https://theses.gla.ac.uk/

Theses Digitisation:

https://www.gla.ac.uk/myglasgow/research/enlighten/theses/digitisation/

This is a digitised version of the original print thesis.

Copyright and moral rights for this work are retained by the author

A copy can be downloaded for personal non-commercial research or study, without prior permission or charge

This work cannot be reproduced or quoted extensively from without first obtaining permission in writing from the author

The content must not be changed in any way or sold commercially in any format or medium without the formal permission of the author

When referring to this work, full bibliographic details including the author, title, awarding institution and date of the thesis must be given

Enlighten: Theses
https://theses.gla.ac.uk/
research-enlighten@glasgow.ac.uk

STUDIES IN THE TECHNIQUE OF SHORT TIME MEASUREMENT AND ITS APPLICATION TO NUCLEAR ISOMERISM.

by

W.M. CURRIE

(June 1962)

Submitted to the University of Glasgow as a Thesis for the degree of Doctor of Philosophy.

ProQuest Number: 10656368

All rights reserved

INFORMATION TO ALL USERS
The quality of this reproduction is dependent upon the quality of the copy submitted.

In the unlikely event that the author did not send a complete manuscript
and there are missing pages, these will be noted. Also, if material had to be removed,
a note will indicate the deletion.

ProQuest 10656368

Published by ProQuest LLC (2017). Copyright of the Dissertation is held by the Author.

All rights reserved.
This work is protected against unauthorized copying under Title 17, United States Code
Microform Edition © ProQuest LLC.

ProQuest LLC.
789 East Eisenhower Parkway
P.O. Box 1346
Ann Arbor, MI 48106 – 1346

CONTENTS.

PREFACE AND ACKNOWLEDGMENTS.

All the experimental work described in this thesis was carried out solely by myself. The work on instrumental time delays and resolution was first proposed by Dr. G.M.Lewis and was published jointly with Dr.Lewis and Dr. R.E.Azuma. The work on Hf^{181} was suggested to me at the start of my research studentship by Drs. Lewis and Azuma who also in the course of my studies advised the measurement of some isomeric lifetimes. The subject matter, the experimental details and the interpretation of these lifetime studies is, however, entirely my own responsibility.

I would like to pay tribute to several people, especially to Dr. G.M. Lewis and Dr. R.E. Azuma whose advice and guidance has been essential to the work reported herein. Dr. Lewis's counsel and encouragement have been given generously throughout the investigations, and in the initial stages Dr. Azuma's practical co-operation in all matters was the most significant influence in the development of my ideas and understanding. I can only say that all this has been very much appreciated.

Most of the later work was made possible only through the co-operation of Dr. W.Jack and Mr. A. Duncan who, respectively, made available and operated the small H.T. set for the production of sources. Much of this work was also greatly facilitated by the recent assistance of Mr. E.Thomas. To these people I am very grateful.

I am particularly grateful to Professor P.I. Dee for his interest and help in furthering these studies, especially for his assistance in the work on hafnium and for the many facilities made available in his department.

I would like to make a special reference to the impressive assistance offered by the Wah Chang Corporation, Albany, Oregon (see chapter 7), in particular to the prompt attention of Mr. R.H. Nielson in dealing with my requests.

Finally, I wish to thank the Department of Scientific and Industrial Research for the provision of a maintenance grant over three years.

W. M. Currie

PUBLICATIONS.

Measurements of Instrumental Time Delay and Resolution in a Fast Coincidence System by W.M. Currie, R.E. Azuma and G.M. Lewis: Nuc. Instr. and Meth. 13 (1961) 215.

Lifetime of the 2.083 MeV State in Ce^{140} by W.M.Currie, Nuc. Phys. 32 (1962) 574.

Isomeric Lifetimes in Ba^{138} and Sn^{120}, by W.M. Currie: to be submitted to Nuclear Physics.

Lifetime of the 152 keV Level in V^{49}, by W.M. Currie: to be submitted to Proc. Phys. Soc.

SUMMARY.

The work reported in this thesis was concerned with the use of a fast coincidence measuring system, i.e. an apparatus using scintillation counters for the measurement of short time intervals between nuclear radiations. The results deal partly with the technique itself and partly with its application to the study of nuclear isomerism.

It has been recognised for a long time now that there are certain inherent limitations to the measurements which can be made with a fast coincidence system. In the first place there is a lower limit to the resolving time which can be obtained and in the second place almost all fast coincidence systems generate by virtue of their detection processes energy dependent, instrumental time delays. This means that the apparent time of an event is influenced by the energy of the radiation. These two aspects of instrumentation are of great practical importance where very short times are being measured .

Chapters 2 and 3 are concerned with these problems of instrumentation, chapter 2 with the development and theory of the subject and chapter 3 with a precise experimental study of instrumental time delays and resolution. The results are very satisfactory. They demonstrate the actual performance of a system, provide illustrative curves and numbers, and indicate the manner in which any other system may be quickly assessed and its limitations ascertained. In addition the

measurements provide pleasing confirmation of the latest theoretical work which has been done on the subject and reveal the inadequacy of some of the earlier treatments.

The rest of the thesis is concerned mainly with the measurement of isomeric lifetimes, four new results being reported and discussed. The background to the subject is considered in chapter 1 where the various features of γ-ray emission from nuclei are reviewed in simple terms and the relationship between these electromagnetic phenomena and the shell and collective models of the nucleus is described. The value of the measurements lies principally in their bearing on these models, and while they provide only a small addition to the already substantial data on the subject they are not insignificant. Three of the measurements have yielded results which do not accord with the general tendency of enhanced rates for E2 transition probabilities , thus emphasising the need for more detailed knowledge of nuclear states, particularly where there is mixing of collective and single particle excitations.

The first lifetime measured was in semi-magic Ce^{140}. It is an E2 lifetime, 17 times longer than the single proton estimate. This was at first found rather surprising since another E2 lifetime in Ce^{140} had already been determined as 17 times shorter than this estimate. As explained in chapter 4, the result is not quite so surprising when more careful consideration is given to the results for other nuclei.

This investigation suggested that there might be some other retarded E2 transitions in nuclei similar to Ce^{140}, that is to say in other semi-magic nuclei which seemed to exhibit mixed excitation modes. An immediate choice for further study was Ba^{138}, and Sn^{120}, with Z = 50 rather than N = 82, was also selected for experiment. This work is described in chapter 5. In both cases successful measurements were made, the result for Ba^{138} being very similar to that for Ce^{140}, and the Sn^{120} result not only giving a lifetime but also correcting an earlier misinterpretation of the decay scheme.

In chapter 6 the measurement of a mixed E2 and M1 transition rate in V^{49} is reported. This work was carried out as part of a plan for the investigation of many isomeric levels using sources prepared on the H.T. set by 14 MeV neutron activation. The work on Ba^{138} and Sn^{120} was also carried out by this means but only after the efficacy of the procedure had been demonstrated in other cases.

The four measured mean lives are:-

2.083 MeV level in	Ce^{140}	.....$(4.97 \pm 0.09) \times 10^{-9}$ sec.
1.890 " " "	Ba^{138}	.....$(2.8 \pm 0.2) \times 10^{-9}$ sec.
2.304 " " "	Sn^{120}	.....$(8.45 \pm 0.18) \times 10^{-9}$ sec.
152 keV " "	V^{49}	.....$(3.05 \pm 0.08) \times 10^{-8}$ sec.

Finally, in chapter 7 (and part of the introduction) there is a discussion of an unsuccessful attempt to observe the electric quadrupole perturbation in the delayed angular correlation between the 133 and the 482 keV γ-rays of Ta^{181}

This was the initial project undertaken by the author. It took up the greater part of 3½ years without yielding any positive results. The reason for this lies simply in the difficulty of the experiment, which was tackled in several ways and which will be the subject of still further study.

CHAPTER 1.

INTRODUCTION

(1.1) Preamble

Most of our present knowledge of nuclear properties and our understanding of nuclear structure has been derived from the study of nuclear spectroscopy, i.e. the study of nuclear radiations. Since the nucleus is small and massive and normally lies at the centre of an envelope of easily disturbed electrons its direct observation is possible only through the medium of radiations which do not interact strongly with these surrounding electrons. Interactions between the nucleus and the electrons do occur and give rise to optical effects from which some of the static properties of nuclei may be derived. Further properties may be studied by microwave methods, atomic beam measurements and mass spectrometry but it is nevertheless largely true that the radiations resulting either from the spontaneous decay of nuclei or from nuclear reactions constitute the prime source of information about the nucleus. Consequently the detection, analysis and interpretation of these radiations has been and still is of paramount importance in nuclear physics.

A great deal of information, particularly regarding the lighter nuclei, has been obtained from nuclear reactions, while at the other end of the scale, among the high - Z elements, our understanding of nuclear structure first blossomed with the detailed study of the α-particles emitted in spontaneous decay. It was through the investigation of α-particle reactions that the very notion of the nucleus was first conceived and it was the analysis of α-particle spectra which first indicated the existence of energy levels in nuclei.

Perhaps the most fruitful source of ideas in nuclear physics has been the study of β- and γ-ray spectroscopy. Throughout the entire range of nuclides, from the neutron to the trans-uranic elements there are more than 1,200 nuclei which emit β-particles or γ-rays or both. The number of nuclei emitting β- particles is about 12 times the number of stable isotopes and there is a vast number of possible excited nuclear states which decay by γ-emission thus greatly extending the range of available information on which theories may be based and put to the test.

Of nuclear theories there is none which is comprehensive and which accounts even in principle for all the properties of all nuclei. Instead there are

several models each of which furnishes a description of a limited range of phenomena. Two of these which have together proved extremely successful in correlating many nuclear data over a wide range of atomic weight are the shell model and the collective or unified model, and one of the most profitable ways of obtaining information concerning these models has been the production and analysis of data on γ-ray emission from nuclei, i.e. the study of nuclear isomerism. The reason for this is that, by comparison with, say, β-decay the emission of electromagnetic radiation by nuclei is a simple process, well understood and involving only a few parameters and concepts. The basic properties of the nuclear states involved can be obtained by direct measurement or by the examination of side effects, such as internal conversion and angular correlations, which do not depend on the nuclear wave functions. In this way unambiguous values for the energies, spins, parities and moments of nuclear states as well as the transition probabilities for decay by γ-ray emission may frequently be obtained and compared with the predictions of one or other of the models.

The extreme usefulness of γ-ray spectroscopy as a nuclear probe has resulted in the devotion of

considerable experimental effort and skill to the development and improvement of measuring techniques. The present day scintillation counter is very much the outcome of this stimulus and in association with the latest electronic devices greatly simplifies the practical tasks of the nuclear spectroscopist. In particular, since the most important feature of any transition process is its probability of occurrence, and since γ-ray transition probabilities are generally very short and difficult to measure, numerous methods have been devised for the determination of the lifetimes of excited states.

It is with this field of γ-ray spectroscopy and in particular with the measurement of very short times between events detected in scintillation counters that the present work is concerned. The investigations have been twofold. Firstly, a thorough and precise study has been made of the delayed coincidence technique and of the performance of scintillation counters when used in a delayed coincidence apparatus, and secondly, this technique has been used to obtain new information on several nuclear levels, most of this information bearing specifically on the collective model and on the shell model.

(1.2) Nuclear Isomerism.

(a) Elementary electromagnetic theory.

An isomer is an unstable or excited nuclear state which exists for a measurable length of time and decays by the emission of electromagnetic radiation. Were sufficient excitation energy available the nucleus would decay very rapidly by heavy particle emission. For this to happen, however, the energy required is generally several MeV, which means that de-excitation by γ-ray emission can take place at energies of up to a few MeV. The process is intrinsically slower than heavy particle emission and in many cases is greatly inhibited by selection rules, so much so that there are numerous isomers with lifetimes comparable to those exhibited in the still weaker β-decay process, and in quite a few instances the two decay modes are in competition.

The first case of isomerism was reported by Hahn (1921) who found that UX_2 and UZ, which have the same atomic weight and number, and which both result from the decay of UX_1, decayed with different periods and different β-particle energies. The explanation is that 1.18 minute UX_2 is more highly excited than UZ and 0.15% of the UX_2 nuclei decay to the ground state UZ by the emission of a 394 keV γ-ray. Fourteen years later further evidence of isomerism was found in indium (Szilard and Chalmers 1935)

and the phenomenon was confirmed by Amaldi and Kurchatov (1935) who established the existence of the 44 hour isomer Br^{80m}. Since then more than ~200 isomers with directly observable lifetimes have been found and a further 670 nuclear levels have had their lifetimes established by indirect methods such as Coulomb excitation and resonance fluorescence. Whether the latter are classified as isomers or not is merely a matter of definition. From the standpoint of nuclear physics the important thing is that such states do exist and that their properties can be determined.

Until 1936 it had been thought that γ-ray emission by nuclei must be very fast, with mean lives in the region of 10^{-13} sec. In that year however von Weisacker (1936) showed that large spin changes in the emission process would account for isomers. He estimated that for a given energy each additional unit of spin change could slow down the transition by a factor of $\sim 10^6$. This result was an extension of the theory of atomic spectra (Condon and Shortley 1935) which was itself based on straightforward classical electromagnetic theory modified in accordance with the correspondence principle (Heisenberg 1925). The theory was extended and made more applicable to nuclei by Heitler (1936a, 1936b) who gave a more precise account of the relationship between angular momentum and radiation.

This pseudo-classical approach is quite simple and since the results are basic to any discussion of isomerism it will be considered briefly here.

In classical theory radiation is produced by the oscillation of charges. For a charge q oscillating with a frequency ν over a distance d it can be shown (e.g. Richtmeyer and Kennard 1950) that the energy radiated per second is

$$W = \frac{16}{3} \frac{\pi^4 \nu^4 q^2 d^2}{c^3} \qquad (1.1)$$

in which the product qd is simply the dipole moment D. If two assumptions are now made this result can be carried over quite satisfactorily into quantum mechanics. Firstly, in dealing with discrete energy quanta, it is supposed that the transition probability is given by

$$A = \frac{W}{h\nu}$$

and secondly, the term D^2 is replaced by the squared matrix element D_{if}^2 where

$$D_{if}^2 = 2 \langle i | D_{op} | f \rangle \exp 2\pi i \nu t$$

That is to say, the dipole moment is replaced by the average over the two states of the corresponding quantum mechanical operator. Hence,

$$A = \frac{64}{3} \frac{\pi^4 \nu^3 D_{if}^2}{hc^3} \qquad (1.2)$$

gives the transition probability for dipole radiation between states i and f. The lifetime of the state i is therefore given by

$$\tau = \frac{3}{64} \frac{hc}{\pi^4 \nu^3 D_{if}^2} \qquad (1.3)$$

This can be applied crudely to the nucleus. If it is assumed that $D_{if} \approx er$ where e is the electronic charge and r the nuclear radius then for a γ-ray of 100 KeV $\tau \approx 10^{-12}$ sec. and for one of 1 MeV $\tau \approx 10^{-15}$ sec.

From the foregoing it would seem very improbable that dipole radiation could account for isomers. These latter must therefore be the result of higher order transitions. Such transitions can be treated in a semi-classical way by the method of retarded potentials.

The electromagnetic field vectors in free space at a point far from the radiating charge system can be expressed in terms of the vector potential $\underline{A}$:-

$$\underline{H} = \text{curl } \underline{A} \qquad \text{in free space} \qquad (1.4)$$

$$\underline{E} = -\frac{1}{c} \partial \underline{A}/\partial t$$

Consequently the radiated power, given by Poynting's vector $\underline{G} = (\underline{E} \times \underline{H})\, c/4\pi$, is derivable from $\underline{A}$. For radiation of angular frequency ω, at a distance r from the source $\underline{A}$ can

be approximated by the expression

$$\underset{\sim}{A}(xyzt) = \frac{\exp[i(\omega t - kr)]}{r} \times \int \underset{\sim}{j}(x'y'z')\,d\tau'$$

$$+ \quad " \quad \times ik \int r' \cos\theta\, \underset{\sim}{j}(x'y'z')\,d\tau'$$

$$- \quad " \quad \times k^2 \int r'^2 (3\cos^2\theta - 1)\, \underset{\sim}{j}(x'y'z')\,d\tau'$$

$$+ \quad - \quad - \quad - \quad - \quad - \quad - \qquad (1.5)$$

where the integrals refer to the interior of the charge system and k is the wave number $2\pi/\lambda$ or $1/\lambda$. Each term in this expansion is a different multipole component of the radiation, dipole, quadrupole, octupole etc., and the integrals correspond to the different multipole moments of the radiating system. It can be seen that the integrals are weighted by the factor $(1/\lambda)^{\ell-1}$ for the 2^{ℓ}th component and that each integral contains a term $(r')^{\ell-1}$. The relative intensities of the components therefore vary as $(r'/\lambda)^{2(\ell-1)}$ and successive multipoles will increase in probability by a factor $(r'/\lambda)^2$. For nuclear radiation of 100 keV this ratio is 10^{-5} which, in combination with eq.(1.3), makes a 100 keV isomer of many seconds duration seem feasible provided that the radiation is of the 2^4th pole.

This simple treatment is capable of producing further results. If the vector potential $\underline{A}$ is expanded not in the form (1.5) but to a higher degree of accuracy it becomes apparent that the radiation is not entirely transverse. Thus radial components of $\underline{E}$ and $\underline{H}$ exist, implying the transport of angular momentum. When the calculation is completed for the dipole case the rate of transmission of angular momentum turns out to be W/ω, or, in terms of quantum mechanics $\hbar$ units of angular momentum for a photon of energy $\hbar\omega$. Heitler(1936a) showed that in general a photon of the 2^{ℓ} th pole carries off $\ell\hbar$ units of angular momentum. It follows that for a nuclear transition between states i and f

$$\underline{I}_i = \underline{I}_f + \underline{\ell}$$
$$\text{or} \qquad \ell \geq |I_i - I_f| = \Delta I \tag{1.6}$$

Thus the multipole order of the radiation cannot be less than the spin change, and the 100 keV isomer mentioned already would seem reasonable where a spin change of 4 was involved.

By a more general extension of eq.(1.2) it can be shown(Fierz 1949, Weisskopf 1951) that for any multipole component the transition probability is:

$$A_\ell = \frac{8\pi}{\ell} \frac{(\ell+1)\, k^{2\ell+1} Q_\ell^2}{[(2\ell+1)!!]^2 \hbar} \tag{1.7}$$

where Q_ℓ is the matrix element associated with the 2^ℓ electric (E) or magnetic (M) moment.

When simple assumptions are made about $Q_{E,\ell}$ and $Q_{M,\ell}$ it appears that $A_{E,\ell} > A_{M,\ell}$ always, by a factor of $\sim 10^3$, suggesting that for a given ΔI the electric transition should always take preference over the magnetic transition, and that the latter should therefore not occur. However, there are further selection rules which prevent this state of affairs.

The term Q_ℓ^2, given by:

$$Q_\ell = \iiint \psi_i \, Q_{op} \, \psi_f \, dx \, dy \, dz$$

vanishes if the total integrand is odd. Thus if ψ_i and ψ_f both have odd parity the operator Q_{op} must also have odd parity, since otherwise the transition would be forbidden. Q_{E1}, the electric dipole operator, is essentially a length and therefore has odd parity, Q_{E2} is an area and has even parity while Q_{M1} is derived from the angular momentum $\underline{r} \times \underline{p}$ and has even parity. In this way the following table for parity changes is obtained. This indicates which type of transition should occur in a given situation.

Table 1.1

Multipole	Dipole	Quad.	Oct.	16-	32-	64-
Electric	Yes	No	Yes	No	Yes	No
Magnetic	No	Yes	No	Yes	No	Yes

(b) Applications in nuclear physics

As soon as isomerism had been established in several cases and the main features of the transition process understood, there followed several investigations of associated phenomena and there were a few abortive efforts to predict transition probabilities from various assumptions about the nucleus. The competing process of internal conversion was studied and found very helpful in the assessment of multipolarities and nuclear spins, the reason being that this process depends not on the nuclear wave function but on the magnitude of the electron wave functions at the nucleus.

Except for $Z \lesssim 20$ and $E \gtrsim 2.5$ MeV the process is very common and in some cases is much more favoured than γ-emission. The relevant parameters are the internal conversion coefficients defined by:

$$\left.\begin{aligned} \alpha_K &= N_K/N_\gamma \\ \alpha_{L_1} = N_{L_1}/N_\gamma \,,\ \alpha_{L_2} &= N_{L_2}/N_\gamma,\quad \alpha_{L_3} = N_{L_3}/N_\gamma \end{aligned}\right\} \qquad (1.1)$$

and the internal conversion ratios K/L, L_1/L_2, L_1/L_3 etc. It follows from the definitions in eq.(1.8) that the total number of transitions, N, is given by

$$N = N_\gamma \left(1 + \alpha_K + \alpha_{L_1} + \text{---}\right)$$

$$= N_\gamma \left(1 + \alpha_{TOT}\right)$$

and that the radiation lifetime and the observed liftime are related by

$$\tau_\gamma = \tau_{obs} \left(1 + \alpha_{TOT}\right) \qquad (1.9)$$

Thus, if α_{TOT} is large the observed isomeric lifetime is much less than the lifetime for γ-emission which means that precise determinations of γ-ray transition probabilities cannot be made unless the conversion coefficients are known.

But, as has been suggested already, it is desirable to know conversion coefficients for other reasons. These coefficients can be calculated very accurately at the present time (Rose 1958) and even before the second world war (Hebb and Uhlenbeck 1938, Dancoff and Morrison 1939) reasonable estimates of their magnitudes were possible. Since they depend on the multipolarity and character of the associated radiation these properties may often be inferred from measurements of the coefficients. Not only that, in many cases of doubt supplementary measurements of the internal conversion ratios, which are generally simpler to make, will

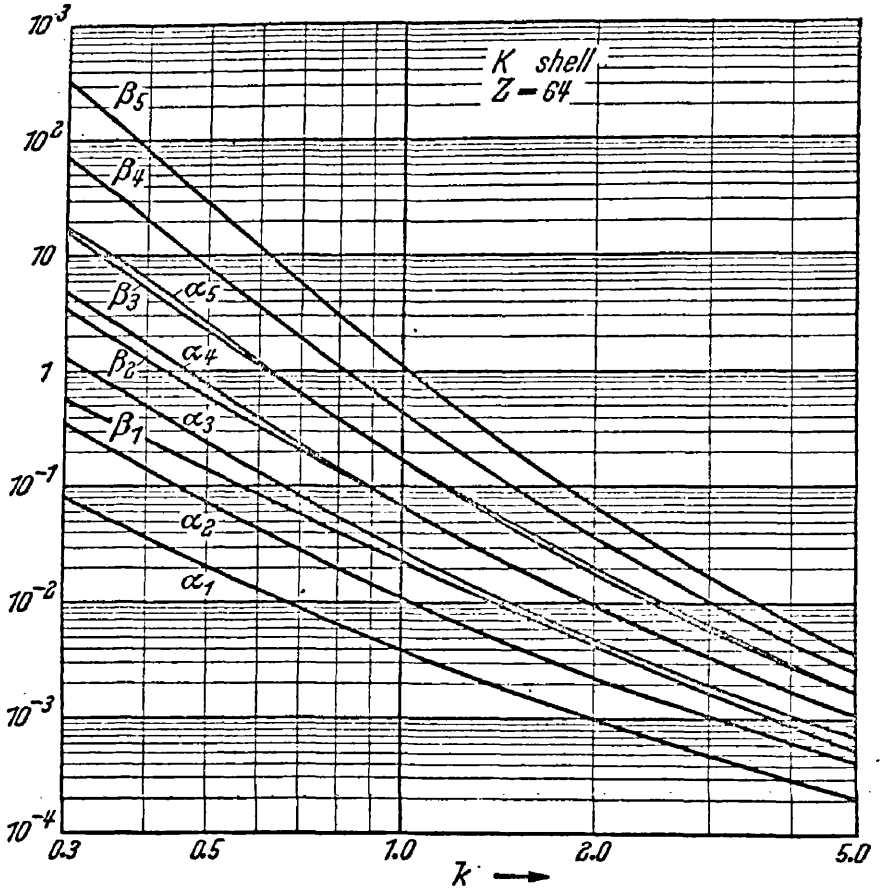

FIG. 1.1a *K*-shell internal conversion coefficients versus transition energy in units of m_0c^2 for $Z = 64$. The α's and β's correspond to electric and magnetic radiations respectively and the subscript denotes the multipole order.

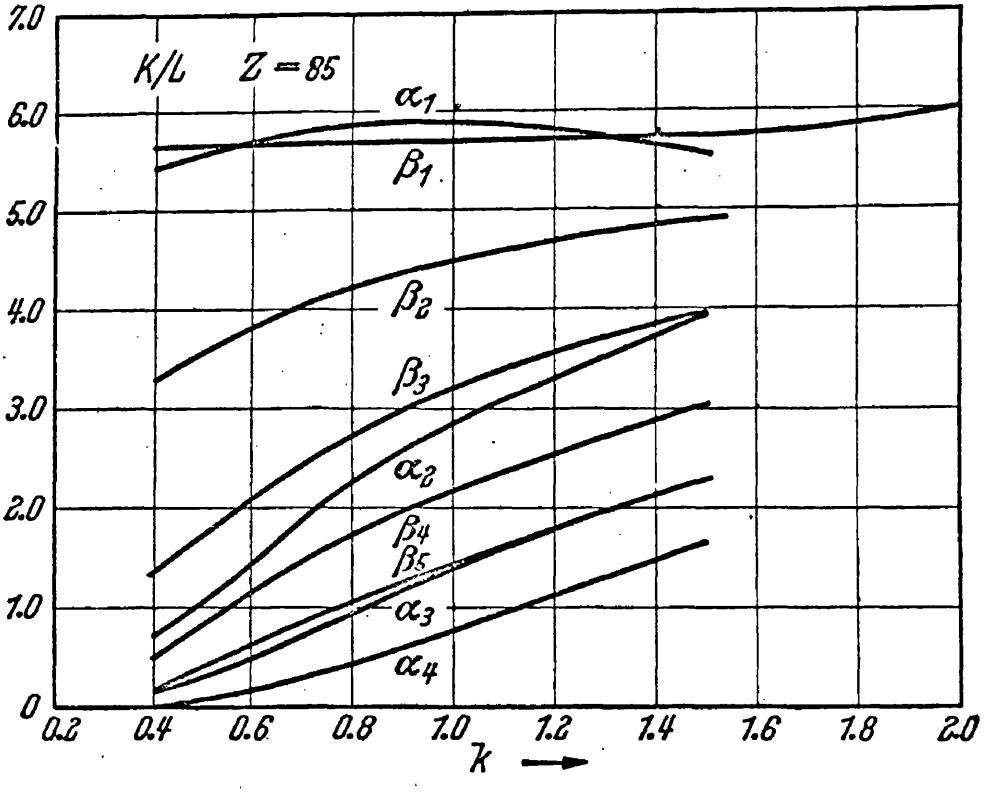

FIG. 1.1b $K/L_{I+II+III}$ internal conversion ratios versus transition energy in units of m_0c^2 for $Z = 85$. The α's and β's correspond to electric and magnetic radiations respectively and the subscript denotes the multipole order.

substantiate these findings and allow an unambiguous assignment to be made. This is illustrated in fig. 1.1.

Another way of determining nuclear spins was provided by Hamilton (1940) in the theory of angular correlations. The measurement of directional and polarization correlations is now a very powerful method of investigation in nuclear spectroscopy, and since it is particularly relevant to some of the work reported in this thesis it will be discussed in more detail in the next section.

The first part of this section outlined the theory of γ-ray emission as it stood between the years 1936 and 1949, when 75 isomers were known and the subject was reviewed by Segrè and Helmholtz (1949). As far as it goes the theory is perfectly correct but of little interest in nuclear physics. The chief limitation at that time was the dearth of information on the nuclear wave functions which meant that the matrix elements could not be evaluated. Some attempts at evaluation were in fact made, but with littl success until the introduction of the nuclear shell model in 1950 (Haxel et al. 1950, Mayer 1951). At this juncture the subject of nuclear isomerism received a great impetus and during the next few years much theoretical and experimental work was done on all its aspects.

In 1951, following the advent of the shell model, Weisskopf used a crude version of the single particle model to estimate transition probabilities for γ-ray

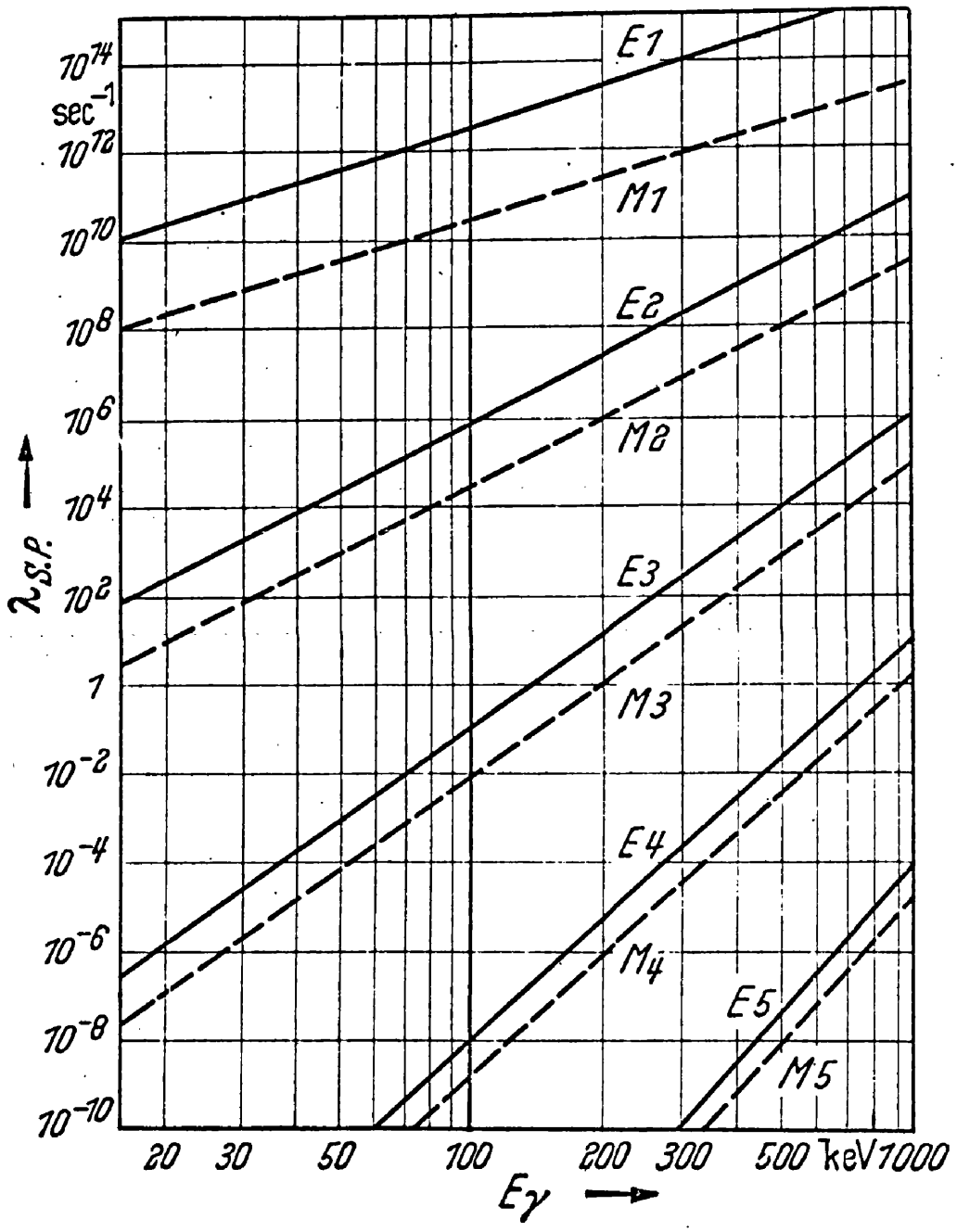

Fig. 1.2 Gamma-ray transition probabilities for a single proton.

omission. By assuming that the radiation was produced by a single independent proton decaying to an s-state he obtained the results:

$$A_{E,\ell} = \frac{4.4(\ell+1)}{\ell[(2\ell+1)!!]^2}\left(\frac{3}{\ell+3}\right)^2\left(\frac{E_\gamma}{197\,MeV}\right)^{2\ell+1}\left(1.5A^{1/3}\right)^{2\ell}\times 10^{21} \quad (1.10)$$

$$A_{M,\ell} = \frac{1.9(\ell+1)}{\ell[(2\ell+1)!!]^2}\left(\frac{3}{\ell+3}\right)^2\left(\frac{E_\gamma}{197\,MeV}\right)^{2\ell+1}\left(1.5A^{1/3}\right)^{2\ell-2}\times 10^{21} \quad (1.11)$$

which lead to the values given in table 1.2 and are

Table 1.2 Average lifetimes in seconds, for A = 100

E MeV	E1	M1	E2	M2	E3	M3	E4	M4	E5	M5
0.01	4×10^{-10}	4×10^{-8}	2×10^{-2}	2	10^{8}	10^{10}	10^{17}	10^{19}	10^{26}	10^{28}
0.1	4×10^{-13}	4×10^{-11}	10^{-6}	10^{-4}	10	10^{3}	10^{8}	10^{10}	10^{15}	10^{17}
1	6×10^{-16}	6×10^{-14}	10^{-11}	10^{-9}	10^{-6}	10^{-4}	10^{-1}	10	10^{4}	10^{6}
10	4×10^{-19}	4×10^{-17}	10^{-16}	10^{-13}	10^{-13}	10^{-11}	10^{-10}	10^{-8}	10^{-7}	10^{-5}

illustrated in fig. 1.2 opposite. From these results it

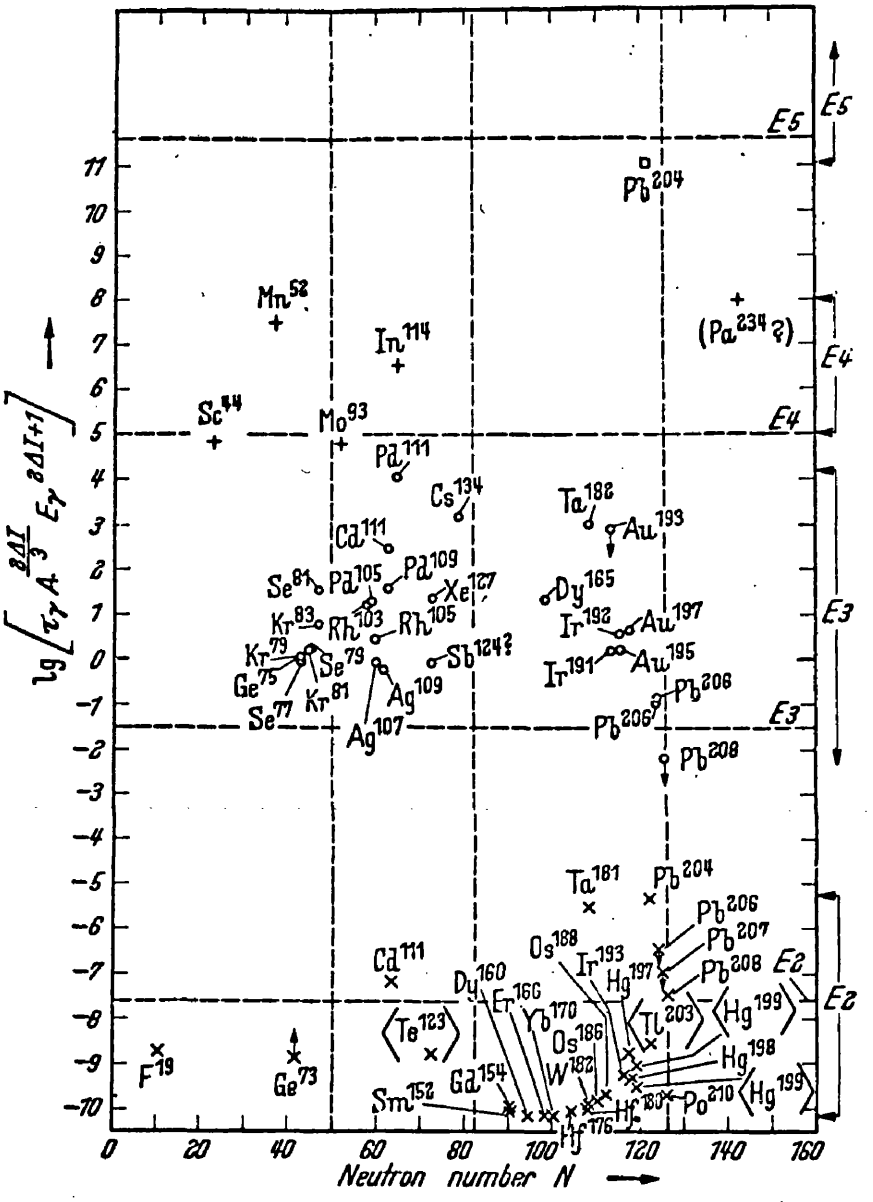

Fig. 13 Comparative lifetimes for $E2$, $E3$, $E4$ and $E5$ transitions, plotted against neutron number N. The theoretical lines, corresponding to matrix elements equal to unity for single particle proton transitions, are also shown. Points marked $\langle\rangle$ are based on mixed transitions.

can be seen that unless the matrix element computed according to the Weisskopf model is in error by $\gtrsim 10^{\pm 3}$ it should be possible to assign the multipolarity when τ_γ is known. If in addition the conversion coefficients and, in the case of cascades, the angular correlation data are known, then it is nearly always possible to assign the spins and parities of the states unambiguously and to label the radiations precisely, even to the degree of mixing involved.

Following Weisskopf's theory (Goldhaber and Sunyar (1951, 1955) carried out an empirical classification of isomers the results of which, along with equations (1.10) and (1.11) have served until now as a basis of comparison in the subject. The general pattern of their results can be seen in figs. 1.3 and 1.4 (taken from Goldhaber and Sunyar 1955).

In these figures the measured values for τ_γ are expressed in the form of comparative lifetimes, that is to say, the dependence on E and A, as expressed in equations (1.10) and (1.11) is removed by multiplication by a suitable factor. The comparative lifetimes thus obtained are true measures of the transition strength, i.e. of the matrix elements. They indicate the validity of the Weisskopf model and can be

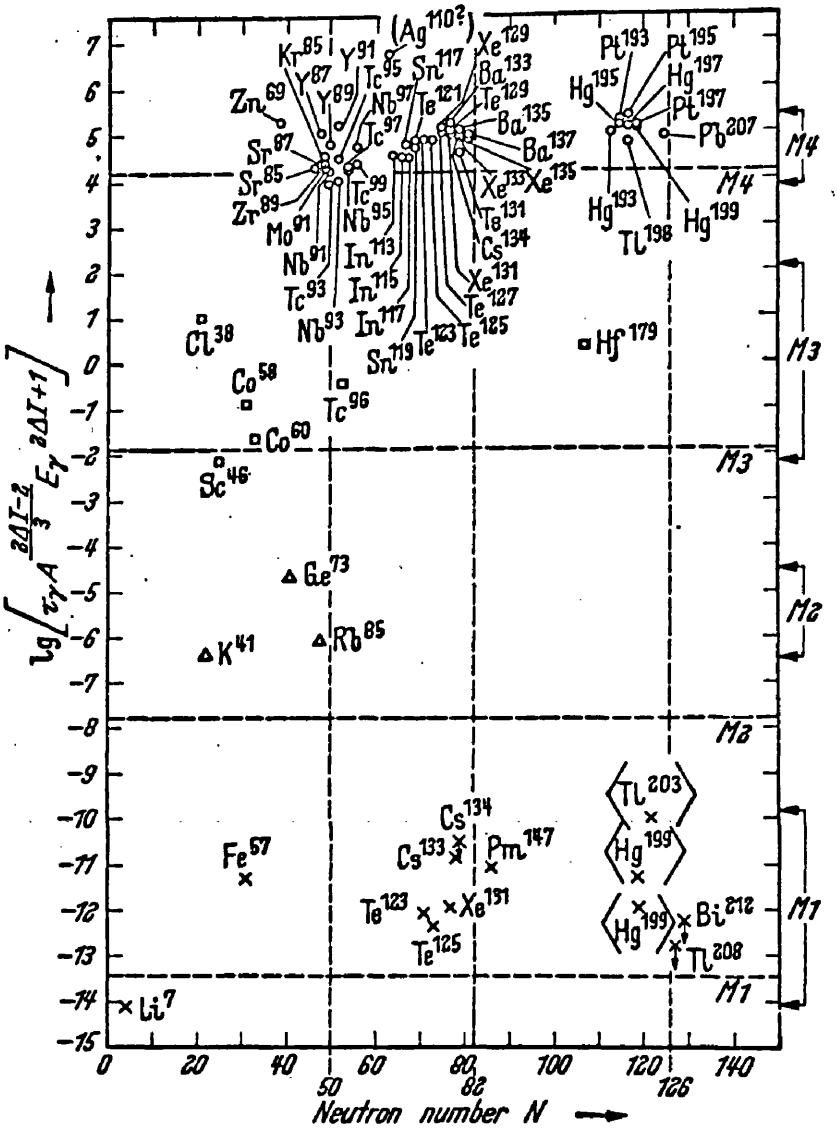

Fig. 1.4 Comparative lifetimes for $M1$, $M2$, $M3$ and $M4$ transitions plotted against neutron number N. The theoretical lines corresponding to matrix elements equal to unity for single proton transitions are also shown. Points marked $\langle\rangle$ are based on mixed transitions.

used in the assessment of other models. To be successful a model must account for the details of these figures, or of their more contemporary equivalents, and, as can be seen, there are a number of irregularities which require explanation. A particularly noticeable feature of fig. 1.3 is the enhancement of E2 transition probabilities. Since the measurements to be reported were all concerned with E2 transitions this particular aspect of isomerism will be discussed more fully later.

(1.3) Angular Correlations

(a) General

The study of angular correlations is one of the most powerful methods of particle and nuclear physics. Indeed, the existence of the nucleus was originally established by an angular distribution experiment (Geiger and Marsden 1913), and more recently the violation of the parity principle has been demonstrated by a measurement of angular distribution (Wu et al. 1957). Any physical process which produces oriented nuclei is amenable to treatment by the general theory of angular distributions and correlations. Such physical processes are: reduction to very low temperatures in a magnetic field, nuclear reactions and all kinds of nuclear decay. Nor need the processes be simple; several radiations can be involved. Clearly then, the subject embraces an extensive field of experimental physics and

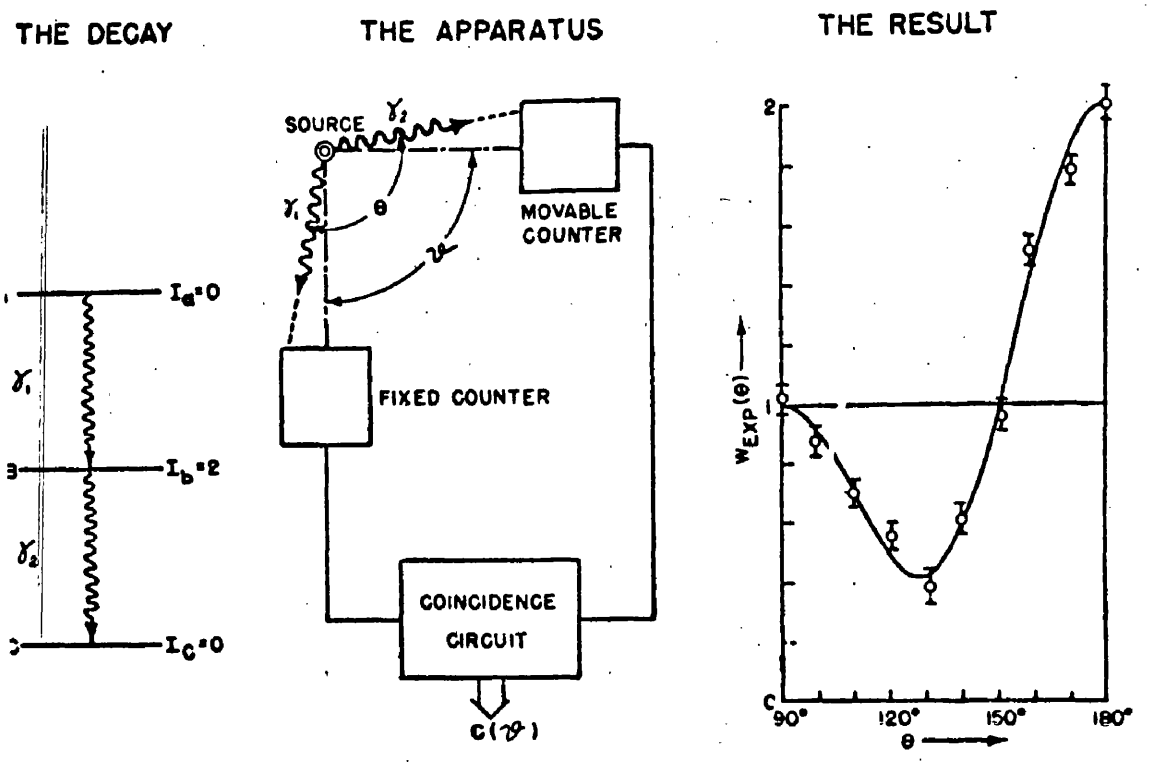

FIG. 1.5a Example of a directional correlation measurement

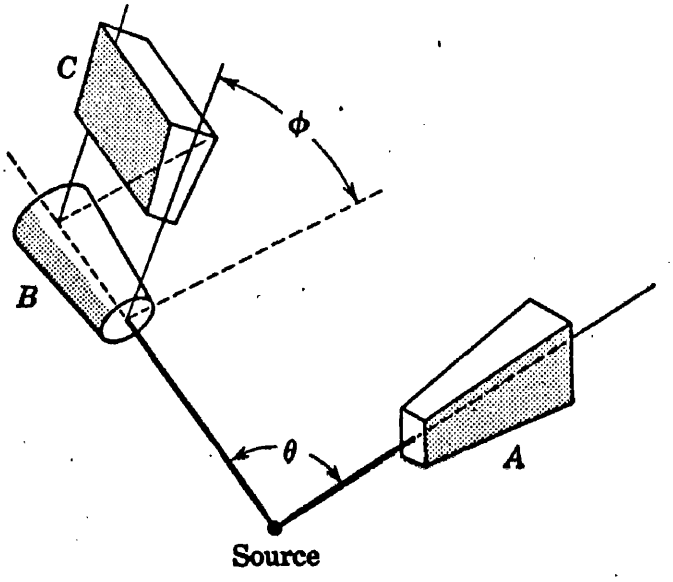

FIG. 1.5b Schematic diagram of a polarimeter. A, B, and C are scintillation crystals.

and only a restricted aspect of it will be considered here. That aspect is the angular correlation of two nuclear γ-rays emitted in cascade. Even for this simple case the theory is quite complicated in its details and only a very condensed account of it will be given here, sufficient to clarify the experimental work reported in chapter 7.

The theory was first developed by Hamilton (1940). Since then it has been greatly improved and extended and has been treated in a very thorough and complete way by several authors (Falcoff and Uhlenbeck 1950, Alder 1952, Fano 1953, Biedenharn and Rose 1953, Fraunfelder et al. 1955, Devons and Goldfarb 1957). Tables of the coefficients referred to below are available in several places (e.g. Biedenharn and Rose, 1953, Siegbahn 1955, Wapstra et al. 1959).

Fig. 1.5a illustrates an angular correlation experiment. γ_1 and γ_2 are emitted in cascade and are detected in two counters one of which can rotate about the source, as shown. The coincidence counting rate, when plotted as a function of θ, gives the angular correlation function $W(\theta)$. The latter can be expanded in the form:

$$W(\theta) = \sum_k A_k P_k (\cos\theta) \qquad (1.12)$$

When parity is conserved only terms with even k occur and k_{max} is given by:

$$k_{max} = \min (2I_b, 2L_1, 2L_2) \qquad (1.13)$$

so that in practise k is unlikely to be greater than 4. Hence:

$$W(\theta) = A_o + A_2 P_2(\cos\theta) + A_4 P_4(\cos\theta) \qquad (1.14)$$

$\partial W/\partial\theta = 0$ at 90° and $W(\theta)$ is symmetrical about 90° so it need only be determined in the range 90° - 180°. The anisotropy A is defined by:

$$A = \frac{W(180^\circ) - W(90^\circ)}{W(90^\circ)} \qquad (1.15)$$

$$\text{i.e.} \quad A = \frac{1 + A_2 + A_4}{1 + \frac{1}{2} A_2 + \frac{3}{8} A_4} - 1 \qquad (1.16)$$

and can be positive or negative.

The coefficients A_k can be written as a product of two factors each of which depends on only one of the two transitions involved:

$$A_k = F_k(1) F_k(2) \qquad (1.17)$$

In the most general case the radiations are mixtures, 2^L- pole plus $2^{L'}$-pole say, with the degree of mixing given by the parameter:

$$\delta^2 = \frac{\text{Intensity of radiation } L'}{\text{Intensity of radiation } L} \qquad (1.18)$$

and the coefficients F_k can then be written:

$$F_k(1) = F_k(L_1 I_a I_b) + 2\delta_1 F_k(L_1 L_1' I_a I_b) + \delta_1^2 F_k(L_1' I_a I_b)$$
$$F_k(2) = F_k(L_2 I_c I_b) + 2\delta_2 F_k(L_2 L_2' I_c I_b) + \delta_2^2 F_k(L_2' I_c I_b) \qquad (1.19)$$

where the middle term in each sum is a measure of the coherent interference in the mixed radiation. The coefficient A_o is given by

$$A_o = (1 + \delta_1^2)(1 + \delta_2^2) \qquad (1.20)$$

and will of course be unity for pure radiations.

These remarks have referred to directional correlations. They say nothing about the parities of states or the character of the radiations. For information on this aspect of a decay scheme a polarisation correlation has to be measured. This involves a determination of the polarisation of γ_2 (or γ_1) as a function of θ and requires the use of some kind of polarimeter. Such a device is provided (fig.1.5b) if the Compton scattered photons from γ_2 stopping in counter B are detected in a third counter (c) which can be rotated about the direction of motion of γ_2. The scattering process is sensitive to the polarisation of the primary radiation and is such that a determination of the amount of scattering both in, and perpendicular to the plane containing the cascade γ-rays provides all the necessary information for the correlation to be determined. This method has been applied to one of the decay schemes to be considered later (Bishop and Perez Y Jorba 1954).

In general the full details of a decay scheme are worked out by a combination of the various methods which have been summarised so far in this chapter, plus additional information from β-decay and nuclear reactions. The decay schemes of the nuclei to be discussed later have been elucidated by all these methods, the limitations of which will become apparent as the thesis proceeds.

(b) Perturbed directional correlations

The foregoing paragraphs were concerned with a special and rather idealised situation. The nucleus was supposed to emit a photon; this left it aligned in some way with respect to the direction of this photon; this alignment was maintained indefinitely until a second photon was emitted, and the direction of the second photon was thus statistically determined. As mentioned earlier this process is but a limited aspect of angular correlations. The elementary treatment of it given in these paragraphs was further simplified by the supposition that in the time interval between the two consecutive transitions nothing happens to the nucleus. In any normal experimental situation this is unlikely because most radioactive nuclei are constituent parts of a solid or liquid source and are consequently liable to perturbations by electric and magnetic

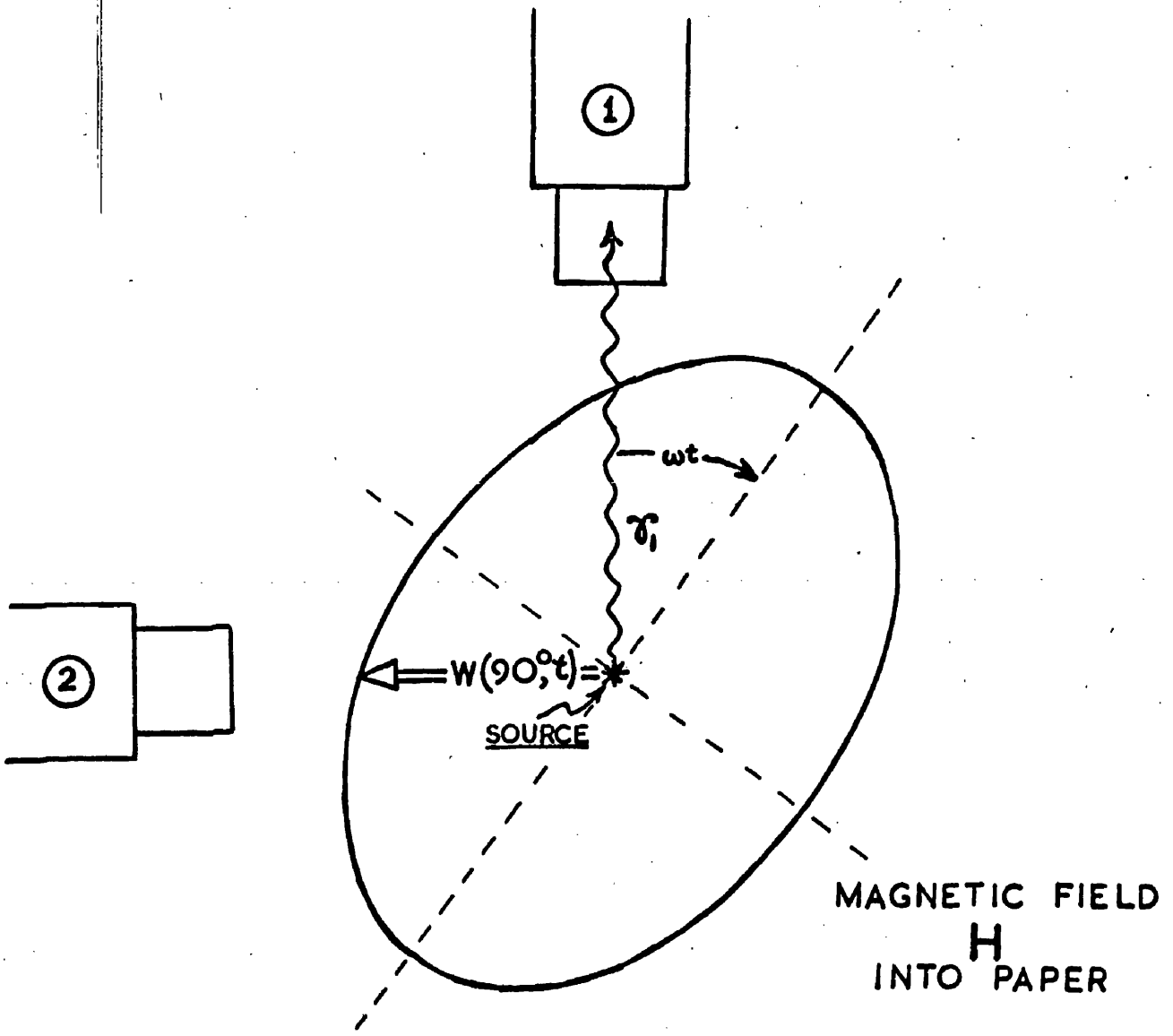

FIG. 1.6

Illustrating the effect of an applied magnetic field on an angular correlation. The elliptical figure represents $W(\theta)$ while ω is the precessional frequency.

fields. This means that in the interval between the transitions a re-alignment is liable to take place by the nuclei rotating in various ways about the impressed fields or field gradients. Not only that, if in the time interval between the transitions the nuclei are subjected to fluctuating fields the population of the intermediate substates is liable to be changed by induced transitions between different m-states. This wipes out the initial preferred direction and is equivalent to a loss of memory.

These various effects produce changes in the angular correlation, and for any given situation the changes thus brought about can be informative. They can yield further information about the electromagnetic characteristics of the intermediate state and/or information about the fields in the source.

Figure 1.6 illustrates for a simple case how an applied field can affect the directional correlation. A constant magnetic field H is applied to the source, perpendicular to the plane containing the source and counters. One result of this is that after the emission of γ_1 the nuclear magnetic moment μ precesses about the field H with angular frequency ω given by:

$$\omega = \frac{\mu H}{I\hbar} = \frac{g\mu_n H}{\hbar} \qquad (1.21)$$

where g is the nuclear g-factor and μ_n is the nuclear magneton. Effectively, therefore, the frame of reference defined by the direction of γ_1 rotates in the laboratory about $\underline{H}$ at this rate, and the angular correlation, defined with respect to this frame, also rotates in the laboratory as shown in fig.1.6. For counter 2, therefore, the probability of detection of γ_2 varies with time as well as with θ. In fact, it may be written down as:

$$W(\theta, t) = \sum_k A_k P_k \left[\cos(\theta - \omega t) \right] \qquad (1.22)$$

Now that a time factor has been introduced the lifetime of the intermediate state must be considered. If this lifetime is very short compared with the precessional period only a small rotation of the nuclear frame of reference will have taken place before the emission of γ_2 and the angular correlation given by eq.(1.14) will hardly be affected. If, on the other hand, several precessional periods, can elapse before the emission of γ_2 then eq.(1.14) will not be applicable at all. These considerations constitute additional grounds for the measurement of isomeric lifetimes.

To deal with the case of perturbations it is necessary to consider in more detail the coincidence arrangement used in the detection of γ_1 and γ_2. In practise the detectors extend over an angular range $\theta_1 - \theta_2$ and measurements are

made with a coincidence system which has a finite resolving time t_R. If a delay is inserted in the system so that only those γ_2's which occur at $t_D \pm t_R$ after γ_1 are registered, then what is actually determined is, after correction for finite $\Delta\theta$ (Rose 1958),

$$W(\theta,t_D) = \frac{\int_{t_D-t_R}^{t_D+t_R} e^{-t/\tau} W(\theta,t)\, dt}{\int_{t_D-t_R}^{t_D+t_R} e^{-t/\tau}\, dt} \qquad (1.23)$$

If $t_R \gg \tau$ (the mean life) and if $t_D = 0$ $W(\theta)$ is called the integral correlation, while if $t_R < \tau$ $W(\theta,t_D)$ is called the delayed angular correlation.

The integral correlation $W(\theta)$ is, in the absence of perturbations, given by eq.(1.14) and is the function most frequently determined in experiments. Applying eq.(1.23) to the case of an applied magnetic field the integral correlation is given by:

$$\left.\begin{aligned} W(\theta) &= \frac{\int_0^\infty \sum A_k P_k [\cos(\theta-\omega t)]\, e^{-t/\tau} dt}{\int_0^\infty e^{-t/\tau} dt} \\ &= \sum \frac{b_k}{\sqrt{1+(k\omega\tau)^2}} \cos k(\theta-\Delta\theta) \end{aligned}\right\} \qquad (1.24)$$

where the b's are the coefficients used when $W(\theta)$ is expanded as a sum of terms $b_k \cos k\theta$, and

$$\Delta\theta = \frac{1}{k} \text{arc tan}(k\omega\tau) \qquad (1.25)$$

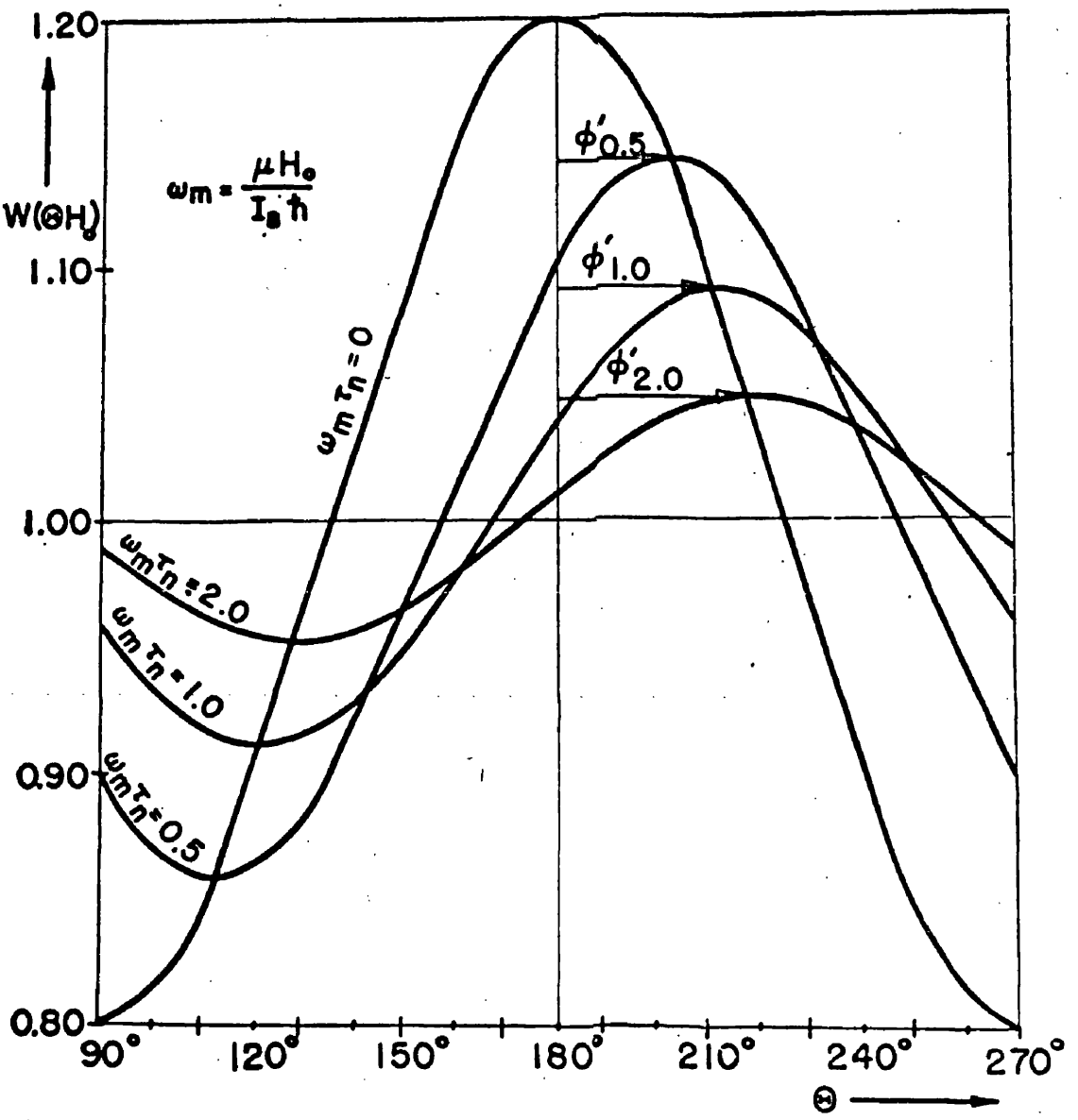

The attenuation and 'azimuthal shift' ϕ of an angular correlation ($W_0(\Theta, 0)=1+0{\cdot}2\cos 2\Theta$) in a magnetic field H_0 perpendicular to the plane ($\mathbf{k}_1, \mathbf{k}_2$).

FIG. 1.7

Thus the integral correlation function is both attenuated and rotated, the attenuation factor being $1/\sqrt{1 + (k\omega\tau)^2}$. If both detectors are equally sensitive to both radiations there is no rotation and the attenuation factor is $1/\left[1 + (k\omega\tau)^2\right]$. Fig.1.7 shows the effect of an applied field on a particular integral correlation. From the measurement of such a correlation the magnetic moment of the intermediate state can be obtained.

If the coincidence system and decay scheme are such that

$$\left.\begin{aligned} t_R &< \tau \\ t_R &< T_L \end{aligned}\right\} \qquad (1.26)$$

where T_L is half the precessional period, i.e. $T_L = \pi/\omega$, then a delayed correlation measurement will yield the precessional period, and hence μ, directly. Counter 2 is set at 90° to the axis of counter 1 and $W(90^\circ, t_D)$ is obtained by the use of variable delays or by time-to-pulse height conversion (see next two chapters). The result is a modulated decay curve, as shown in fig. 1.8 in which T_L is evident. If the axis of counter 2 is now rotated through 90° the modulation should be altered in phase by 180°.

The illustrative case just considered embodies the main features of all other cases. The general case is

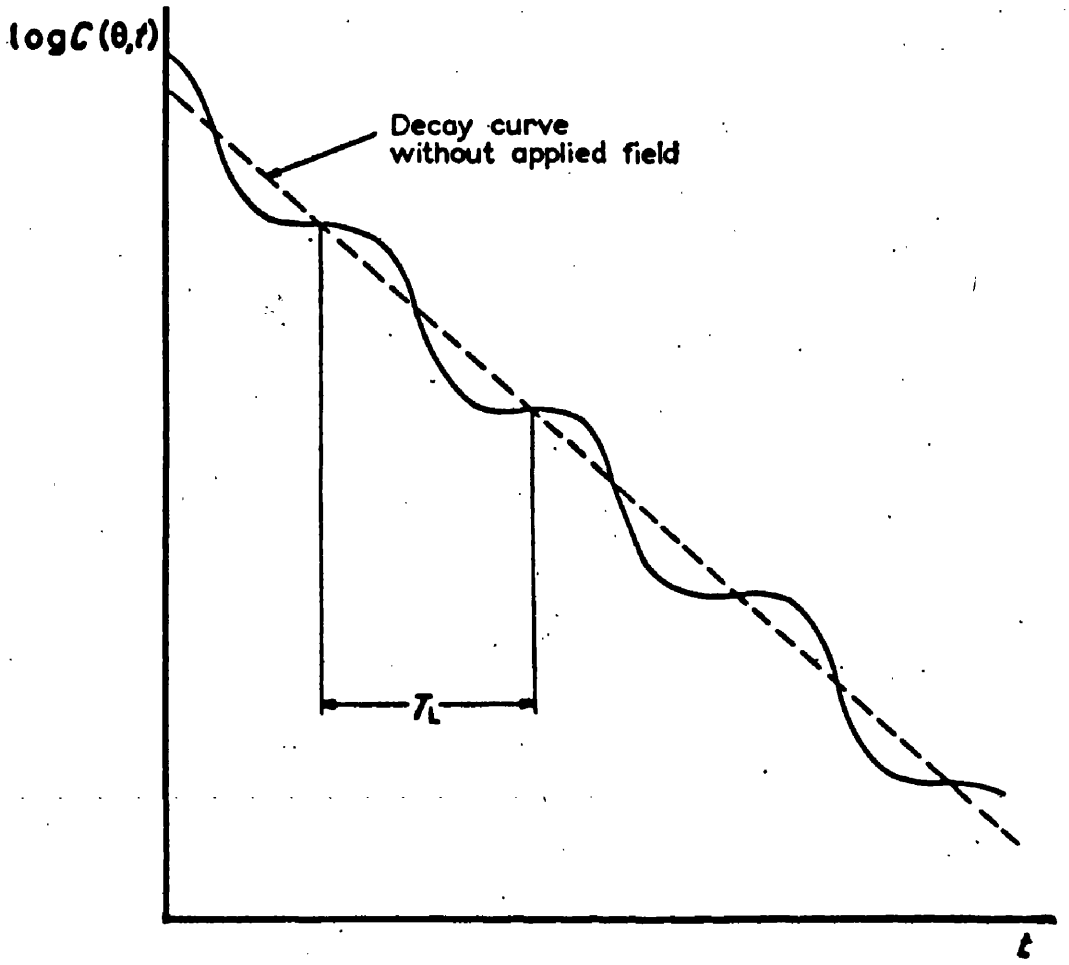

Fig.1.8 Modulated decay curve. Modulation caused by the spin axis precession in the external magnetic field. T_L = time for one half turn of precession.

much more complicated but gives rise to similar results, which will now be given. These results are taken from Steffen (1955) and Beer and Bovey (1959).

In any case where the intermediate nucleus is affected by perturbing fields the coefficients A_k of eq.(1.14) are modified to:

$$A_k = F_k(1) \; G_k(t) \; F_k(2) \tag{1.27}$$

where $G_k(t)$ is called the attenuation factor. It is a function of time and is unity for t = o. Thus (1.14) now becomes:

$$W(\theta,t) = \sum_k F_k(1) \; G_k(t) \; F_k(2) \; P_k(\cos\theta) \tag{1.28}$$

When this is integrated with respect to time $G_k(t) \rightarrow G_k$, and it turns out that for the case of static fields these G_k's can never vanish. That is to say a "hard core" integral correlation always remains, no matter how strong the perturbing field, and for all cases of axial symmetry the minimum value of G_k is given by

$$G_k(\text{min.}) = \frac{1}{4k + 1} \tag{1.29}$$

For static interactions the attenuation functions are always periodic, while in the case of time dependent interactions (eg. lattice vibrations and Brownian motion) they generally take an exponential form. In the latter case therefore the correlation decays with some characteristic half life and after several half lives is

wiped out completely. The intermediate nuclei are no longer aligned with respect to the original preferred direction and the angular distribution of the γ_2's is isotropic. This effect has been studied by the author's supervisors (Azuma and Lewis 1957).

The case with which the author was concerned was that of static electric quadrupole interactions. The quadrupole moment of the nucleus interacts with the electric field gradient produced in the crystal lattice of the source material. The theory has been worked out in detail by Abragam and Pound (1953) who found that for a polycrystalline source the attenuation functions are as follows:

$$\left.\begin{aligned}
&I_b=1 : G_2(t)=1/5(3+2\cos\omega_e^\circ t)\\
&I_b=3/2 : G_2(t)=1/5(1+4\cos\omega_e^\circ t)\\
&I_b=2\begin{cases}G_2(t)=1/35(13+2\cos\omega_e^\circ t+12\cos 3\omega_e^\circ t+8\cos 4\omega_e^\circ t)\\ G_4(t)=1/63(29+12\cos\omega_e^\circ t+16\cos 3\omega_e^\circ t+6\cos 4\omega_e^\circ t)\end{cases}\\
&I_b=5/2\begin{cases}G_2(t)=1/35(7+13\cos\omega_e^\circ t+10\cos 2\omega_e^\circ t+5\cos 3\omega_e^\circ t)\\ G_4(t)=1/63(7+15\cos\omega_e^\circ t+18\cos 2\omega_e^\circ t+23\cos 3\omega_e^\circ t)\end{cases}
\end{aligned}\right\}(1.30)$$

where ω_e° is the fundamental precessional frequency given by

$$\left.\begin{aligned}
\omega_e^\circ &= \frac{3}{4I(2I-1)}\,\frac{eQ}{\hbar}\,\frac{\partial E_z}{\partial z} \quad \text{for integral } I\\
\text{or } \omega_e^\circ &= \frac{3}{2I(2I-1)}\,\frac{eQ}{\hbar}\,\frac{\partial E_z}{\partial z} \quad \text{for half integral } I
\end{aligned}\right\}(1.31)$$

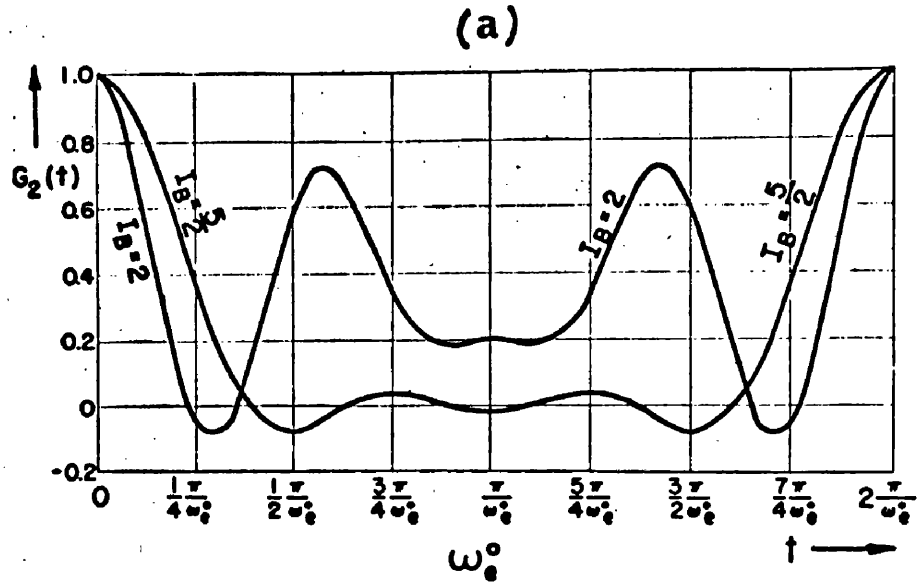

The attenuation coefficient $G_2(t)$ for the delayed correlation as a function of the delay time t for $I_B=\frac{3}{2}$ and $I_B=2$ (according to Abragam and Pound, 1953)

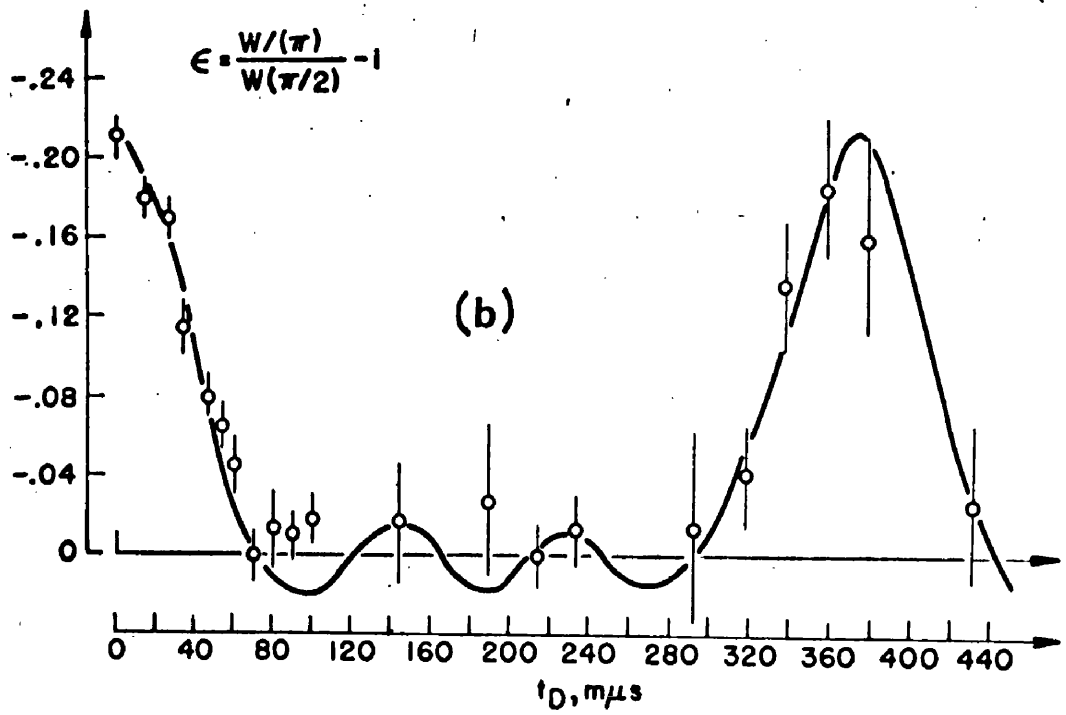

Measurement of the delayed angular correlation in In^{111} with a polycrystalline indium metal source. From a comparison with Eq. (1.30) an interaction strength $\Delta\nu_Q = 17.7$ Mc can be deduced [P. Lehmann and J. Miller, *J. phys. radium* **17**, 526 (1956)].

FIG. 1.9

Fig. 1.9a shows $G_2(t)$ plotted for I_b=2 and 5/2 while fig. 1.9b shows the experimentally observed function obtained by a delayed angular correlation measurement on In^{111} (Lehman and Miller 1956). From this curve the quadrupole interaction frequency ν_Q, given by

$$\nu_Q = \frac{eQ}{h} \frac{\partial E_z}{\partial z} \qquad (1.32)$$

was found to be 17.7 Mc.

From what has been said in this section it is apparent that measurements of perturbed angular correlations can, among other things, yield information about the moments of excited nuclear states. The desirability of this will be dealt with in the next section and unsuccessful attempts to make such measurements on two nuclei will be discussed in the last chapter.

(1.4) Nuclear Models

(a) The shell model

The purpose of all measurements of conversion coefficients, lifetimes, angular correlations etc. is the improvement of nuclear theory. This is concerned largely with the structure of nuclear states but also with the processes whereby these may change. Since, as has been

seen, the decay processes with which this thesis is concerned are straightforward and well understood they may be reliably utilised in the collection of information about nuclear states. Such information can then be related to one or more of the various nuclear models.

It is most unlikely that a few measurements of isomeric lifetimes and such like data will radically affect the postulates and conclusions of any of these models, but the sum total of such data are the facts by which nuclear theories must stand or fall and at the present time there is still a need for more facts on many aspects of the subject.

The subject of nuclear models has been both comprehensively and extensively reviewed. Only two of the models, which are relevant to the ensuing discussion will be considered here, and these only briefly and from the restricted point of view of the present work.

The nuclear shell model (or single particle model) is analogous to the structure of atoms. It results in the magic numbers:

$$N \text{ or } Z = 2,8,20,28,50,82,126,184 \qquad (1.33)$$

which dominate so many empirical data, and accounts for many of the observed properties of nuclei, if not

quantitatively, at least qualitatively. Altogether the ramifications of the model are extensive and attention will be directed here only to the topics of isomerism and quadrupole moments.

It was pointed out by Goldhaber and Hill (1952) that the occurrence of isomers could be related to the magic numbers. From the data available at that time it was apparent that long lived isomers ($T_{\frac{1}{2}} > 1$sec.) occurred in "islands of isomerism" which lay just below the magic numbers N = 50,82 and 126; Z = 50 and 82, and which stretched about halfway to the preceding magic numbers. The reason for this is that, according to the shell model, these regions are associated with high spin states and correspondingly large values for ΔI. At the same time it was pointed out by these authors that there were few isomers for odd Z above Z = 50 and it was recognised that this was probably the result of core effects. Thus in the region of the rare earths where even-even nuclei (the cores of odd-Z nuclei) are characterised by low lying excited states the absence of long lived isomers is due to a breakdown of the simple shell or one particle model.

This breakdown is apparent also in the more detailed classification of Goldhaber and Sunyar (1955). Fig. 1.3 shows that in the region of the rare earths E2 reduced

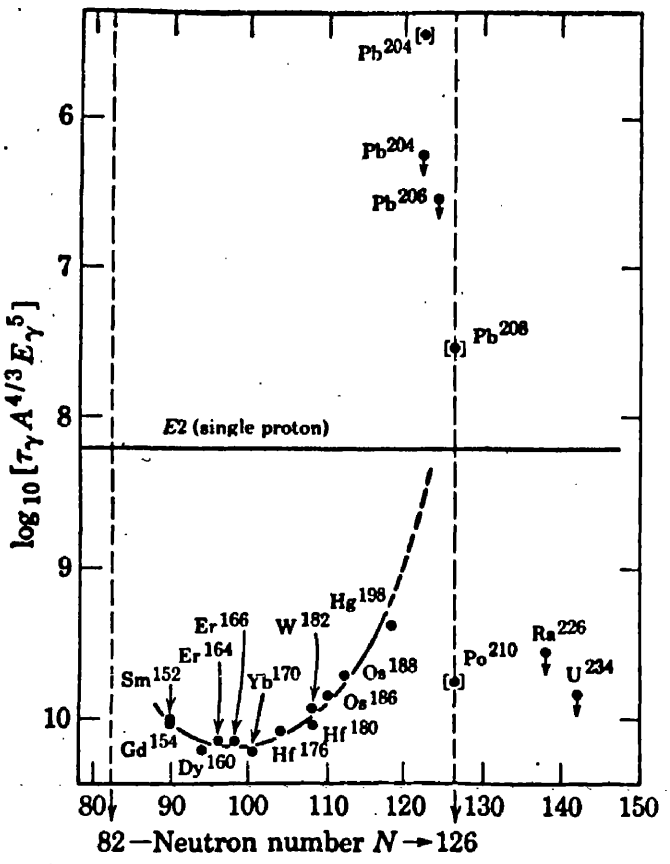

Fig. 1.10 Comparative lifetimes for $E2$ transitions in even-even nuclei against neutron number N. The points are plotted as $\log_{10}(\tau_\gamma A^{4/3} E_\gamma^5)$, where τ_γ is obtained from the half-lives by correcting for internal conversion. In this plot the theoretical single proton decay rate is a constant when $S(J_f J_i L)$ is put equal to unity. E_γ is measured in Mev and τ_γ in sec. All points except those marked [ ] are $2^+ \rightarrow 0^+$ transitions. The solid line through the points represents an average for the experimental data.

transition probabilities are generally greater than the single particle prediction by factors of up to 100. Moreover this enhancement can be seen to disappear as the magic number N = 126 is approached. This is especially true for even-even nuclei, as shown in fig.1.10 (Sunyar,1955).

Here then there is regular disagreement with the single particle model and it is clear that some systematic effect is present. The same systematic effect is also evident in other data, notably in quadrupole moments.

The shell model predicts qualitatively the variation of quadrupole moments with increasing N or Z. When a new shell begins to form the quadrupole moment is negative; as the number of protons, say, is increased Q becomes positive and increases in magnitude until the shell is about 2/3 full; Q then decreases to zero at the next magic proton number after which it again becomes negative. To this extent the shell model provides a valid description of quadrupole moments, but when the observed magnitudes are compared with the predictions of the model the latter are found to be much too small in many cases, e.g. Ta^{181}. Also there are many nuclei with only odd neutrons outside the closed shell core. According to the single particle model such nuclei should have little or no quadrupole moment, yet O^{17}, for instance, with one odd neutron has a

quadrupole moment just as large as would be expected for a single proton.

The first proposal for dealing with these anomalies was made by Rainwater (1950). He showed that greater stability and larger quadrupole moments would be produced in a spheroidal nucleus. This was taken up by Bohr (1952) who developed a "quasi-molecular" model to deal with the vibrations and rotations of a deformable nucleus. The theory was extensively developed and applied to numerous nuclei by Bohr and Mottelson (1953). Since then this unified model which embraces both collective and individual-particle aspects of nuclear structure has proved extremely fruitful and has been the subject of many investigations, including most of those reported herein. Accordingly some simple aspects of the theory and some of the results will now be considered.

(b) Collective effects in nuclei.

First of all there are collective effects which occur in spherical nuclei and which are relevant to the discussion of Ce^{140}, Ba^{138} and Sn^{120}. These take the form of harmonic oscillations of the nuclear surface, like those of an incompressible liquid drop — hence the name hydrodynamical model. The nuclear surface may be expressed as:

$$R(\theta,\phi) = R_0\left[1 + \sum_{\lambda\mu} \alpha_{\lambda\mu} Y_{\lambda\mu}(\theta,\phi)\right] \qquad (1.34)$$

where R_0 is the equilibrium radius, $Y_{\lambda\mu}$ is the normalised spherical harmonic of order $\lambda\mu$ and the amplitudes $\alpha\lambda\mu$ are are the normal coordinates of the oscillating system. Thus the normal modes of oscillation are multipoles with eigenfunctions $Y_{\lambda\mu}$ which are the same as the eigenfunctions of total angular momentum λ, with $(2\lambda + 1)$ degeneracy. The value $\lambda = 1$ corresponds to an oscillating dipole, i.e. a translation of the whole system, which cannot occur. Hence the lowest order of oscillation to be expected is the quadrupole oscillation with $\lambda = 2$.

By a straightforward application of classical mechanics the energy can be written as:

$$H = \sum_{\lambda\mu} \left\{ \tfrac{1}{2} B_\lambda |\dot{\alpha}_{\lambda\mu}|^2 + \tfrac{1}{2} C_\lambda |\alpha_{\lambda\mu}|^2 \right\} \qquad (1.35)$$

which represents a set of harmonic oscillators with frequencies

$$\omega_\lambda = \sqrt{\frac{C_\lambda}{B_\lambda}} \qquad (1.36)$$

Here B_λ and C_λ are constants which, by hydrodynamical analogy, can be determined roughly for nuclei. The quadrupole oscillations (and it is only there that are of importance) will be characterised by excited states with

energies $\hbar\omega_\lambda$, $2\hbar\omega_\lambda$, $3\hbar\omega_\lambda$ etc. The first excited state resulting from one excitation quantum or boson will have angular momentum 2, the second one consisting of two bosons will have J = 0, 2, 4(only symmetric combinations of bosons are allowed), the third one J = 0, 2, 3, 4, 6, and all the states will have even parity.

On the basis of this model energies, moments and transition probabilities can be calculated. Paradoxically the quadrupole moments should be vanishingly small while the transition probabilities for $\hbar\omega_\lambda \longrightarrow 0$ should be considerably larger than the Weisskopf estimate. Transitions from the second 2+ state ⟶ ground state should be forbidden and cascades rather than cross over transitions are thus to be expected. The excitation energies are generally high and particle states are usually excited before an energy of $2\hbar\omega_\lambda$ is reached. In practise therefore the model is generally restricted in its usefulness to the first excited state.

Antithetical in some respects to the foregoing is the case of deformed nuclei. Spheroidal deformation can result from strong coupling between the core and a few odd nucleons (e.g. the case of O^{17} referred to already) or it can arise quite simply by particle alignment when a shell is being filled up (e.g. among the rare earths).

Thus a nucleus with several particles outside a closed shell can be thought of as an oblate spheroid. As in the case of spherical nuclei classical mechanics proves useful in dealing with this situation.

For a rotating rigid body the energy is given by

$$E_{rot} = \sum_{i=1}^{3} \frac{R_i^2}{2\mathcal{I}_i} \qquad (1.37)$$

where R_i is the angular momentum about the ith axis and $\mathcal{I}_i$ is the corresponding moment of inertia. If the rigid body has axial symmetry orientations about this axis, 3 say, are indistinguishable and hence for a nucleus $R_3 = 0$. Also $\mathcal{I}_1 = \mathcal{I}_2 = \mathcal{I}$ say. Then:

$$E_{rot} = \frac{1}{2\mathcal{I}} (\underline{R})^2 \qquad (1.38)$$

and in quantum mechanics this becomes:

$$E_{rot} = \frac{\hbar^2}{2\mathcal{I}} J(J+1) \qquad (1.39)$$

where J is the rotational angular momentum.

This result is valid for a nucleus with zero intrinsic angular momentum. Due to the symmetry of the spheroidal nucleus on reflection through a central plane perpendicular to the symmetry axis only even values of J can occur in the rotational excitations. Moreover the excited states must have the same parity as the intrinsic ground state. Hence the excited states are:

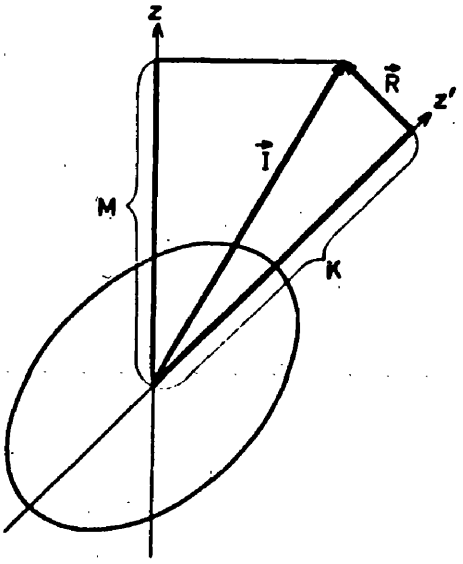

FIG.1.11 *Angular momentum coupling scheme for deformed nuclei.* The total angular momentum, I, has the component M along the fixed z-axis and the component K along the nuclear symmetry axis, z'. The collective rotational angular momentum, R, is perpendicular to the nuclear symmetry axis; thus, K is entirely a property of the intrinsic motion.

$$(J\pi) = 0+,\ 2+,\ 4+,\ 6+,\ 8+ \text{ etc.} \qquad (1.40)$$

with $E_{rot} = 0,\ 6,\ 20,\ 42,\ 72$ etc. times $\frac{\hbar^2}{2\mathcal{I}}$ (1.41)

i.e. $E_{rot} = 0,\ 1,\ 3.33,\ 7,\ 12$, etc. times

E_{rot} for $J = 2$. (1.42)

As an illustration Hf^{180} has spin 0 and $J = 2,4,6,8$ for the first four excited states. The energy of the first excited state is 93 keV, that of the second is 3.3 x 93 keV, that of the third 6.9 x 93 keV and that of the fourth 11.7 x 93 keV. The above simple approach is therefore quite sound.

In general the intrinsic angular momentum of the nucleus is not zero. Its wave function can however be expressed in terms of the rotation operator $D(\alpha\beta\gamma)$ (see Edmonds 1957) which refers to rotations through the three Eulerian angles α, β and γ. The eigenfunctions of this operator $\mathcal{D}^{J}_{MK}(\alpha\beta\gamma)$ are those of a symmetric top with total angular momentum $\sqrt{J(J+1)}\,\hbar$, projection $M\hbar$ on the z-axis and projection $K\hbar$ on the "intrinsic" z-axis, i.e. on the axis of symmetry in the rotating frame.

In the nuclear case, as has been seen, the rotational angular momentum $\underline{R}$ must be perpendicular to the symmetry axis. Hence fig. 1.11 is obtained, in which $\underline{K}$ represents the contribution of the intrinsic angular momentum to the total angular momentum. Thus there will be a rotational band of levels corresponding to $K = 0$ and others

corresponding to $K \neq 0$. The total wave function of the nucleus can be written:

$$\psi = \sqrt{\frac{2I+1}{8\pi^2}}\, \phi_{\tau K}\, \mathcal{D}^{I}_{MK}(\alpha\beta\gamma) \qquad (1.43)$$

where ϕ represents the intrinsic structure characterised by K and additional quantum numbers τ. By an extension of the simple argument given above the following results for $K \neq 0$ are obtained:

$$\begin{aligned} &\text{excited state spins} = K,\ K+1,\ K+2 \\ &\quad \text{parity same as for } \phi_{\tau K} \end{aligned} \qquad (1.44)$$

and the energies of the excited states are:

$$E_J = E_K + \frac{\hbar^2}{2\mathcal{I}}\left\{J(J+1) + a(-1)^{I+\frac{1}{2}}(J+\tfrac{1}{2})\,\delta_{K\frac{1}{2}}\right\} \qquad (1.45)$$

In view of eq. (1.43) any nuclear parameter or process can be thought of as having two aspects, a rotational and an intrinsic aspect. The rotational aspect can be dealt with explicitly since the $\mathcal{D}^{I}_{MK}$ are known. This means that:

a) States having a common $\phi_{\tau K}$ (i.e. states in same rotational band) can be precisely compared.

b) Transitions for which $\langle \phi_{\tau K} | \phi_{\tau' K'} \rangle$ is the same can be precisely compared. (This includes transitions within a rotational band).

Applying point a) to the matter of quadrupole moments, the intrinsic state $\phi_{\tau K}$ will have an intrinsic quadrupole moment Q_o. Due to the rotation of the nucleus the quadrupole moment observed in the laboratory is less than Q_o. Essentially there is a smearing out of the nuclear shape so that the faster the rotation the more spherical is the appearance of the nucleus (see fig. 1.11). The result is that

$$Q = \frac{3K^2 - J(J+1)}{(2J+3)(J+1)} Q_o \qquad (1.46)$$

According to eq. (1.46) $Q < Q_o$ even for the ground state. This is because of the zero point rotation.

Thus in the case of Ta^{181} the ground state has $K = J = 7/2$ (Mottelson and Nilsson 1959). From the hyperfine structure of spectral lines Q has been determined as 2.7×10^{-24} cm^2 (Murakawa and Kamei 1957) implying that $Q_o = 5.8 \times 10^{-24}$ cm^2. On the other hand Q_o has been derived (Huus et al. 1956) from Coulomb excitation to be 7×10^{-24} cm^2. If Q could be obtained for an excited state eq.(1.46) could be checked and the different results compared. The details of this will be considered in chapter 7.

Applying point b) to transition probabilities the relative probabilities for transitions in the same

rotational band can be calculated. Applying the results of Bohr and Mottelson (1953) to the case of K = 0 the following ratio is obtained:

$$\frac{B_e\ (2) \quad (J = 4 \longrightarrow J = 2)}{B_e\ (2) \quad (J = 2 \longrightarrow J = 0)} = \frac{10}{7} \qquad (1.47)$$

This result will be referred to in chapter 4.

Whenever $\Delta K > L$ the change in the intrinsic wave function gives rise to K-forbiddenness (Alaga et al. 1955); i.e. the transitions are inhibited. The number $\nu = \Delta K - L$ is the degree of forbiddenness, and its effect on transition probabilities will be referred to in chapter 4.

A more complete treatment of the intrinsic states can be given in terms of the so called Nilsson asymptotic quantum numbers (Nilsson 1955, Mottelson and Nilsson 1959). On the basis of changes in these three numbers and in ΔK transitions can be classified as hindered or unhindered. For instance the 480 keV M1 transition in Ta^{181} is hindered according to the asymptotic selection rules. The measured hindrance factor is $\sim 3 \times 10^6$. The transition is therefore 97% E2 since the hindrance factor for the latter is only ~ 30.

It is apparent from all that has just been said that the extreme single particle description of γ-ray emission

has to be greatly modified when applied to nuclei in which collective effects are dominant. The case of rotational collective effects is, strictly speaking, only relevant to the experimental work described in chapter 7, but it has been discussed in some detail here because these effects have been the subject of much theoretical and experimental study and are now well understood. To some extent therefore they serve as a qualitative guide to the phenomena encountered in spherical nuclei and in nuclei of the intermediate region where neither the hydrodynamical nor the rotational model is applicable and in which the single particle model is quite inadequate. Hence, lacking a neat theory to apply to the results for Ce^{140}, Ba^{138}, Sn^{120}, the author was forced to make crude comparisons with examples taken from the theory of rotational states. In this way the measured lifetimes were found to be qualitatively acceptable although nothing positive or precise could be done to compare them with theory.

CHAPTER 2

THE DELAYED COINCIDENCE METHOD* AND ITS LIMITATIONS

(2.1) Fast Coincidence Techniques and Time-to-Pulse Height Conversion.

(a) Fast coincidence circuits.

The techniques of delayed coincidence counting and time-to-pulse height conversion were developed for use with scintillation counters. The latter respond rapidly to ionising radiations and produce pulses with exceedingly f fast rising edges and with falling edges that can also be much faster than anything produced by a Geiger counter. Thus the scintillation counter is the obvious choice of detector for resolving the small time intervals between closely consecutive radiations such as occur in the decay of short lived excited states of nuclei.

A coincidence circuit is one which accepts at two or more input points pulses of width T' say, and which gives an output pulse when these overlap. Ideally therefore the circuit should give an output whenever the centres of two pulses occur within T' seconds of one another; otherwise it should give no output. In practise the input pulses

---

* Following general practise this expression is here used to mean time-to-pulse height conversion as well as the original technique of delayed coincidence counting.

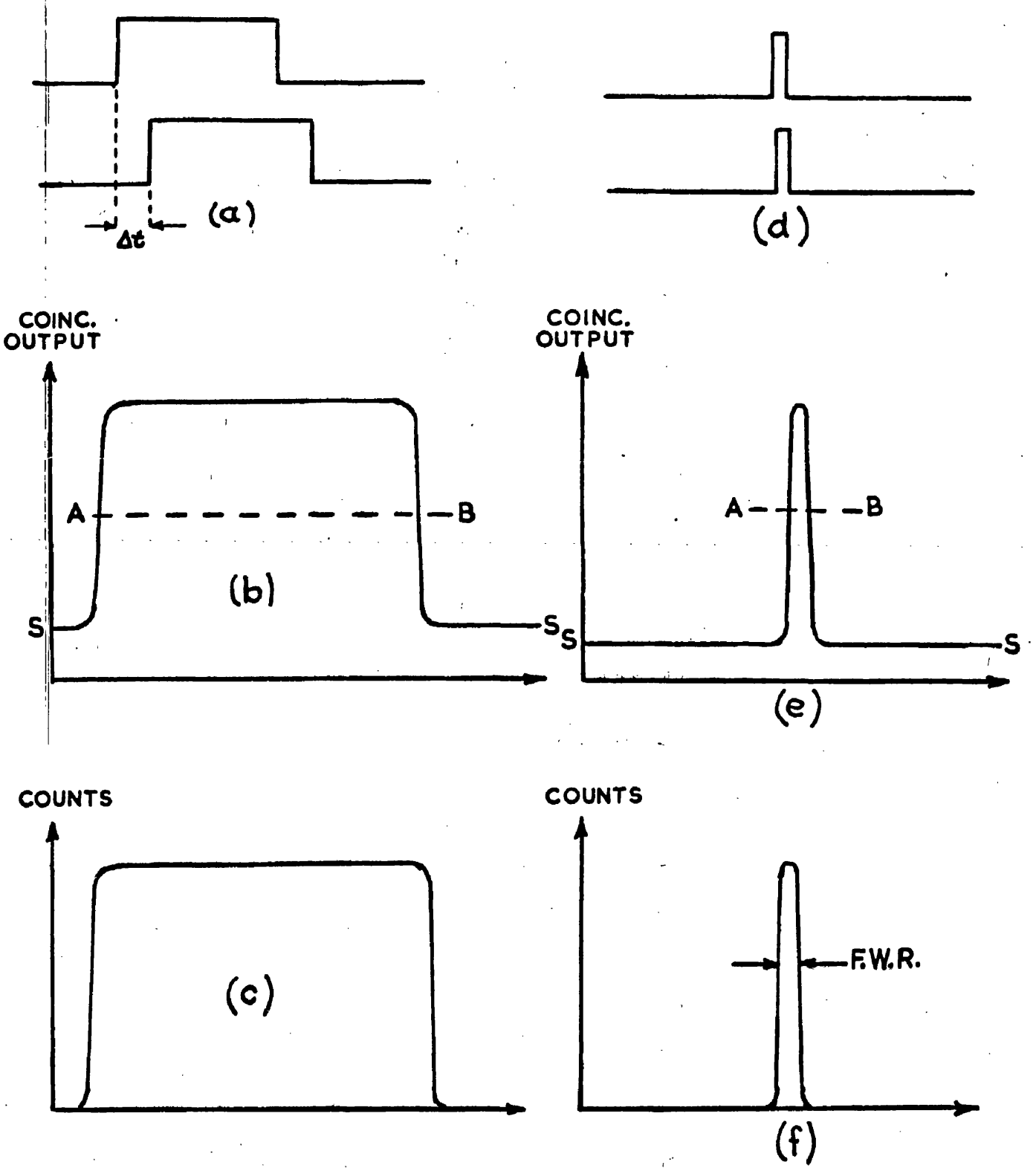

FIG. 2.1

Illustrating what is meant by "resolving time". (a,b,c) for long pulses, (d,e,f) for short pulses. F.W.R. = full width resolution.

are never perfect step functions and the circuits are in any case always limited in response so that as the time interval between the centres of the input pulses varies the coincidence output varies also in a continuous way. Moreover coincidence circuits always give some kind of output for just a single pulse.

Fig. 2.1 illustrates the performance of a coincidence circuit both for long pulses (fig. 2.1a) and for short pulses (fig. 2.1d). If the input pulse length is T' the resolving time is given by

$$T = \frac{N_c}{2N_1N_2} \qquad (2.1)$$

where N_1 and N_2 are the input pulse rates and N_c is the number of chance coincidences counted above the discriminator level AB. When the rise time of the coincidence output pulse, T_R, is much less than T', then $T' \approx T$.

The resolving time can also be obtained by plotting the coincidence counting rate as a function of Δt the time interval between the pulses (fig. 2.1c,f). The width at half height of this curve is called the full width resolution, hereafter referred to as the FWR. The FWR = 2T. When $T' \approx T_R$ the best resolution can be obtained. If the level AB (fig. 2.1e) is varied the

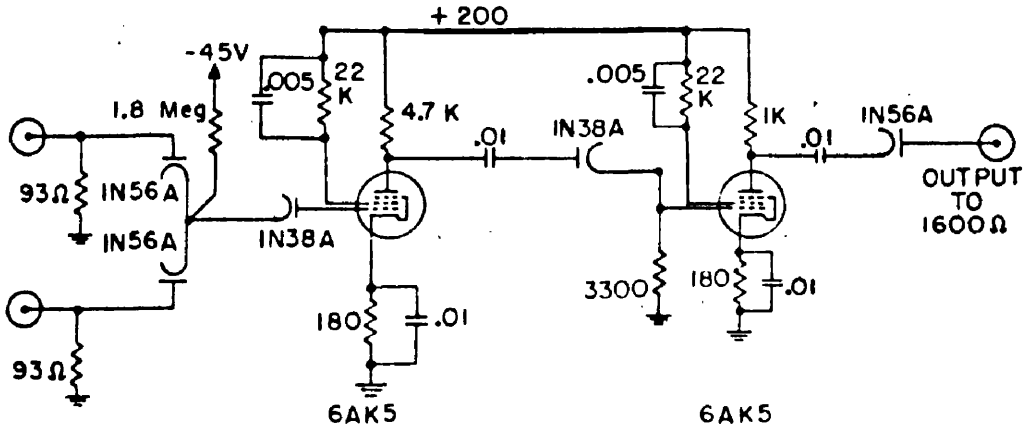

FIGURE 2.2a *High-resolution coincidence circuit for negative pulses from the anodes of two photomultiplier tubes.*

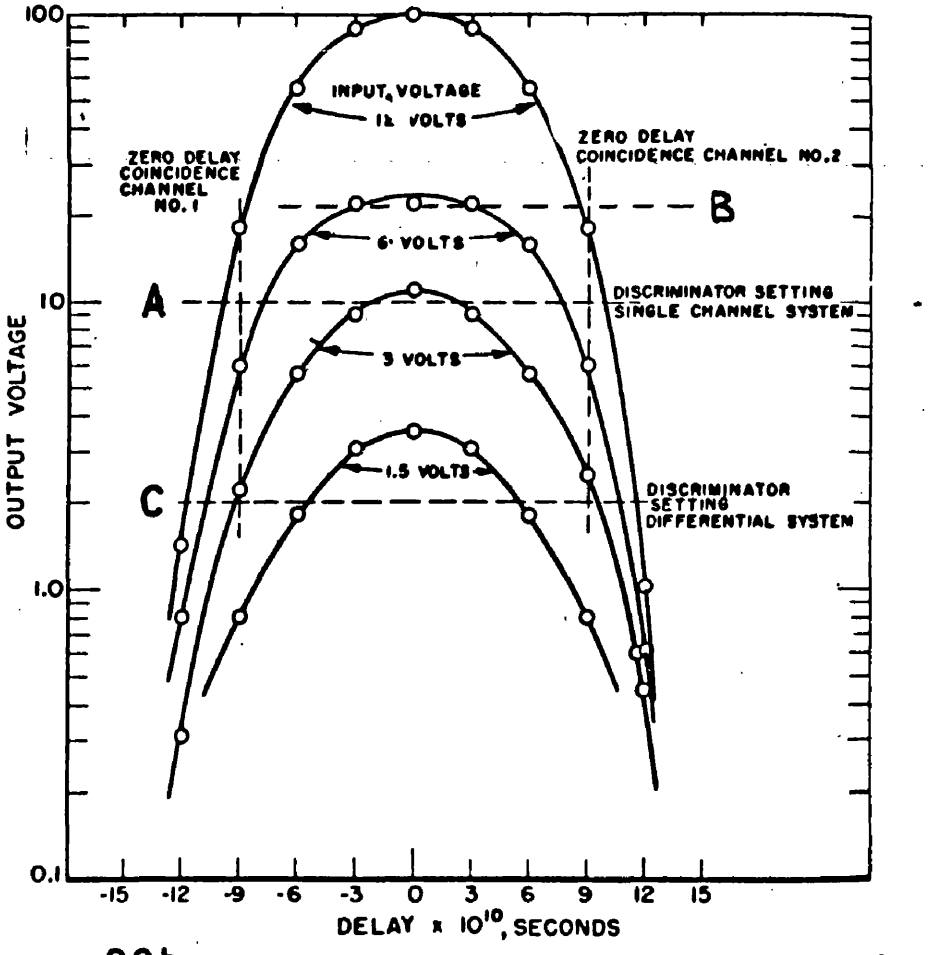

FIGURE 2.2b *Response of the coincidence circuit of figure 1 and associated amplifier as a function of the time separation of a pair of equal amplitude pulses from the mercury-relay pulse generator.*

The dashed lines refer to operation of the circuit as part of a differential coincidence system (see text).

resolution curve (fig. 2.1f) will vary and the minimum FWR will be obtained when the level AB is set high enough to eliminate the flat top on the resolution curve.

Fig. 2.2a shows a diode coincidence circuit used by Minton (1956) and fig. 2.2b shows the characteristics of this circuit when handling fast pulses from a mercury switch. With input pulses of 6 volts and the discriminator set at A the FWR will be $\sim 1.5 \times 10^{-9}$ sec. If the discriminator setting is raised to B the FWR should in principle be $\sim 5 \times 10^{-10}$ sec. However this is not a very satisfactory mode of operation since the characteristic varies so slowly at this level. Thus, this circuit could not be used reliably with less than $\sim 10^{-9}$ sec. for the FWR.

A method for improving the resolving time of such circuits was proposed by Bay (1951) and was in fact adopted by Minton. This is the method of differential coincidence counting in which only the rising and falling edges of the pulses are utilised. Two circuits like those of fig. 2.2a are used, each biased at the level C in fig. 2.2b. But in this case (fig. 2.6a) artificial delays are included in the circuitry so that coincident pulses do not overlap fully in the two circuits. Instead the zeros occur as shown in fig. 2.2b, with the result that just as the pulses come into coincidence in the second unit

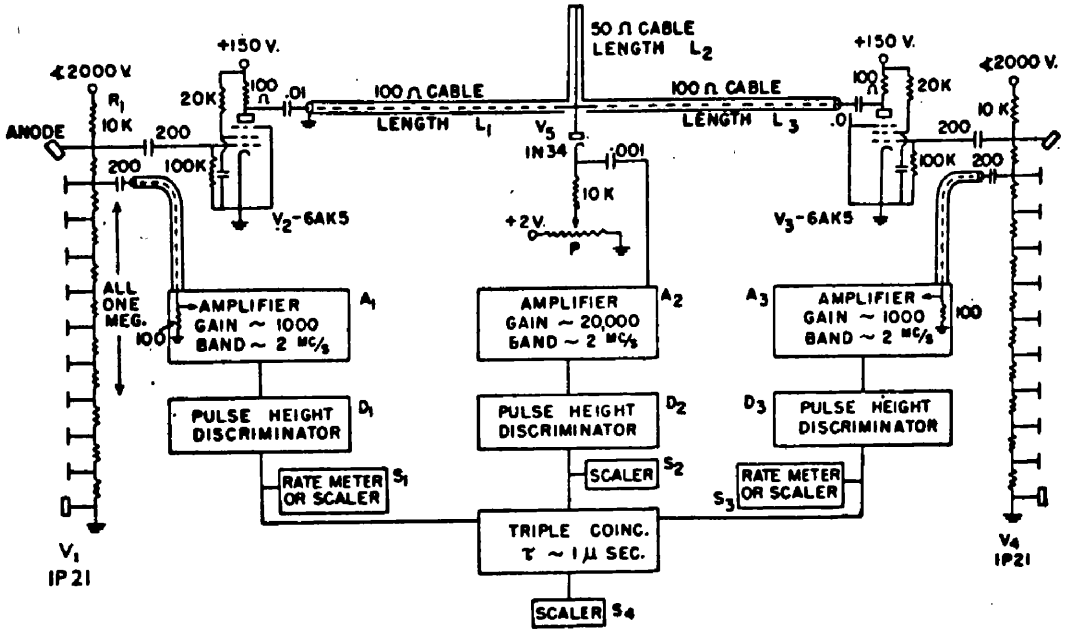

FIG. 2.3a Diagram of a coincidence circuit capable of resolving times near 10^{-9} seconds, after Bell et al. 1952.

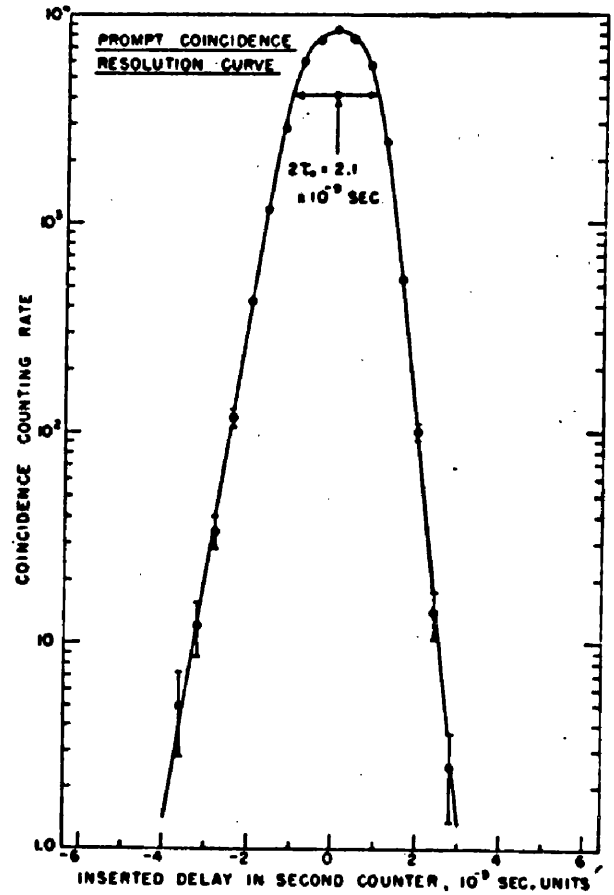

FIG. 2.3b Prompt coincidence resolution curve observed in testing the coincidence circuit of Fig. 5. The observed coincidences were produced by passing hard beta-rays through the thin stilbene crystal of the first counter into the stilbene crystal of the second counter.

they start to go out of coincidence in the first unit. The outputs from the two units are combined in a slow coincidence unit whose efficiency (i.e. bias) can also be varied. By this means Hinton was able to achieve an electronic FWH of 2.8×10^{-10} sec.

(b) Measurements with fast coincidence systems.

By "fast coincidence system" is meant the complete arrangement of scintillators, photomultipliers and electronics. In such a system the pulses being fed to the coincidence device are taken from the output (usually the anode) of the photomultiplier, they are generally passed through a non-linear limiting valve to standardise their heights, and their length is also fixed by a length of shorted delay line, normally referred to as a clipping line. Ideally therefore the pulses ought to be square. The apparatus also includes independent auxiliary equipment (side channels) which permit the selection of a limited energy range in either detector. These side channels are comparatively slow and so the complete arrangement (see fig. 2.3a) is called a fast-slow system.

If such a system is used to detect prompt radiations, i.e. two simultaneous or nearly simultaneous events such as annihilation quanta, and if artificial

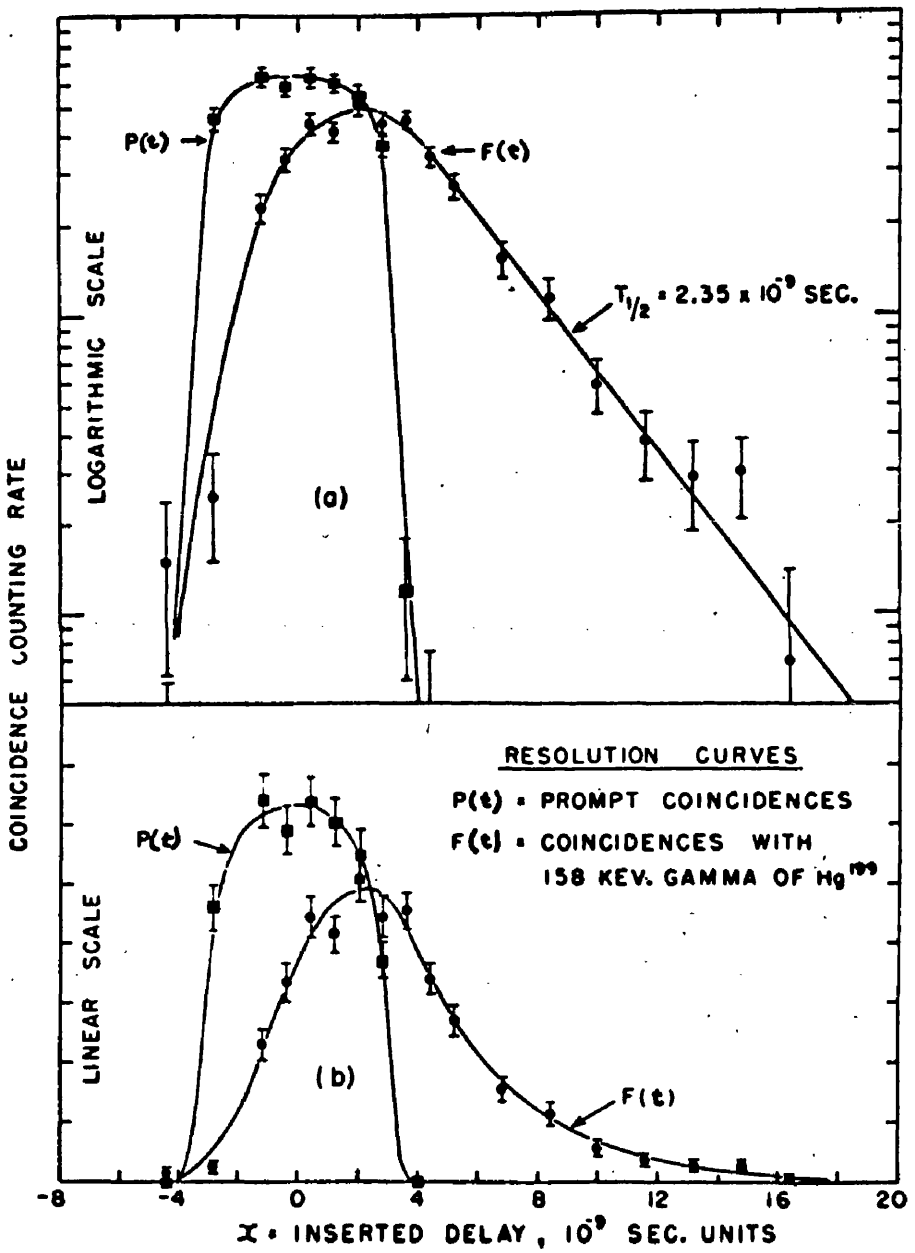

Fig 24 *P(t)* prompt and *F(t)* delayed coincidence resolution curve for a radiation of Hg^{199} having a half life of 2.35×10^{-9} seconds. Diagram (*a*) logarithmic scale, diagram (*b*) linear scale. Chance coincidences have been subtracted.

delays are introduced and Δt varied while the coincidence counting rate is observed a curve like that of fig. 2.3b is obtained (Bell et al. 1952). In this case the FWR arises not only from the electronics but also from time fluctuations in the scintillators and multipliers.

It is essentially this FWR which determines the lower limit to time measurement with this kind of apparatus. When the time distribution under study is much more dispersed than the prompt resolution curve the measurements are relatively easy.

For instance in the measurement of an isomeric lifetime with mean life τ the procedure is as illustrated in fig. 2.4 (Bell et al. 1952). P(t) is the prompt resolution curve and F(t) the delayed resolution curve. If the decay of the state in question is given by $f(t) \propto e^{-t/\tau}$ then:

$$F(t) = \int_{-\infty}^{\infty} f(x) \left[P(t-x)dx \right] \qquad (2.2)$$

from which it follows that:

$$\frac{d\,F(t)}{dt} = \frac{1}{\tau} \left[P(t) - F(t) \right] \qquad (2.3)$$

$$\frac{d}{dt} \log F(t) = -\frac{1}{\tau} \left[1 - \frac{P(t)}{F(t)} \right] \qquad (2.4)$$

$$\tau = \text{centroid } F(t) - \text{centroid } P(t) \qquad (2.5)$$

Equation (2.3) shows that the maximum of F(t) should occur at its intersection with P(t) ; (2.4) indicates that when $P(t) \ll F(t)$ the lifetime may be obtained from the slope of the curve F(t); and (2.5) reveals that even when this condition does not obtain the lifetime is given by the difference in the centroids of the two curves. This last equation applies therefore to lifetimes which are less than the resolving time of the apparatus and provides the basis for the centroid shift method of lifetime measurement.

When the lifetime is determined from the slope of F(t) the prompt curve P(t) is not really necessary. However in the basic centroid shift method both curves are necessary to determine τ. P(t) is obtained with a source of prompt radiations and F(t) is obtained with the source containing the delayed level. Sometimes a method called the self comparison method is used. In this F(t) is recorded with the first radiation detected in counter 1 say, and the second in counter 2. A second "inverse" curve F'(t) is then obtained with the order of the radiations reversed. The centroid shift from F(t) to F'(t) is then twice the mean life of the delayed level.

A recent method developed by Weaver and Bell (1960) involves the calculation of the third moment of the curve F(t) and makes possible a slight improvement on the centroid shift method. This is essentially an

improvement in analysis, not in techniques. The latter have also been refined however. Simms et al. (1961) have measured lifetimes by a method which allows both the prompt and the delayed peaks P(t) and F(t) to be recorded simultaneously. The method can be applied to only a few decay schemes, but since errors due to instability, drifting etc. are greatly reduced the method yields an accuracy of 5×10^{-12} sec.

(c) Time-to-pulse height conversion.

In 1952 Marshall used a special gated-beam tube, the 6BN6, in a fast coincidence circuit and obtained a resolving time of better than 3×10^{-10} sec. with pulses from a mercury switch. This valve has two control grids. These can be biased in such a way that the valve passes negligible current in the quiescent state and very little current when a signal is applied to one grid only. But when coincident signals are applied to both grids there is a large flow of current through the valve producing a prominent signal at its anode (see fig. 3.1b).

Neilson and James (1955) used this valve in a development which has in the intervening years altogether superseded the earlier type of delayed coincidence circuitry. Instead of applying very short pulses these

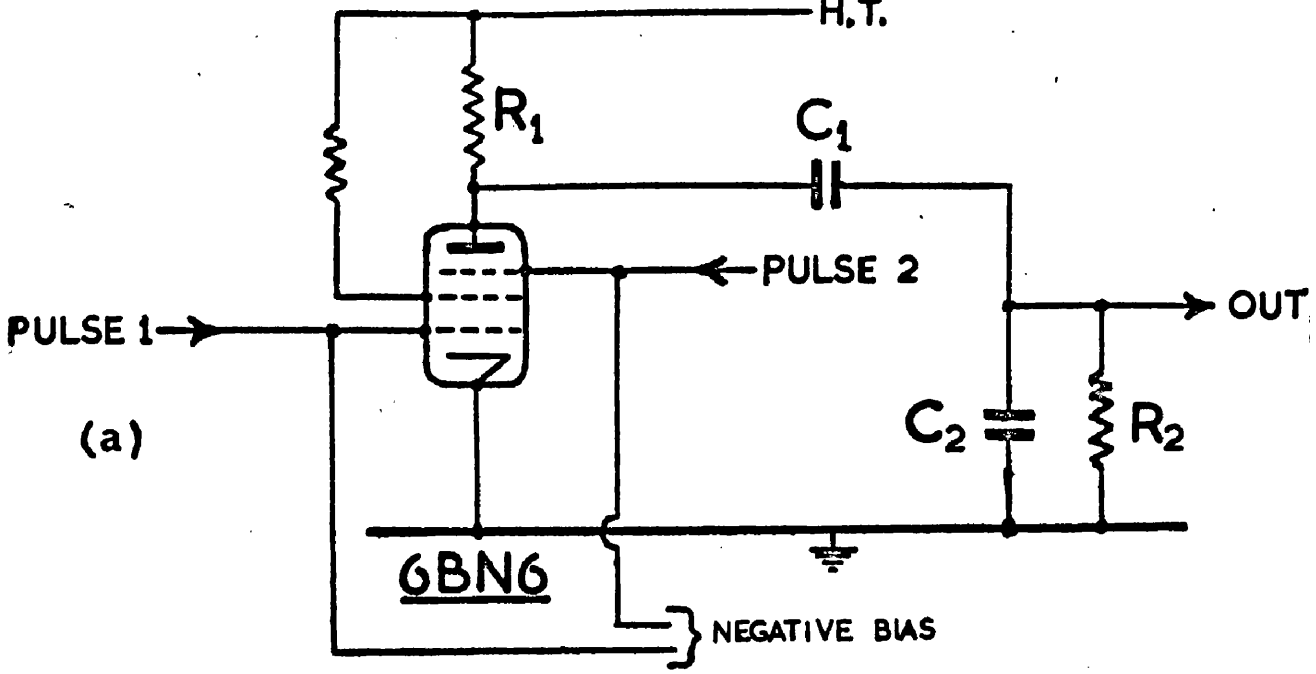

time-to-pulse height converter

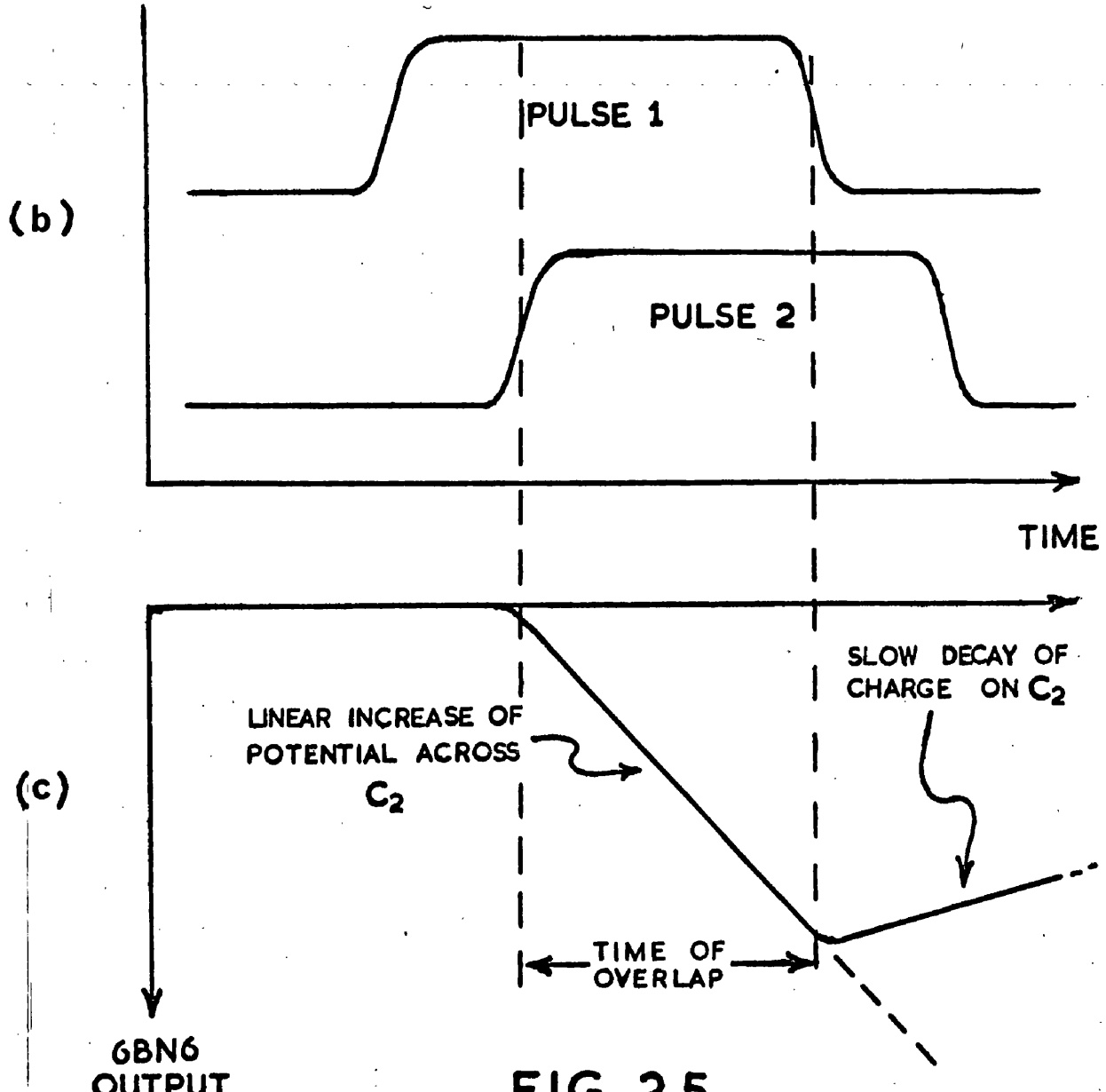

FIG. 2.5

performance of time-to-height converter.

workers used a relatively long clipping line to produce pulses of ~40 nsec. length. These are shown in fig. 2.5b. The pulses are applied to the 6BN6 in the manner shown in fig. 2.5a. During the period of overlap, 20 nsec. say, the 6BN6 valve passes (in the author's apparatus) ~0.1 mA of current; this current is fed through a coupling condenser C_1 to C_2 where it is integrated to produce a potential as shown in fig. 2.5c. Since $RC_2 \gg 20$ nsec., where $R = R_1R_2/(R_1 + R_2)$, the voltage developed across C_2 is proportional to the period of overlap of the original pulses. Thus a time interval has been converted to a pulse height and the circuit is called a time-to-pulse height or time-to-amplitude converter. Green and Bell (1958) improved the circuit and made it possible to distinguish the order in which the pulses arrive at the 6BN6, thus cutting down the chance coincidence rate.

The beauty of the time-to-height converter is that information over almost any desired time range is obtained continuously provided that facilities are available for analysing the pulse heights. Hence information about a time distribution can be obtained much more rapidly than by delayed coincidence counting (in the strict sense), also long term instabilities are rendered less troublesome and

the statistics are greatly improved.

The resolving time in a time-to-height converter is obtained by exposing the detectors to prompt radiations so that output pulses of nearly constant amplitude are produced. These are fed to a multichannel pulse height analyser (kicksorter) and will appear on this as a Gaussian distribution. If the correspondence between pulse height or channel number and Δt is known the FWH is obtained directly from the curve on the kicksorter. Curves obtained by this method are similar to those shown in figures 2.3b and 2.4 and are analysed in exactly the same way.

(d) Limitations of the method.

From the foregoing paragraphs it is clear that isomeric lifetimes can be most easily and most reliably determined when $\tau \gtrsim T$(the FWH = 2T). It is therefore very desirable that the resolving time of a delayed coincidence system should be as small as possible, and any improvements in detectors, in circuits, in methods or in understanding which makes possible a reduction of the FWH is to be welcomed. It is essential therefore that the factors determining the FWH be understood quantitatively so that the proper steps can be taken to minimise their effects.

During the past ten years there have been several investigations of the theory of time resolution in scintillation counter systems and in the next section it will be shown that while the early studies were not quite correct a stage has now been reached where the various limiting factors are fairly well understood. Along with this theoretical development there have also been numerous qualitative comparisons of theory and experiment and two or three specific experimental studies of performance; but there has not been any thorough quantitative experimental check of the latest theoretical analysis and no convincing demonstration of its validity.

This gap was filled by the results to be given in chapter 3, obtained by the author and published in collaboration with R.E. Azuma and G.M. Lewis in "Nuclear Instruments and Methods". The measurements are also of value in another very practical way. When a very short lifetime ($< T$) is being measured the centroid shift method is used. Now, as will be seen in the next section and chapter, the position of the centroid of a resolution curve depends not just on the nature of the radiation source but on various instrumental effects, in particular on the energy liberated in the scintillator. This means that unless the energy selection during the production of the curve $F(t)$ corresponds exactly to that used in obtaining

P(t) or P'(t) there will be systematic instrumental effects which could seriously affect the outcome of the measurement. There has been only one investigation (Bashandy 1960) of this effect, known as instrumental time delay, and in that case the results were interpreted with the wrong equations. The results in chapter 3 have therefore provided long overdue corroboration of the correct equations while at the same time demonstrating how serious these time delays are and how they can be assessed in a given application.

(2.2) Development of the Theory of Time Resolution.

(a) The early treatment of Post and Schiff.

Soon after the development of the scintillation counter and its application to the measurement of very short lifetimes it was realised that the factors governing the resolving time must be clearly understood, even if only to allow the improvement of scintillators multipliers and techniques. The first theoretical analysis of fast coincidence performance was by Post and Schiff (1950). They made two important assumptions:-

1) It was assumed that the photomultiplier acts as a perfect amplifier multiplying the primary photoelectrons with precise gain and without time spread.

2) It was assumed that the fast coincidence circuit acts as a perfect discriminator giving a signal when the photomultiplier has accumulated a definite number Q of photoelectrons.

These assumptions are important because it is only their incorrectness in practise which makes the Post-Schiff treatment inadequate, and it has been their unwarranted acceptance which has led some investigators to draw the wrong conclusions in assessing performance.

The treatment of Post and Schiff was therefore concerned entirely with the scintillator and the statistics thereof. The analysis was rigorous and general and capable of application to any intensity function for the scintillator output, but the basic relevant feature of the process in so far as it concerns real scintillators can be understood quite simply.

Suppose that a scintillation event results in the release of R photoelectrons from the photocathode of the multiplier and that their emission follows the law of exponential decay. Then the number of photoelectrons released after a time t is:

$$n(t) = R(1 - e^{-t/\tau}) \qquad (2.6)$$

where $\tau (= 1/\lambda)$ is the decay time of the scintillator.

The rate of emission of photoelectrons will be

$$\frac{dn}{dt} = \frac{R}{\tau} e^{-t/\tau} \qquad (2.7)$$

and for short times such that

$$t << \tau \qquad (2.8)$$

eq. (2.7) can be approximated by

$$\frac{dn}{dt} = \frac{R}{\tau} \qquad (2.9)$$

It follows that the mean time elapsing before the emission of Q photoelectrons is given by

$$Q = \frac{R}{\tau} \quad t_Q$$

$$\text{i.e.} \quad t_Q = Q \frac{\tau}{R} \qquad (2.10)$$

Thus the ideal coincidence circuit will register the event after a mean time t_Q, given approximately by eq.(2.10). This time delay depends on R, the energy essentially , and will be large for small R.

It is now necessary to consider the fluctuations in t_Q. In this time an average of Q photoelectrons are emitted. The error on Q is approximately $\sqrt{Q}$ so that fluctuations in the number of photoelectrons emitted in time t_Q is $\sqrt{Q}$. Crudely, therefore, the fluctuations in the

time t_Q will be the time required to collect $\sqrt{Q}$ photoelectrons. Hence the variance on t_Q is given roughly by

$$\sigma^2 = Q\left(\frac{\tau}{R}\right)^2 \qquad (2.11)$$

Equations (2.10) and (2.11) are in fact perfectly correct to first order which is all that is required in many cases. By their more rigorous methods Post and Schiff obtained, to second order:

$$t_Q = Q\left(\frac{\tau}{R}\right)\left\{ 1 + \frac{(Q+1)}{2R} + \text{----} \right\} \qquad (2.12)$$

$$\sigma^2 = Q\left(\frac{\tau}{R}\right)^2\left\{ 1 + \frac{2(Q+1)}{R} + \text{----} \right\} \qquad (2.13)$$

and, eliminating τ,

$$\sigma^2 = \frac{1}{Q}\, t_Q^{\,2}\left(1 + \frac{Q+1}{R} + \text{----} \right) \qquad (2.14)$$

Equations (2.11) and (2.13) indicate that the best phosphor will be the one for which (τ/R) is least, that is to say the light output should be high and the decay time short. The ratio of the efficiency to the decay time is therefore generally used as a figure of merit for scintillation materials.

Following the paper by Post and Schiff attention was directed to the effect of imperfections in the multiplier.

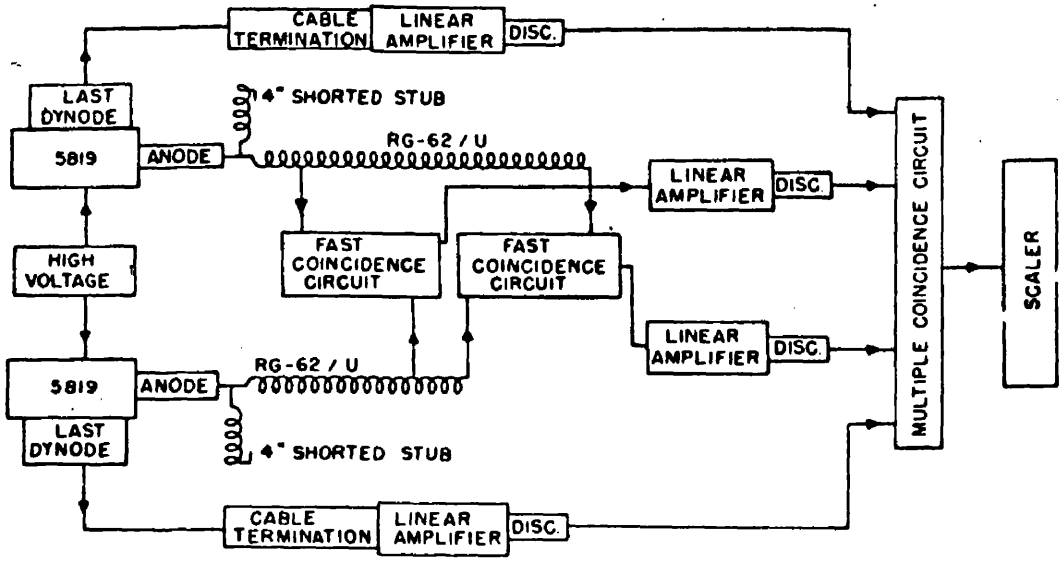

FIGURE 2.6a *Block diagram of the differential coincidence system with gating pulse height selectors.*

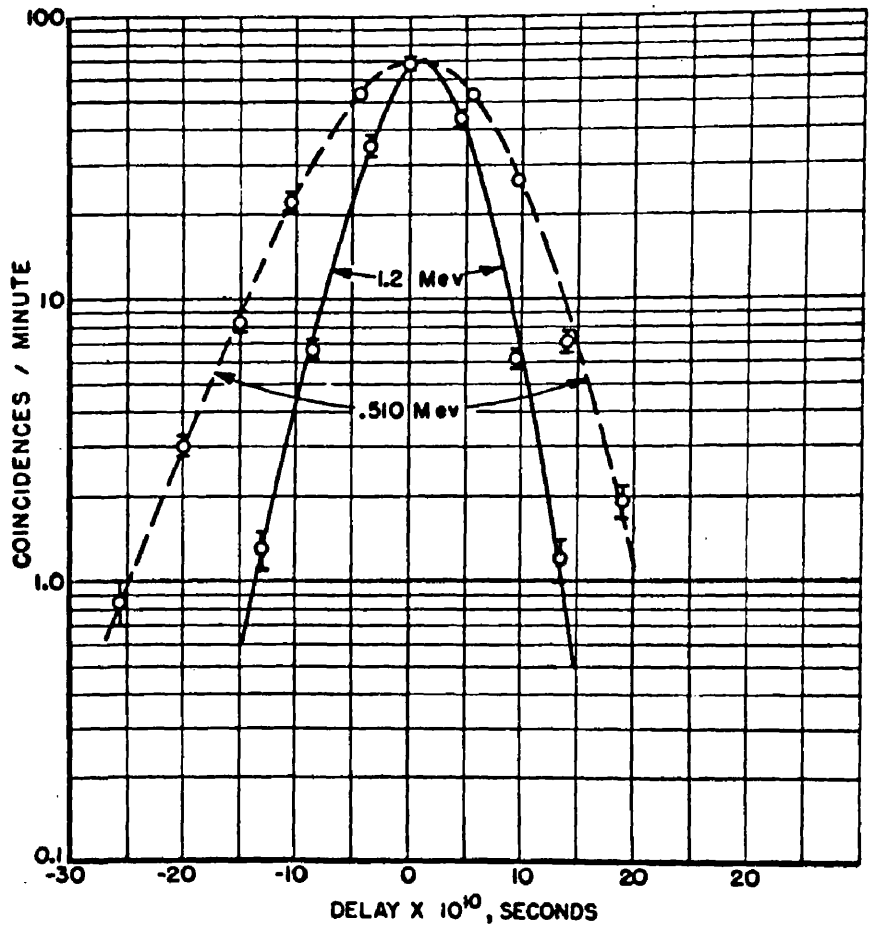

FIGURE 2.6b *Effect on the response of the differential coincidence system of fig. 2.6a produced by a variation in the number of photons emitted by the phosphor.*

5819 photomultipliers and stilbene crystals were used.

At a symposium (Symposium 1952) on scintillation counting Horton pointed out that the variance due to transit time spread would be given by

$$\sigma_M^2 = \frac{\beta^2}{Q} \qquad (2.15)$$

where β is the r.m.s. time spread per stage of the multiplier and the subscript M has been used to indicate "multiplier". On this basis he concluded that the optimum value of Q would be given approximately by:

$$Q = \frac{\beta R}{B\tau} \qquad (2.16)$$

where B is a constant of the order of unity.

Thus the optimum value of Q is energy dependent and is not necessarily small. This point has been ignored by many workers who have advocated (e.g. Garg, as recently as 1960) the desirability of limiting on the first photoelectron, i.e. making Q = 1.

In 1952 Post considered the effects of light collection. Since these are normally of marginal importance and are considerable only when long light guides are used they will not be detailed here.

(b) <u>The treatment of Minton</u>.

Minton (1956) reconsidered the theory of time resolution and used a fast coincidence circuit (fig.2.6)

to check his results numerically. He considered in more detail the response of his fast coincidence circuit to photomultiplier pulses. It seemed unrealistic to assume that the coincidence circuit triggered precisely on the emission of the Qth photoelectron. It was more natural to suppose that each of the first Q photoelectrons played its part in registering the event and that the variance in the time of response of the system to the pulse would be given by the arithmetic mean of the variances associated individually with the first Q electrons. Hinton therefore took as the variance:

$$\sigma_S^2 = \left(\frac{\tau}{R}\right)^2 \left[\frac{1}{Q} \sum_{N=1}^{Q} \left\{ N + \frac{2}{R} N + N^2 \right\} \right]$$

$$= \left(\frac{\tau}{R}\right)^2 \left[\frac{Q(Q+1)}{2Q} + \frac{2(Q+1)(Q+2)}{3R} \right]$$

$$\doteq \frac{Q}{2}\left(\frac{\tau}{R}\right)^2 + \frac{2Q^2}{3R}\left(\frac{\tau}{R}\right)^2 \qquad (2.17)$$

which is correct to second order for $Q \gg 1$. The subscript S here refers to "scintillator". Thus the first order variance is half the Post-Schiff value since it no longer depends on just one photoelectron.

The analysis also dealt with time spread in the photomultiplier. Following Morton (Symposium 1952), Hinton concluded that the multiplier would contribute a

variance

$$\sigma_m^2 \doteq \frac{1}{Q}\left(\varepsilon_{ph}^2 + \frac{\varepsilon_{dd}^2}{g}\right) \qquad (2.18)$$

due to transit time fluctuations. In (2.18) ε_{ph} is the r.m.s. time spread for photoelectrons and ε_{dd} is the same quantity for secondary electrons leaving the first dynode; g is the stage gain and it is to be noted that transit time effects beyond the second dynode have not been considered. To (2.18) was added a variance γ^2/Q which was due to fluctuations in gain. Eq. (2.18) could thus be written

$$\sigma_m^2 = \frac{1}{Q}\left(\varepsilon_{ph}^2 + \frac{\varepsilon_{dd}^2}{g} + \gamma^2\right)$$

i.e. $$\sigma_m^2 = \frac{T_M^2}{Q} \qquad (2.19)$$

where T_M is a constant, characteristic of the multiplier.

Combining (2.17) and (2.19), to first order:

$$\frac{d(\sigma^2)}{dQ} = \frac{1}{2}\left(\frac{\tau}{R}\right)^2 - \frac{T_M^2}{Q^2}$$

and this will be zero, i.e. σ^2 will be minimised when:

$$Q = \frac{\sqrt{2}\,RT_M}{\tau} \qquad (2.20)$$

The minimum value of σ^2 will be:

$$\sigma_{MIN}^2 = \frac{\sqrt{2}\,T_M\tau}{R} \qquad (2.21)$$

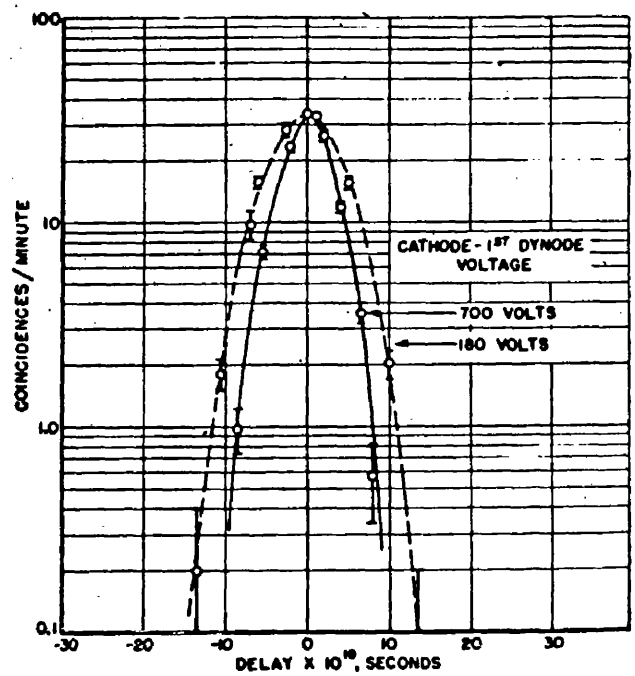

FIGURE 2.7a *Effect on the response of the differential coincidence system of fig 2.6a produced by a change in the transit time in the photocathode-to-dynode region of the photomultiplier.*

5819 photomultipliers and terphenyl-toluene scintillators were used with Co^{60} γ radiation.

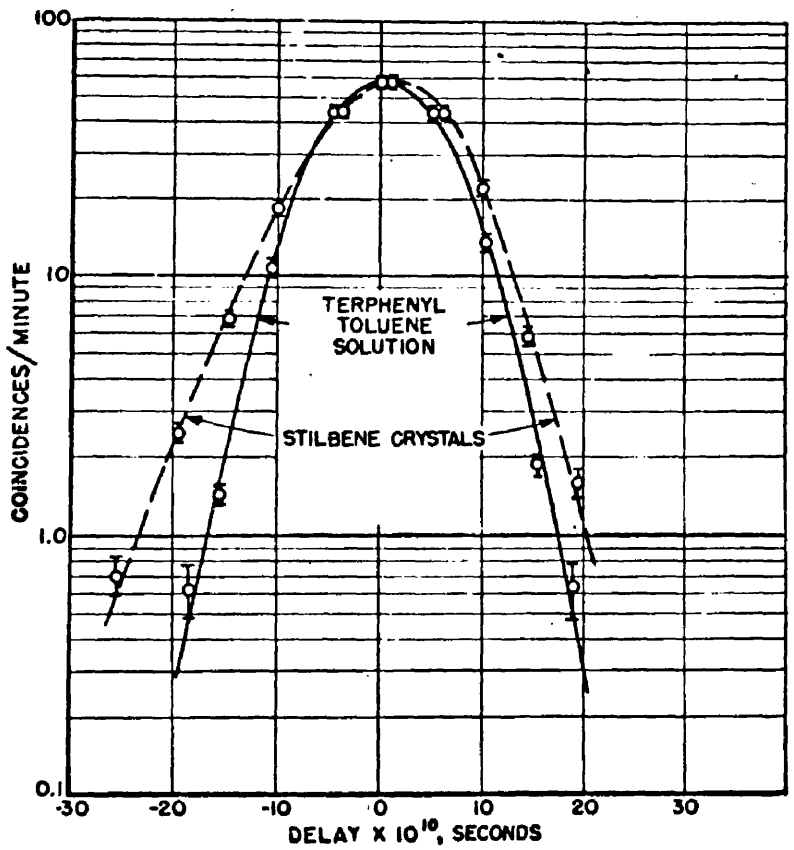

FIGURE 2.7b *Effect on the response of the differential coincidence system of fig. 2.6a produced by a difference in the time distribution of photons incident on the photomultiplier using annihilation radiation.*

The scheme of Hinton's differential coincidence system is shown in fig. 2.6a. Fig. 2.6b illustrates the dependence of σ^2 on the energy liberated in the scintillator. Fig. 2.7b shows how σ^2 can be improved by choice of scintillator and fig. 2.7a shows how photoelectron transit time spread can be reduced with corresponding improvement in σ^2. From an analysis of these curves it was concluded that:

$T_{11} = 1.8 \times 10^{-9}$ sec. for 180 volts between cathode and first dynode.

$T_{11} = 9.5 \times 10^{-10}$ sec. for 700 volts between cathode and first dynode.

and the best FWR obtained was 6.2×10^{-10} sec. with Co^{60} prompt γ-rays.

The various factors influencing resolution were discussed again by de Waard (1958) but with little attention to instrumental time delays. The latter were investigated by Bashandy (1960) but the interpretation was confined to a comparison with the Post-Schiff equations and took no account of multiplier effects. Bonitz and Berlovitch (1960) also reproduced some data on time delays but made no attempt at all to analyse them.

It should perhaps be remarked here that there have

been very few investigations by the centroid shift method in recent years, and some of the results circulated earlier have not in fact been published (e.g. case of Hf^{180} referred to in chapter 4). It would appear that despite the lack of precise data on the subject most investigators have realised the hazard of measuring very short lifetimes by this method. In particular the self comparison method in which time delay effects would be most serious has rarely been used.

(c) The theory of Gatti and his co-workers.

In 1957 Colombo, Gatti and Pignanelli published a rigorous analysis of the performance of a delayed coincidence system and in 1959 Gatti and Svelto went over the theory again amplifying some of the points. With these papers the theory of time delays and time resolution is more or less completed. Unfortunately the results could not be expressed in simple formulae. Instead numerical calculations were made and illustrative results were given in the form of graphs. The main points of the Gatti theory will now be considered.

The chain of processes involved in the detection of a particle in a scintillation counter is as follows:-

1) Slow-down in the scintillator and excitation of optically active states.

2) Decay of the excited states with emission of light

3) Collection of light.

4) Emission of photoelectrons by the photocathode.

5) Secondary emission from dynodes and the formation of the electron avalanche.

6) Processing of the output current pulse.

Processes 1) and 3) will not be considered, and process 2) will be considered through its effect on 4). The first thing to be considered however is 6), because the theory was developed with strict reference to a pulse processing technique rather different from that of time-to-pulse height conversion.

In this technique (Cottini et al. 1956, Cottini and Gatti 1956) the photomultiplier outputs are applied to valves and used to excite transient oscillations at the anodes, 20 Mc in one detector, 20.2 Mc in the other. The two wave trains are then combined in a ring diode modulator whose 200Kc output is used in its first cycle to trigger a discriminator. The output of the discriminator blocks a linearly rising voltage which has been started independently by the multiplier pulses, and since the phase of the 200 Kc oscillation is determined by the phase difference in the original transients the voltage at which this blocking occurs is a measure of the original phase difference, i.e. of the original time difference.

Essentially, the technique of frequency conversion magnifies by a factor of 100 the time to be evaluated by time-to-height conversion. Thus the output is similar to that of a time to height converter.

Gatti et al. analysed the operation of this system and developed the theory accordingly. They distinguished, in the main, two modes of operation:

1) Non-linear working in which only a part of the output pulse from the multiplier is used to excite the oscillations, and the relevant variance is that on the centroid of this partial pulse.
2) Ballistic linear working in which the whole multiplier pulse is used but in which this pulse is much shorter than a period of the 20 Mc oscillation. In this case the variance is that on the centroid of the whole pulse.

It turns out that mode 2) does not give quite such good resolution as mode 1) but does have the advantage that no instrumental time delay is involved. This means that a wide range of energy can be selected without loss of resolution. It will be shown in the next chapter that mode 1) is equivalent to the standard technique of time-to-pulse height conversion.

Attention can now be directed to processes 4) and 5). It is desired to calculate the occurrence time of the

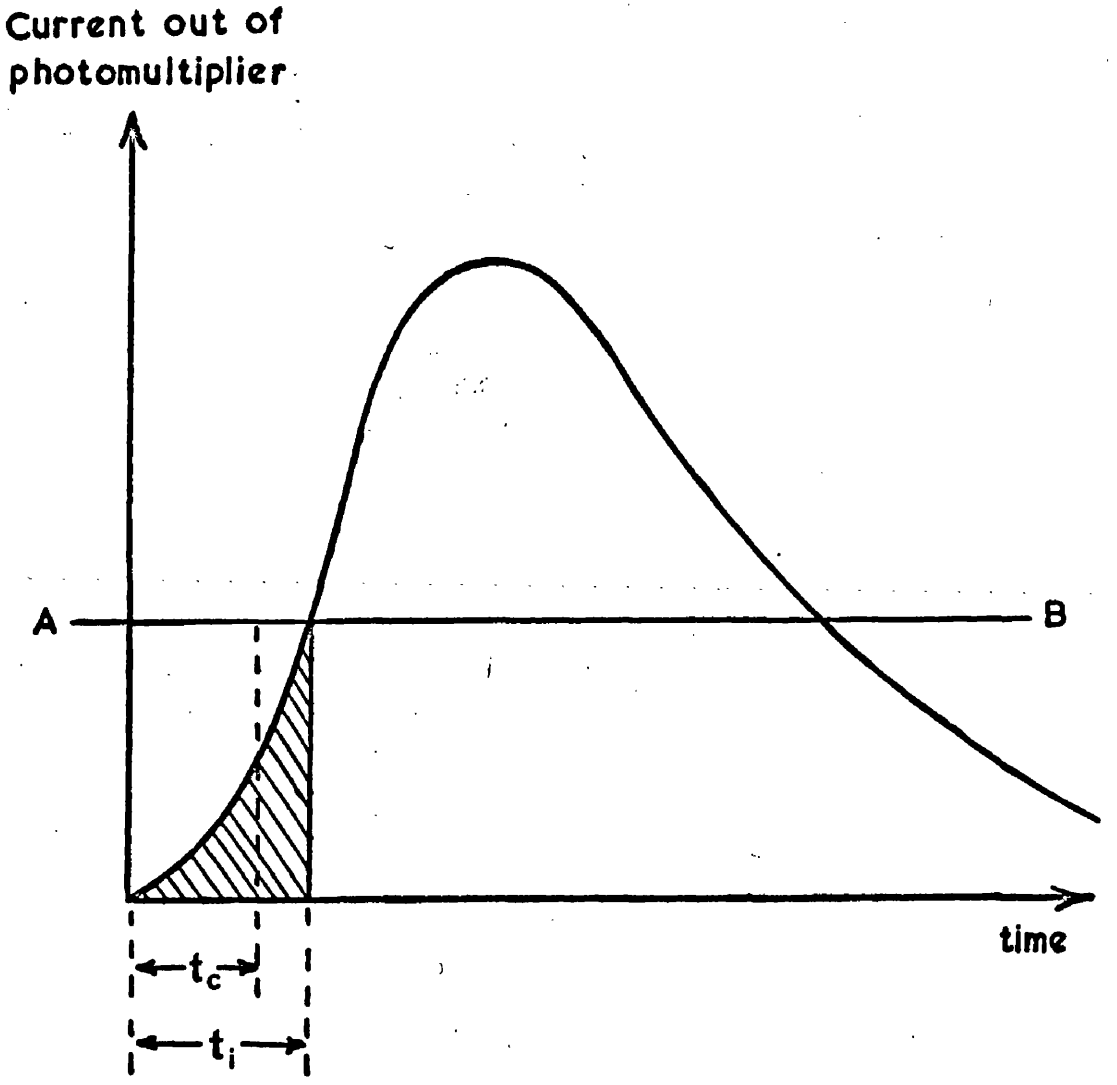

FIG. 2.8

Output pulse from photomultiplier.
Limiter is cut off when level AB is reached; t_i is the time to reach this level, t_c is the time to the centroid of that part of the pulse occurring before time t_i.

centroid of the initial part of the pulse which is exciting the oscillations. This is illustrated as the hatched area in fig. 2.8 where t_c is the time to the centroid and t_1 is the time required to cut off the first valve, i.e. the time required to collect Q photoelectrons. It is desired then to calculate t_c and its variance.

From the Post-Schiff treatment it is known that the mean time of emission of the nth photoelectron is, from eq.(2.13)

$$t_n = n\left(\frac{\tau}{R}\right)\left[1 + \frac{n+1}{2R} + \cdots\right]$$

Therefore the mean time t_c of the centroid of the first Q photoelectrons is:

$$t_c = \frac{1}{Q}\left(\frac{\tau}{R}\right)\sum_{n=1}^{Q}\left[n + \frac{n(n+1)}{2R} + \cdots\right]$$

$$= \frac{Q+1}{2}\left(\frac{\tau}{R}\right)\left(1 + \frac{Q+2}{3R} + \cdots\right) \qquad (2.22)$$

which is different from the Post-Schiff result. Eq.(2.22) has just been obtained by the same summation method as was used by Hinton in deriving σ_1^2. Applied to t_c this summation is quite valid, but Hinton's application of it to σ_1^2 was not. This can be seen as follows:

$$\sigma_Q = \sqrt{Q}\,\frac{\tau}{R}$$

but $$t_Q = Q\,\frac{\tau}{R}$$

i.e. $$t_Q - t_{Q-1} = \frac{\tau}{R}$$

Now $\tau/R < \sqrt{Q}(\tau/R)$ which means that when the Qth photoelectron arrives early by an amount σ_Q, the (Q - 1)th and possibly the (Q - 2)th etc. photoelectrons must also arrive before their meantimes. Thus the actual arrival times of individual photoelectrons are not independent. There is a constraint on them. As a result of this Minton's equation (2.17) is incorrect and should , according to Gatti, be replaced by

$$\sigma_s^2 = \frac{Q}{3}\left(\frac{\tau}{R}\right)^2 + \text{----} \qquad (2.23)$$

In the Gatti theory Minton's proposals for dealing with the multiplier are accepted and improved upon. The r.m.s. transit time spread is taken to include time spread between all the dynodes. For a fixed stage gain g it can easily be shown that:

$$\varepsilon_{ph}^2 = \varepsilon_{cd}^2 + \frac{\varepsilon_{dd}^2}{g-1}\left(1+\frac{2}{g}\right) \qquad (2.24)$$

where "cd" refers to photoelectrons and "dd" to secondary electrons. Hence:

$$\sigma_M^2 = \frac{\varepsilon_{ph}^2}{Q} \qquad (2.25)$$

The effects of gain fluctuations will not be considered here.

Thus far the Gatti theory is not very different from that of Minton, but at this stage a new and very important parameter is introduced. This is λ, defined as the second

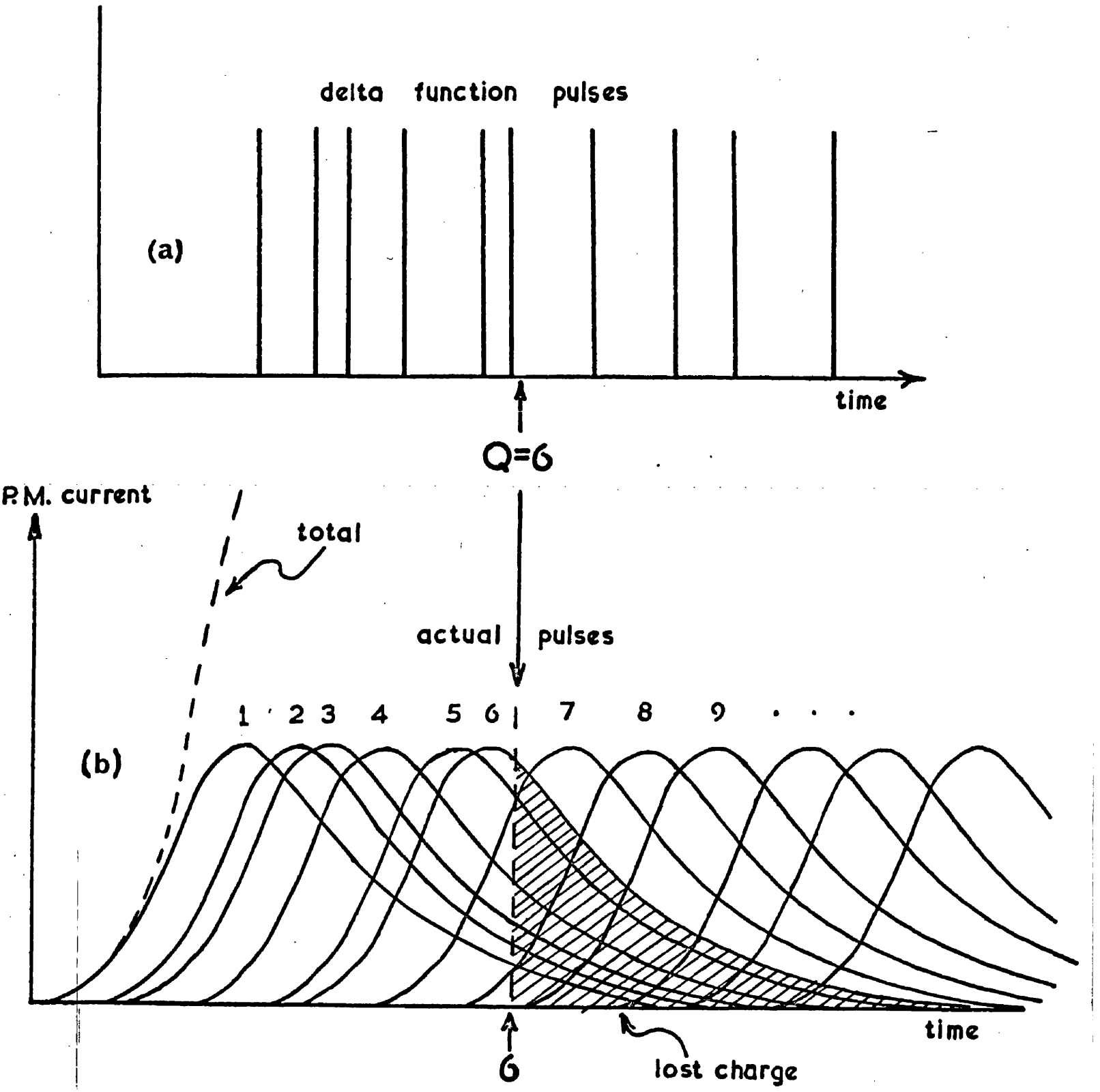

FIG. 2.9

Illustrating the effect of the parameter λ .

moment of the multiplier current pulse resulting from a single photoelectron:

$$\lambda^2 = \int_0^\infty (t-a)^2 f(t)\, dt \qquad (2.26)$$

where $f(t)$ is the single electron response of the photomultiplier and a the time of its centroid. The effect of λ is illustrated in fig. 2.9. Fig. 2.9a shows the first 10 single electron delta function pulses coming out of an ideal photomultiplier. Fig. 2.9b shows how the actual multiplier pulse is a superposition of pulses, each with finite λ. The arrow in each figure indicates the time of emission of the 6th photoelectron. In fig. 2.9a all the charge corresponding to the six photoelectrons has been collected in this time t_6, but in fig. 2.9b, due to the dispersive effect of λ, all the charge in the shaded area has not been collected. A little of the 7th and 8th photoelectron pulses has been collected but the net result is that the charge collected in time t_6 corresponds to less than six photoelectrons. The photoelectron equivalent of this charge is therefore designated C and it follows that

$$Q \geq C \text{ always} \qquad (2.27)$$

In view of this, if a charge equivalent to C photoelectrons is required to cut off a limiter valve the time required to collect this charge is not t_c but t_Q and since $Q > C$

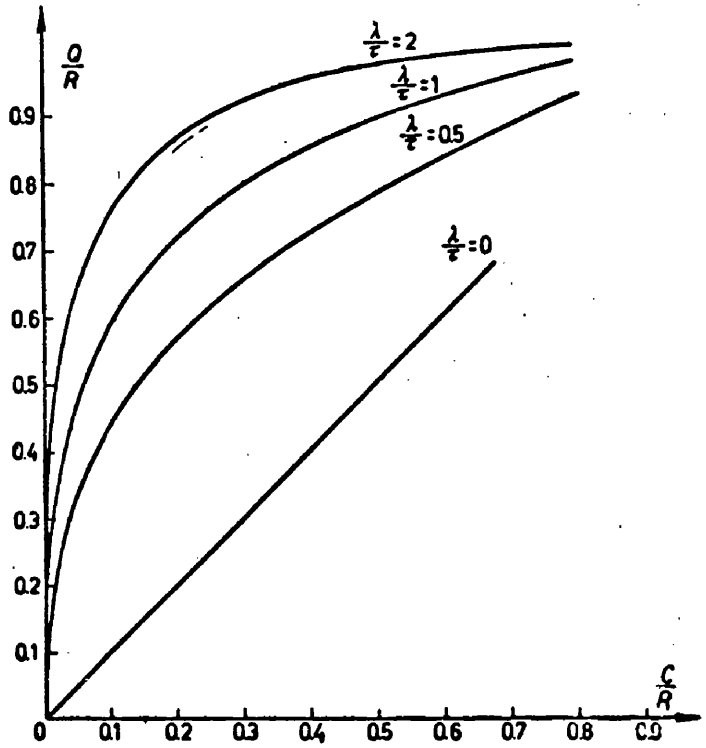

Fig.2.10a Charge collected versus number of photoelectrons emitted with phototube response « width » λ as parameter.

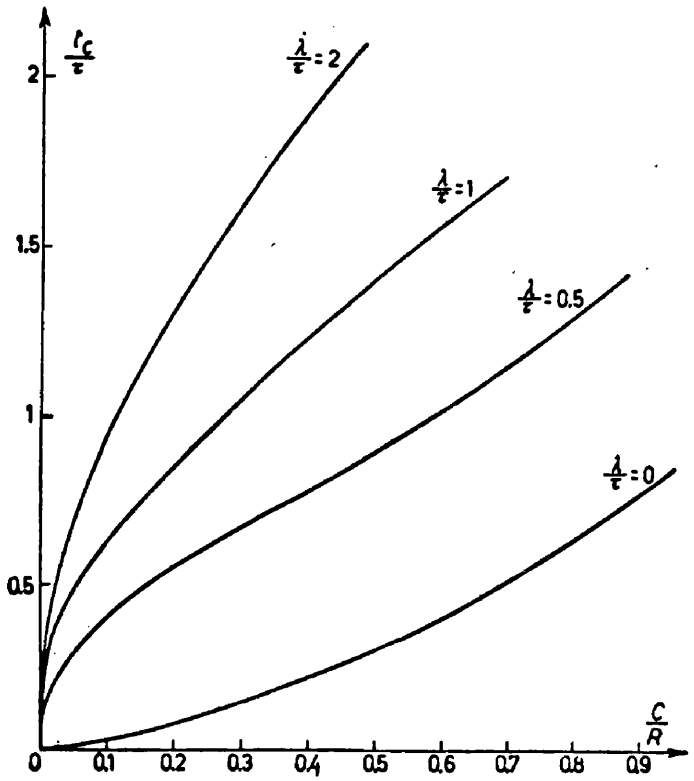

Fig. 2.10b « Machine time » dependence from pulse height R.

generally, $t_Q > t_c$.

This distinction between C and Q is one of the most important results of the Gatti theory and most of the practical consequences of λ can be understood simply in terms of this feature. Fig. 2.10a shows how C and Q are related. It can be seen that as λ/τ increases the effect becomes very serious.

If all other things are fixed except the energy the effect of λ can be incorporated in the earlier equations by writing in place of equations (2.22), (2.23) and (2.25):

$$t_c = \frac{Q(R) + 1}{2} \left(\frac{\tau}{R}\right) \qquad (2.28)$$

$$\sigma_s^2 = \frac{Q(R)}{3} \left(\frac{\tau}{R}\right)^2 \qquad (2.29)$$

$$\text{and } \sigma_n^2 = \frac{\varepsilon_{ph}^2}{Q(R)} \qquad (2.30)$$

where (2.28) and (2.29) are correct to first order. The function Q(R) is always greater than the simple constant Q(C in the new terminology) and can be obtained graphically from fig. 2.10a. Fig.2.10b shows how λ affects the instrumental time delay t_c.

It was to clarify the various matters discussed in this section and to investigate the completeness of the theory that the measurements now to be described were undertaken.

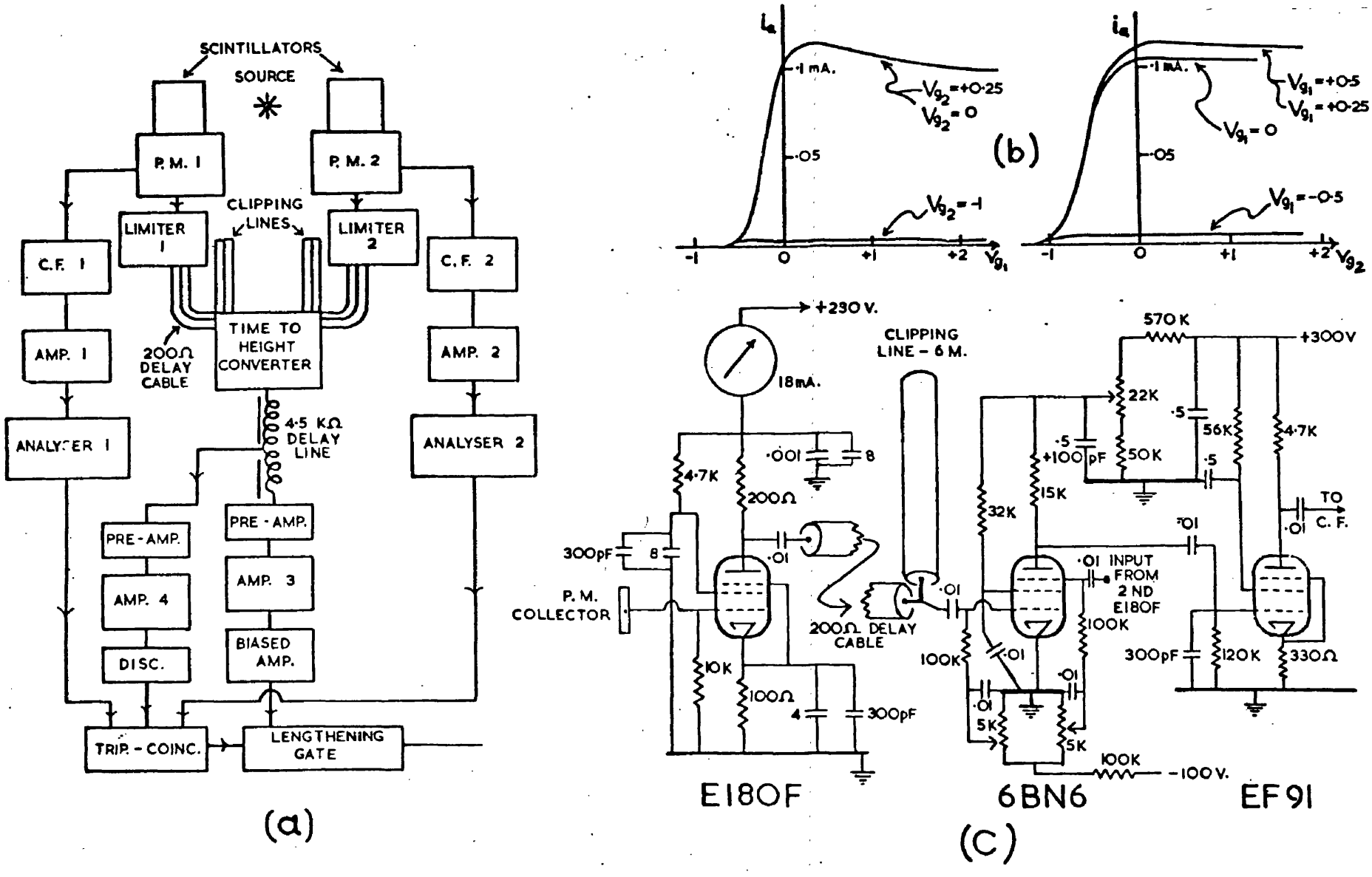

FIG. 3.1

Details of circuitry.

CHAPTER 3

MEASUREMENTS OF RESOLUTION AND INSTRUMENTAL TIME DELAY

(3.1) The Apparatus

The apparatus which was used for all the measurements reported in this thesis is a time-to-pulse height converter of the type first used by Neilson and James (1955) and developed by Green and Bell (1958). It does not incorporate the supervisory diode circuit used by Green and Bell to determine the order in which the pulses must overlap. Without such a control the pulses of fig. 2.5 can give the same pulse height at the output for two possible positions, 1-2 and 2-1. This fact doubles the random counting rate and could be troublesome in certain measurements. However, in what follows it is not relevant.

Fig. 3.1a is a block diagram of the system. The anode pulse of the photomultiplier is applied to a limiter valve, as shown in fig. 3.1c, cutting it off and producing a positive step at its anode. This step is passed down a variable length of 200 Ω delay cable to the time-to-height converter. The latter unit is not situated at the end of the delay line. Instead it is a fixed distance, say 6 metres, from the end and this final 6m is terminated with a short circuit and so acts as a clipping line. The result is that a rectangular pulse $\sim$45 nsec. long is applied

to one control grid of the 6BN6 valve. A similar pulse from the other detector is applied to the other control grid.

The 6BN6 valve is operated at very low voltages, 15 volts on the anode and 6 volts on the accelerator. Under these conditions the static characteristics are as shown in fig. 3.1b where it can be seen that just a little more than one volt applied to both grids should produce a saturation current of 0.1 mA. Switching off the 14 mA anode current in an E180F limiter will result in a 1.4 volt pulse going down the 200 Ω cable (in parallel with a 200Ω anode resistor) to the 6BN6. The overlaps of the two pulses will therefore turn on a current of 0.1 mA in the 6BN6 and this current will charge up the 300pF integrating condenser for the time of overlap. For 10 nsec. of overlap the accumulated charge will be 10^{-12} coulombs and the voltage developed across the condenser will be 3.3 mV. The time constant of this integrating circuit is determined largely by the anode load on the 6BN6. It will therefore be $\sim 4.5 \times 10^{-6}$ sec. which is much longer than the maximum time of integration, 40 nsec. The circuit therefore converts time to amplitude linearly in the range 0 - 40 nsec., producing initially a pulse of up to ~ 14 mV with a decay time of 4.5 μsec.

Fig. 3.1a also shows the side channels and auxiliary units. The side channels derive their signals from the third last dynode of the photomultiplier. These energy pulses are integrated, amplified and passed to differential pulse height analysers which allow any desired range of energies to be selected. If the outputs of these analysers were combined in a simple coincidence unit and thus used to gate the centre channel signals the random coincidence rate would be quite high on account of the large (~ 1.3 μsec.) resolving time of the slow coincidence unit. This is overcome by making the unit a triple coincidence device which means that the chance coincidence rate depends only on the short resolving time of the fast part of the circuit. It is therefore greatly reduced.

The biased amplifier and lengthening gate were developed specifically for this work. The amplifier has a bias control which can be set at anything between 0 and 50 volts. When a pulse is fed into the unit only that part which exceeds the bias level is transmitted. This portion of the pulse can then be linearly amplified. The unit therefore permits magnification of the time scale so that any selected portion of the coincidence pulse height spectrum can be expanded to cover the 150 channels of a kicksorter. This was invaluable in the measurements of resolution and time delay. The lengthening gate is a

(a)

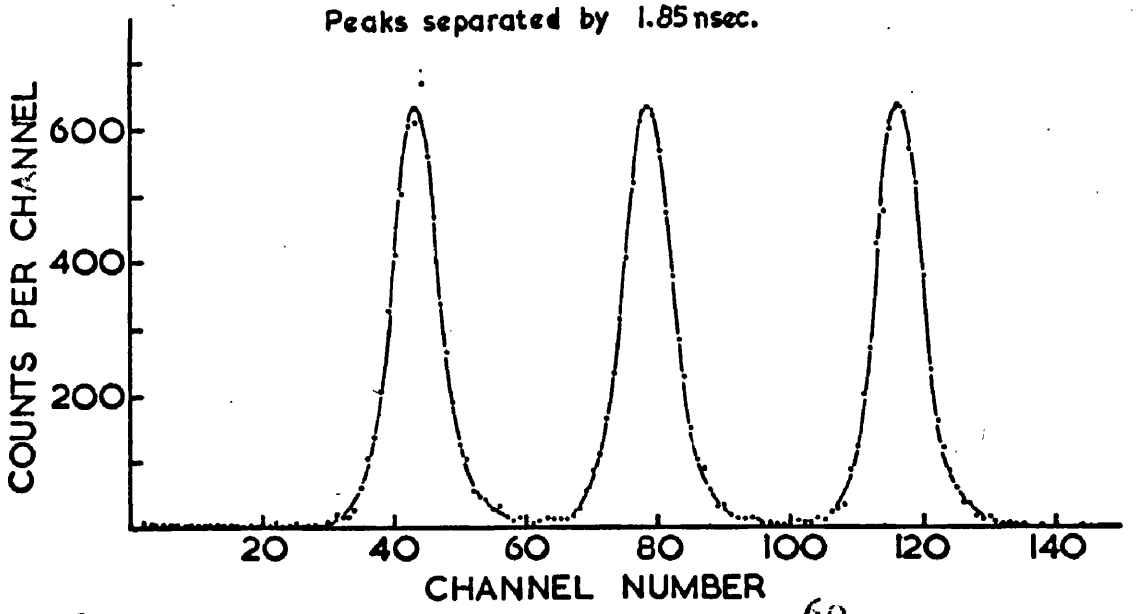

Resolution curves obtained with a Co^{60} source. Peak separation produced by 50 cm of delay cable (1.85 mμs).

(b)

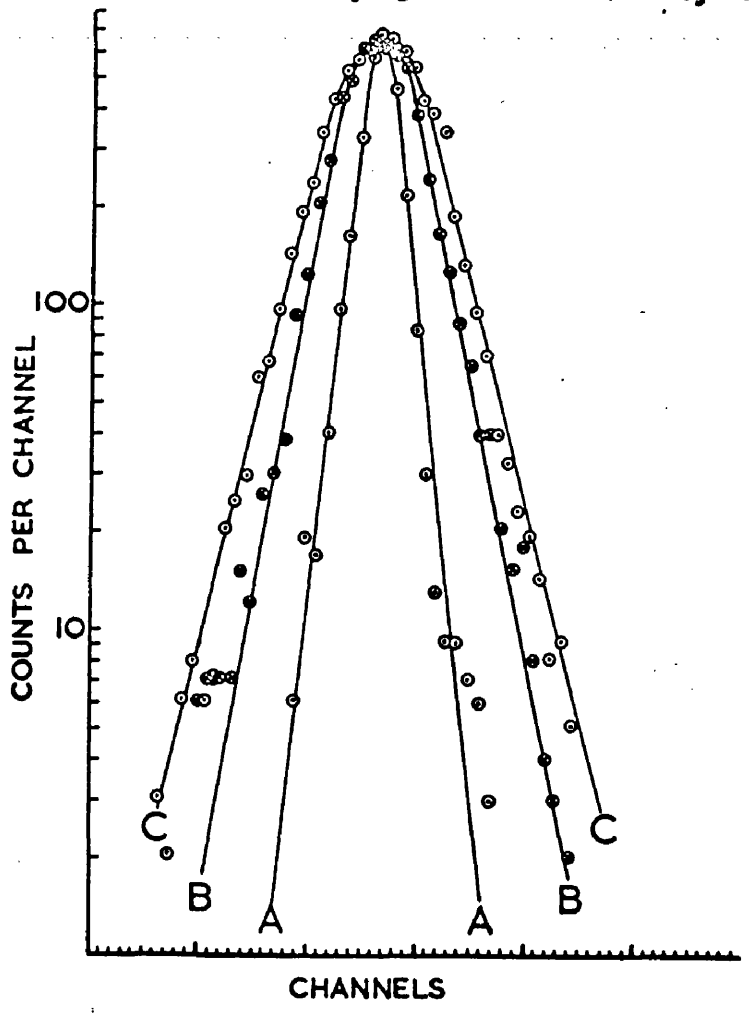

FIG. 3.2

Typical resolution curves: A: with self coincidences, B: with Co^{60} γ's, C: with Na^{22} ½-MeV γ's.

coincidence/anti-coincidence device, very necessary for lengthening the sharp pulses from the biased amplifier and for preventing large pulses entering the kicksorter. It produces at its output rectangular pulses of about 10 μsec. length.

The apparatus was calibrated by the insertion of various lengths of 200Ω delay cable between the limiters and the 6BN6. Fig. 3.2a shows three resolution curves which were obtained with lengths of cable differing by 50 cm. The performance was found to compare favourably with quotations by other workers (Bell and Jørgensen 1960, Bonitz and Berlovitch 1960, Kane et al. 1960, Simms et al. 1961). Fig. 3.2b illustrates this. For curve A the output of the photomultiplier was applied to both channels of the time-to-height converter. This is referred to as self-coincidences. Curve B was obtained with high energy Y-rays from Co^{60} and curve C with $\frac{1}{2}$-MeV annihilation radiation from Na^{22}. For the Co^{60} Y-rays thebest FWR was 4.3×10^{-10} sec., a figure scarcely bettered at the time of this work.

In order to compare measurements made on this apparatus with the predictions of the Gatti theory it is necessary to establish that the results of that theory are applicable. Fig. 3.3a shows the current pulse out of the photomultiplier. The hatched area is the portion which registers the event

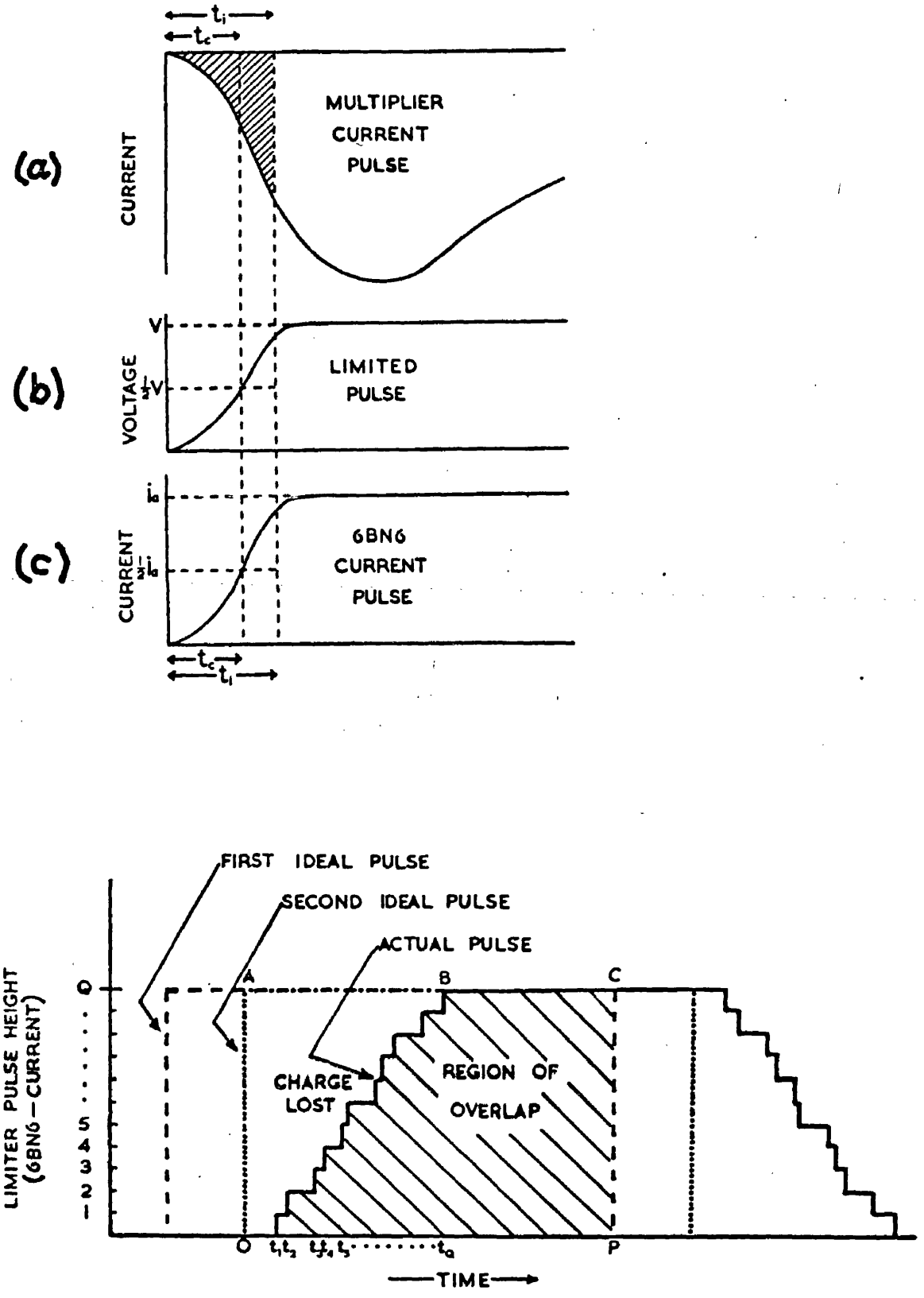

FIG. 3.3

Idealised representations of the fast pulses.

by blocking the E180F limiter and creating the limited step pulse at the anode of this valve, fig. 3.3b. This limited pulse is then used to turn on the saturation current i_a in the 6BN6, fig. 3.3c. If the E180F and 6BN6 have linear characteristics, then, ignoring for the moment the effect of λ, the rising edge of the current pulse through the 6BN6 will correspond to the emission of Q photoelectrons from the photocathode of the multiplier. This is illustrated in fig. 3.3d. If two ideal pulses coincide at the 6BN6 grids then the ideal current pulse will be given by OACP and the charge passed to the integrating condenser will correspond to the area OACP. If, on the other hand, the second pulse is not ideal but results from the arrival of discrete units of charge at times t_1, t_2, t_3 ------- t_Q corresponding to the original Q electrons an amount of charge equal to the area OAB will be lost to the 6BN6 integrating condenser. Since charge = current x time, the time delay will be

$$t = \frac{OAB}{CA}$$

$$= \frac{t_1 i + t_2 i + \text{-------} t_Q i}{Qi}$$

$$= \frac{1}{Q} \sum_{i=1}^{Q} t_i \qquad (3.1)$$

which is the same as was assumed in the derivation of eq. (2.22). Thus it is the centroid of the hatched part (fig. 3.3a) of the multiplier pulse, i.e. the centroid of the first Q electrons, which determines the time delay and resolution.

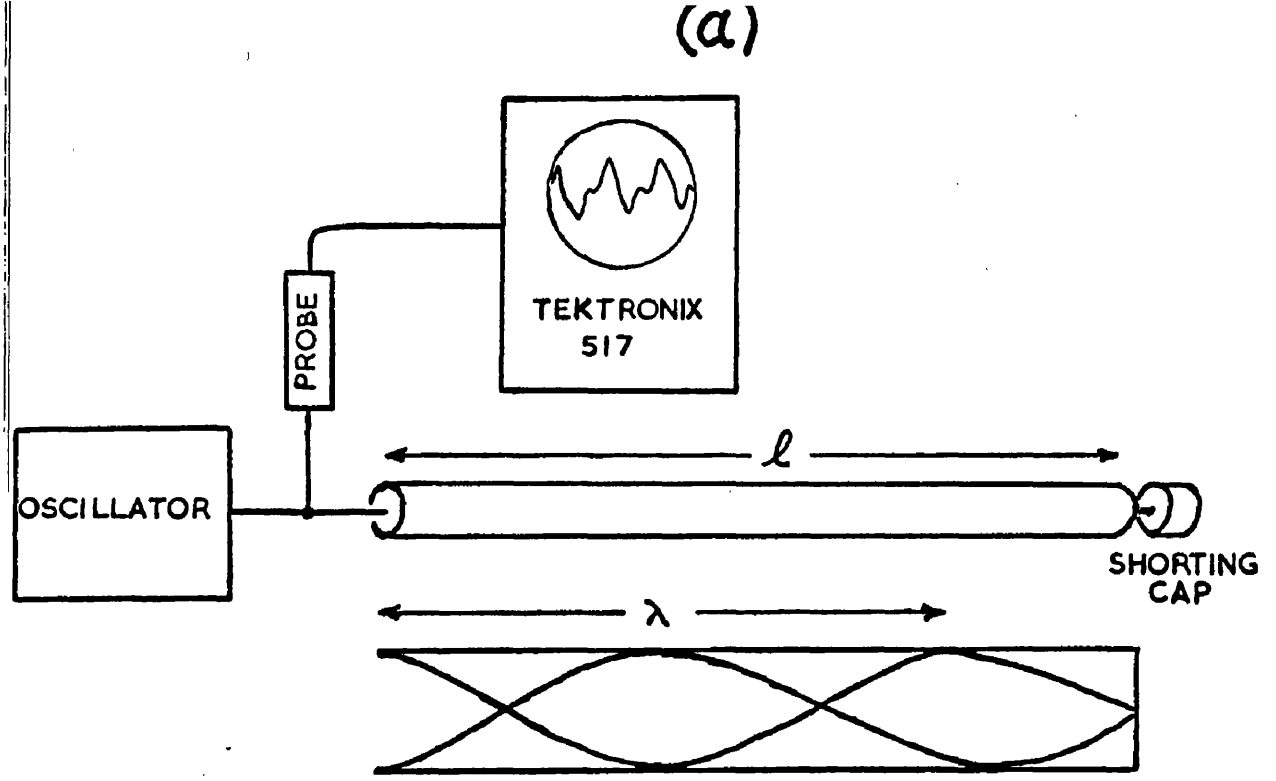

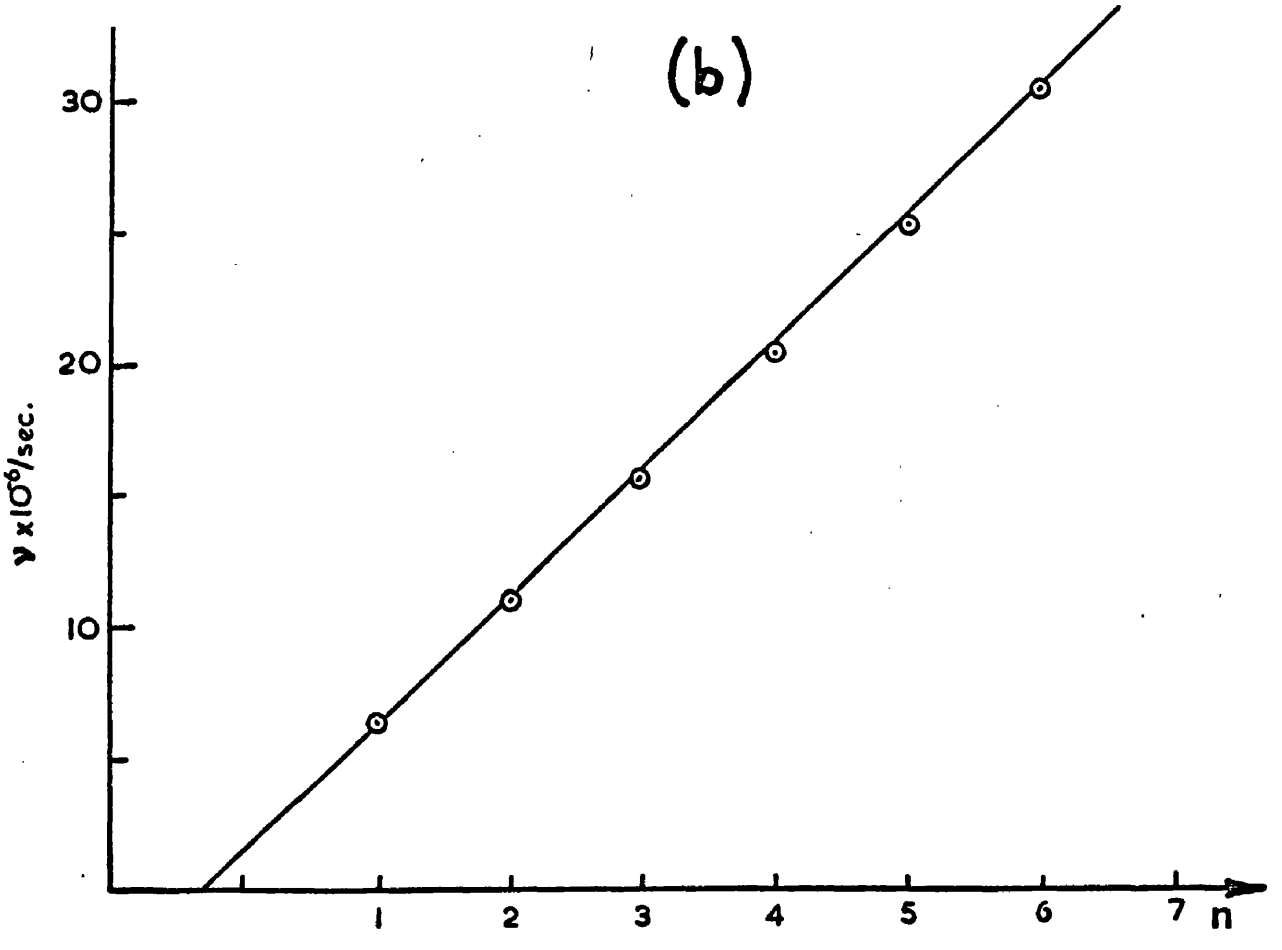

FIG 3.4

Illustrating the standing wave method for determining the cable velocity.

(3.2) Ancillary Measurements.

(a) Velocity of propagation in the 200Ω cable.

To allow the precise determination of small time intervals the apparatus must be carefully calibrated. This requires an accurate knowledge of the velocity of propagation of pulses down the 200Ω delay cable. This was determined by two methods.

The first method is illustrated in fig. 3.4. Fig. 3.4a shows a signal generator feeding a sine wave oscillation into the cable with a fast oscilloscope displaying the voltage at the input to the cable. When the transmission line is terminated by a short circuit and a good sine wave appears at its input the length of the line is related to the signal wavelength by:

$$2\ell = \frac{\lambda}{4} + n\lambda$$

$$\text{i.e.} \quad 2\ell\nu = (n + \tfrac{1}{4})v \qquad (3.2)$$

where ν is the frequency, v is the velocity of propagation and n is an integer. Hence if ℓ is known and ν is varied n and v can be found. Fig. 3.4b shows the frequency plotted against n. From this graph

$$2\ell(\nu_1 - \nu_2) = (n_1 - n_2)\, v$$

$$\text{i.e.} \quad v = \frac{2\ell(\nu_1 - \nu_2)}{n_1 - n_2} \qquad (3.3)$$

From this equation, by the method of least squares:

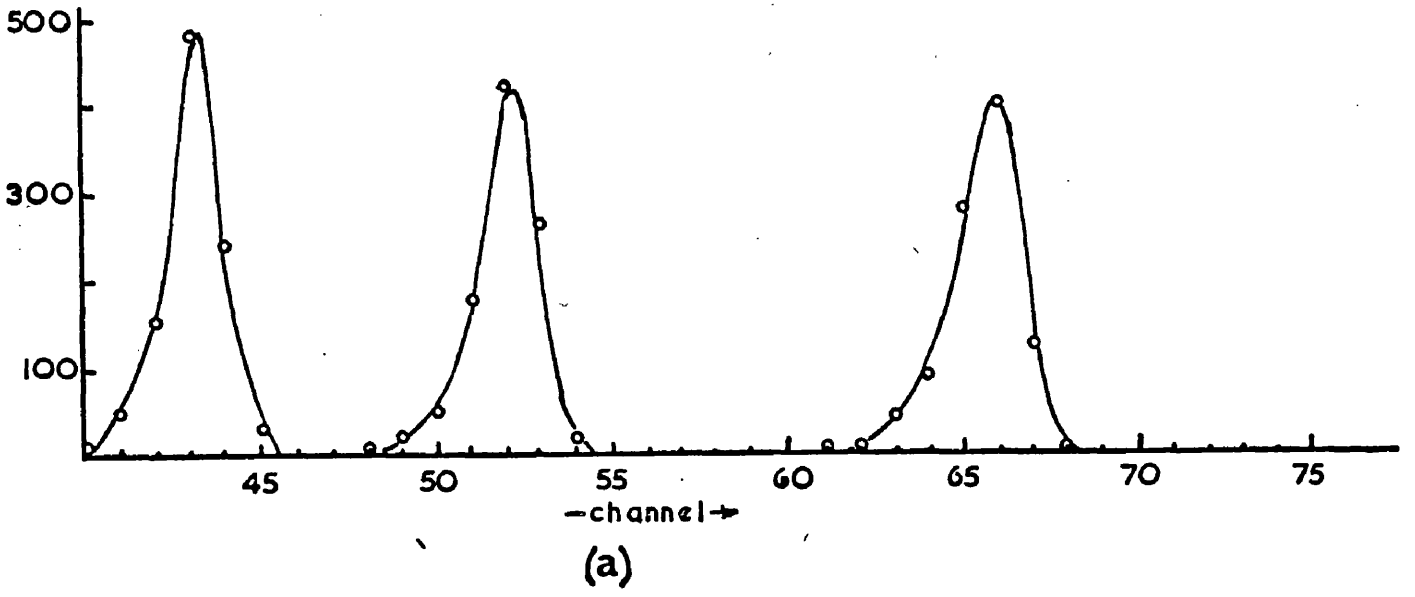

(a)

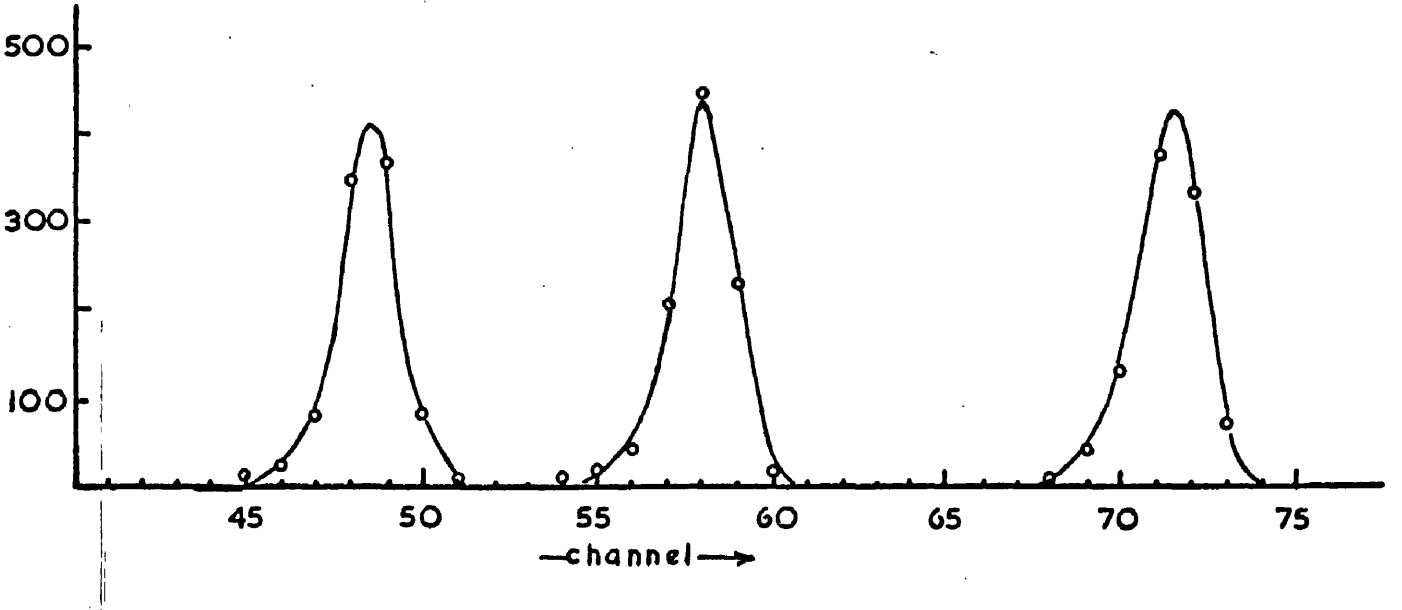

(b)

FIG. 3.5

Peaks obtained by the method of time of flight of photons for determining the cable velocity.

$$v = (0.90 \pm 0.01) \text{ times the velocity of light} \qquad (3.4)$$

A second method of estimating the velocity of propagation down the cable is the time of flight technique. A source of prompt annihilation radiation (Na^{22}) was placed between the detectors on the common axis of both photomultipliers, but nearer to one than the other. Three resolution curves were recorded with different lengths of delay cable. These are shown in fig. 3.5a. The source was then moved 72 cm. nearer the other detector and the same three resolution curves recorded again, fig. 3.5b. The displacement of these curves corresponds to the time taken by light in travelling 1.44m. From the separations between the curves of figs. 3.5a and b the length of cable required to produce the same displacement can be found to be 1.27m Hence the velocity of propagation down the cable is:

$$v = 1.27c/1.44 = 0.885\ c$$

This result was not regarded as very reliable since the counting rates were changed in the two counters when the source was moved. An increased counting rate can cause pile up effects and spurious time delays and since no precautions were taken against these effects a precise agreement between the two estimates can hardly be expected. The agreement is nevertheless moderately good and in all subsequent work it has been assumed that (3.4) is correct;

i.e. that 1 metre of cable is equivalent to 3.7×10^{-9} sec.

(b) Efficiencies of scintillators.

The relative efficiencies of the different scintillators were determined by direct comparison under the conditions of the experiment. After a series of measurements with say, NaI(Tl), several standard photopeaks were recorded on a kicksorter. The E.H.T. was then switched off, the NaI(Tl) replaced by anthracene, for instance, E.H.T. switched on and Compton distributions recorded for the second scintillator. In this way the relative efficiencies were accurately determined each time a change was made.

(c) Decay times of scintillators.

Before the equations given in chapter 2 could be used for a comparison of different scintillators the decay times of these scintillators had to be known. There are plenty of quotations for those (e.g. by the manufacturers) but decay times are known to vary with composition and temperature in the case of NaI(Tl) (Van Sciver 1956, Eby and Jentschke 1954), with crystal size in the case of anthracene (Brooks 1956), and with oxygen content in the case of liquid scintillators (manufacturer's report). In view of these facts it was necessary to determine the decay times of the phosphors used in the measurements.

(a)

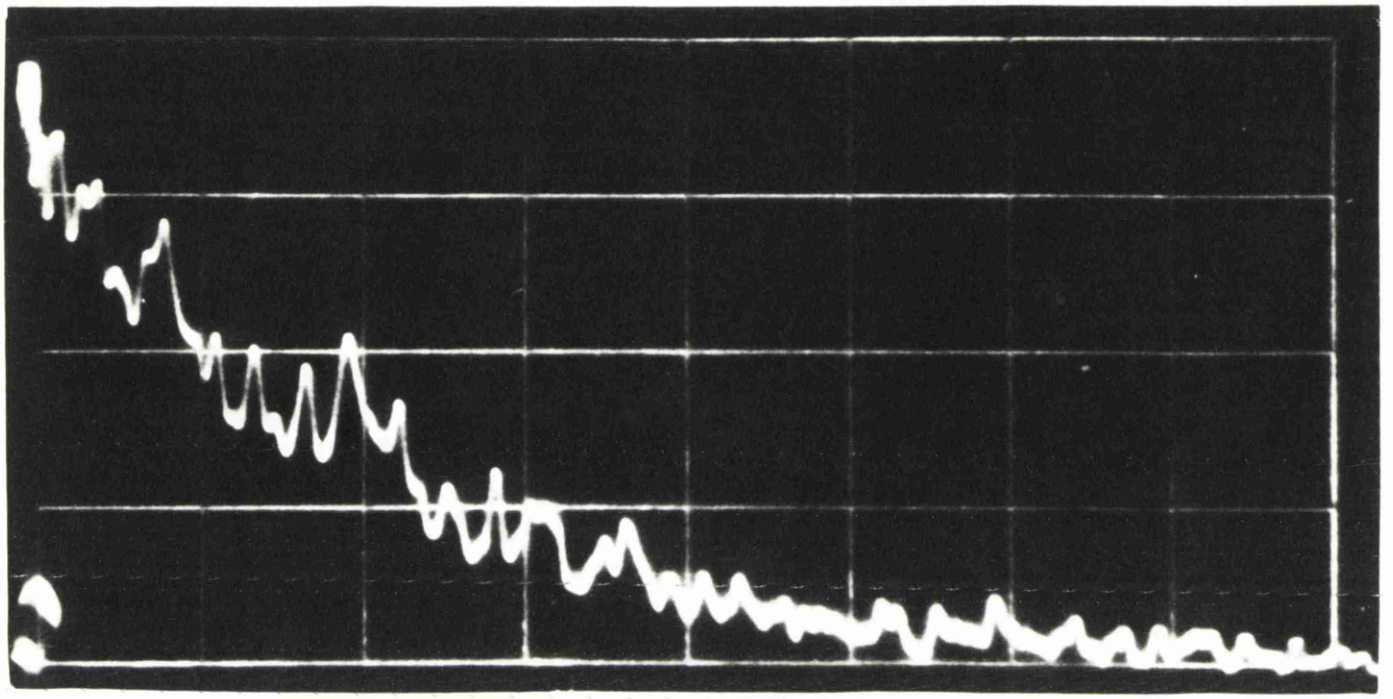

10^{-7} SEC./CM.

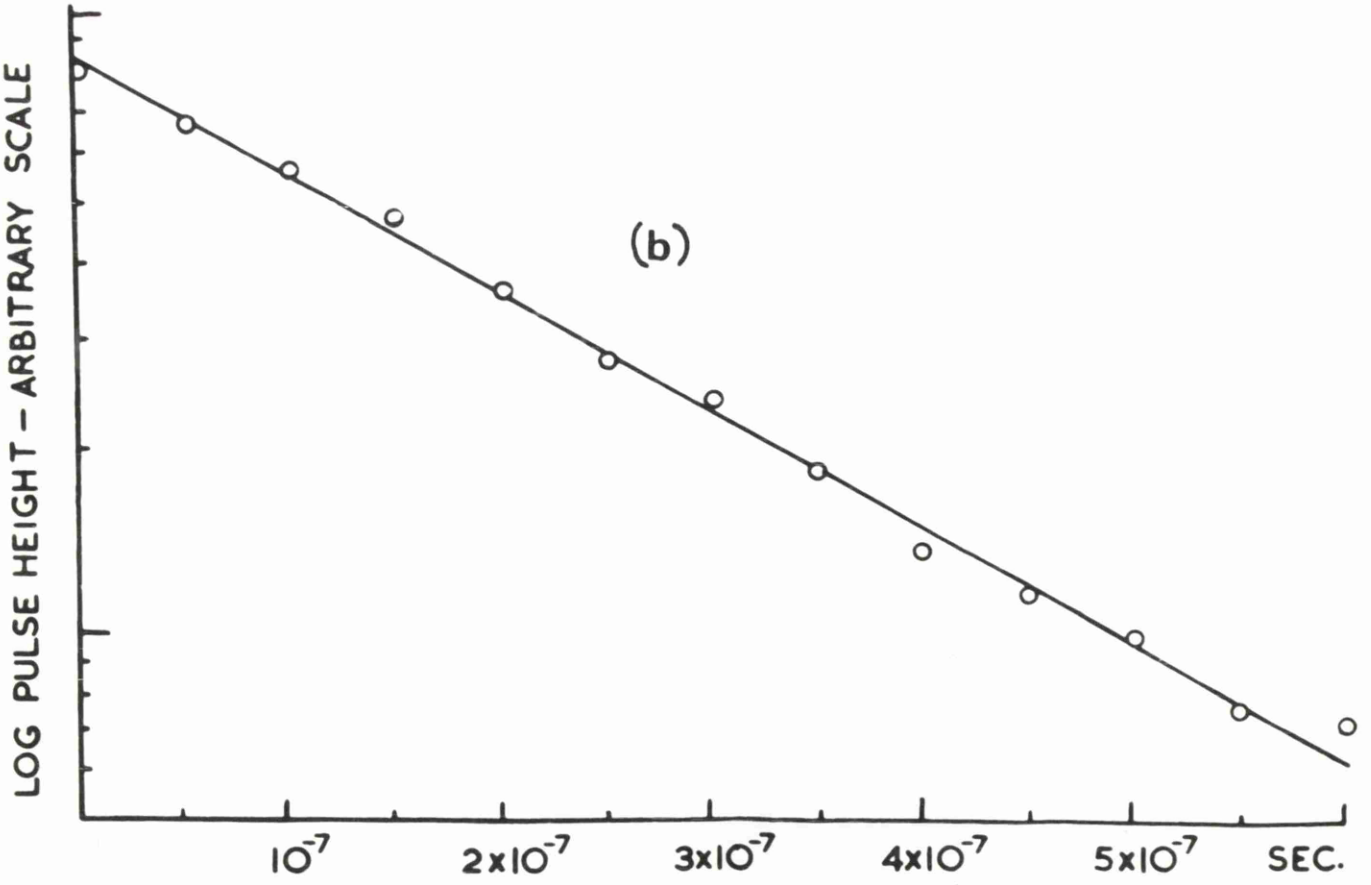

FIG. 3.6

Scintillation pulse from NaI(Tl).

The method used to obtain the scintillation decay times was a direct oscilloscope method similar to that used by Phillips and Swank (1953). The anode of the photomultiplier was connected to ground through a 100Ω resistor and the current pulse (time constant $\sim 10^{-9}$ sec.) viewed in a fast oscilloscope. The fastest scope found compatible with available film speeds was the Tektronix 517 with a rise time of 7 nsec. Fig. 3.6a shows a current pulse from NaI(Tl). The roughness of the trace is due to statistical fluctuations in photoelectron emission. Fig. 3.6b is a graph of pulse height (log) against time, obtained from summing the ordinates of 31 traces. From a least squares analysis of the data

$$\tau = (2.34 \pm 0.12) \times 10^{-7} \text{ sec.}$$

where allowance has been made for a possible inaccuracy in the calibration of the oscilloscope.

The next scintillator investigated by this method was naphthalene. This material was found to have a decay time of 70 nsec. but its light output was very low and good pulses for application to the 6BN6 could not be obtained. Accordingly no further use was made of naphthalene.

A small cube, ~ 1 cm^3, of anthracene was used in the measurements and its decay time was obtained by the above

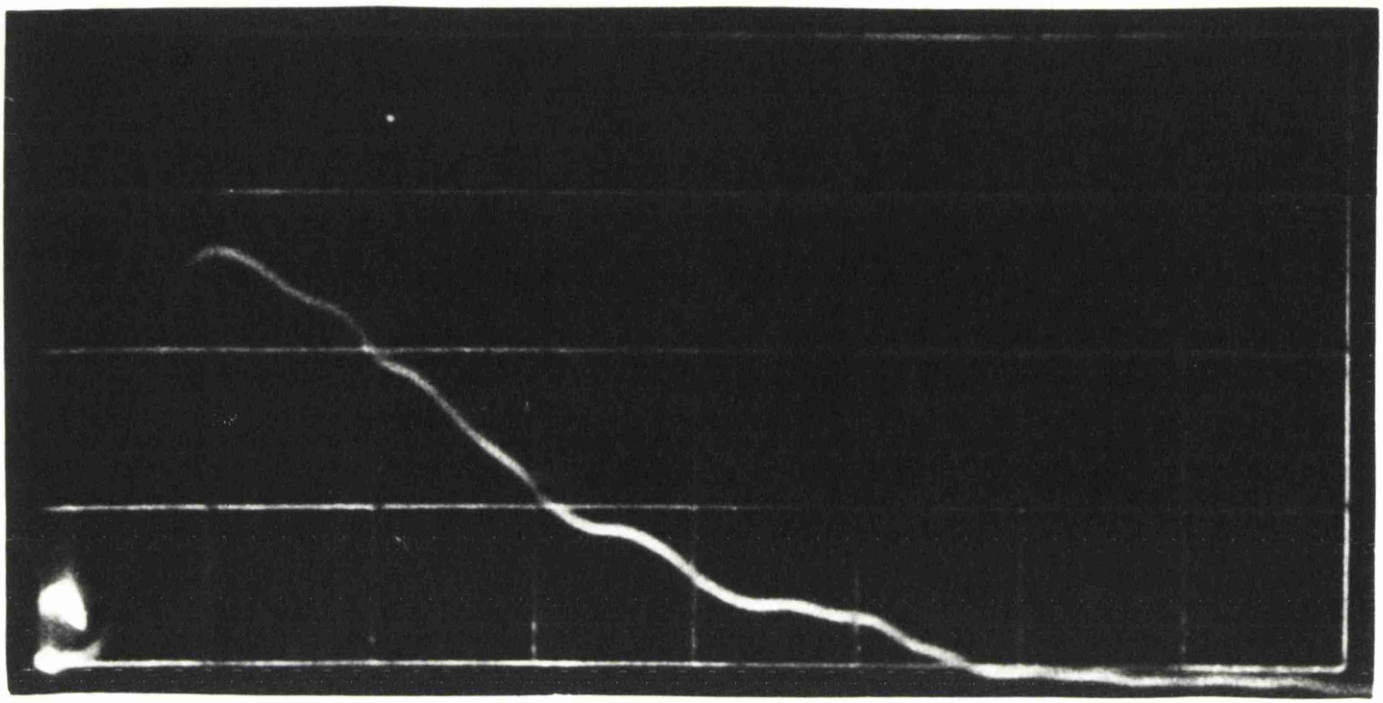

(b)

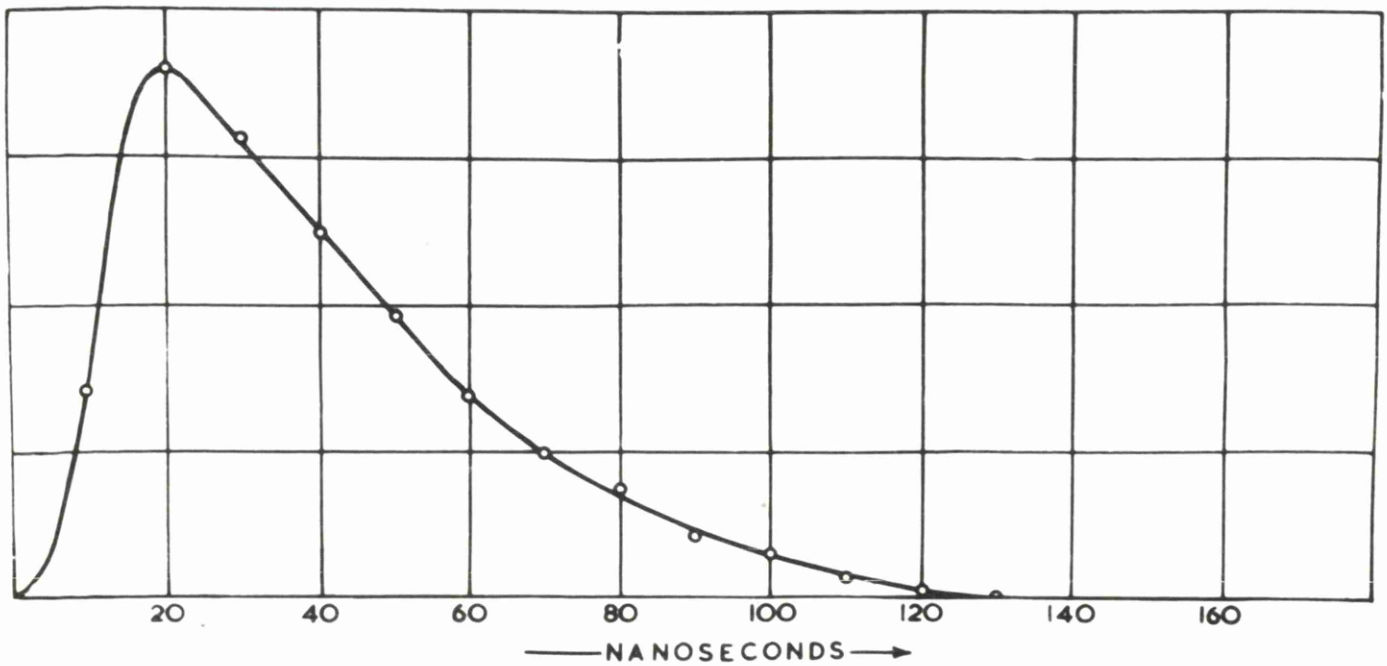

FIG. 3.7

Scintillation pulse from anthracene.

method. Fig. 3.7a shows a typical anthracene pulse and fig. 3.7b shows the mean pulse shape obtained by summing 20 traces. It will be noted that the anthracene pulse decay is not exponential and that the photoelectron emission cannot therefore be described by eq.(2.7). Rather, the decay is linear for about 60 nsec., followed by an exponential Tail. This can be dealt with if eq.(2.9) is replaced by

$$\frac{dn}{dt} = \frac{2R'}{T - t} \qquad (3.5)$$

where R' is the total number of photoelectrons in the linear part of the pulse, i.e. excluding the Tail, and T is the time required for the linear part to fall to zero . For $t \longrightarrow 0$:

$$\frac{dn}{dt} = \frac{2R'}{T} \qquad (3.6)$$

which means that the anthracene has an effective mean life of RT/2R'. In this way the decay time of the anthracene was found to be:

$$\tau = (37 \pm 2) \text{ nsec.}$$

The plastic and liquid scintillators were investigated by the method also but for these cases τ was too short for measurable effects to be seen on the oscilloscope. All that could be concluded about these scintillators was that in

each case $\tau < 7$ nsec. The manufacturers quotations were therefore accepted for them.

(d) Photoelectron yields (P)

The statistical analysis of time resolution depends on the parameters Q and R. These represent numbers of photoelectrons and unless they are known with some precision the analysis is not very meaningful. It was necessary therefore to estimate the numbers of photoelectrons produced by events in the different scintillators. This number is not of course just a property of the scintillators. It depends on the efficiency of the photocathode of the multiplier, usually 5-10%. The photoelectron yield P can therefore be defined as the number of photoelectrons produced per keV of energy for a given scintillator/multiplier combination.

The photoelectron yield P is paramount in determining the energy resolution of a scintillation counter since the statistical uncertainties in pulse size are primarily due to the statistics of electron emission from the photocathode. If R photoelectrons result from a scintillation of energy E the standard deviation on R is $\sigma = \sqrt{R}$. Hence the fractional variance in R is $1/R$. At the first dynode each photoelectron becomes σ secondary electrons. The fractional variance on this number is $1/\sigma$ and if there are R photoelectrons incident on the dynode the fractional variance on the number

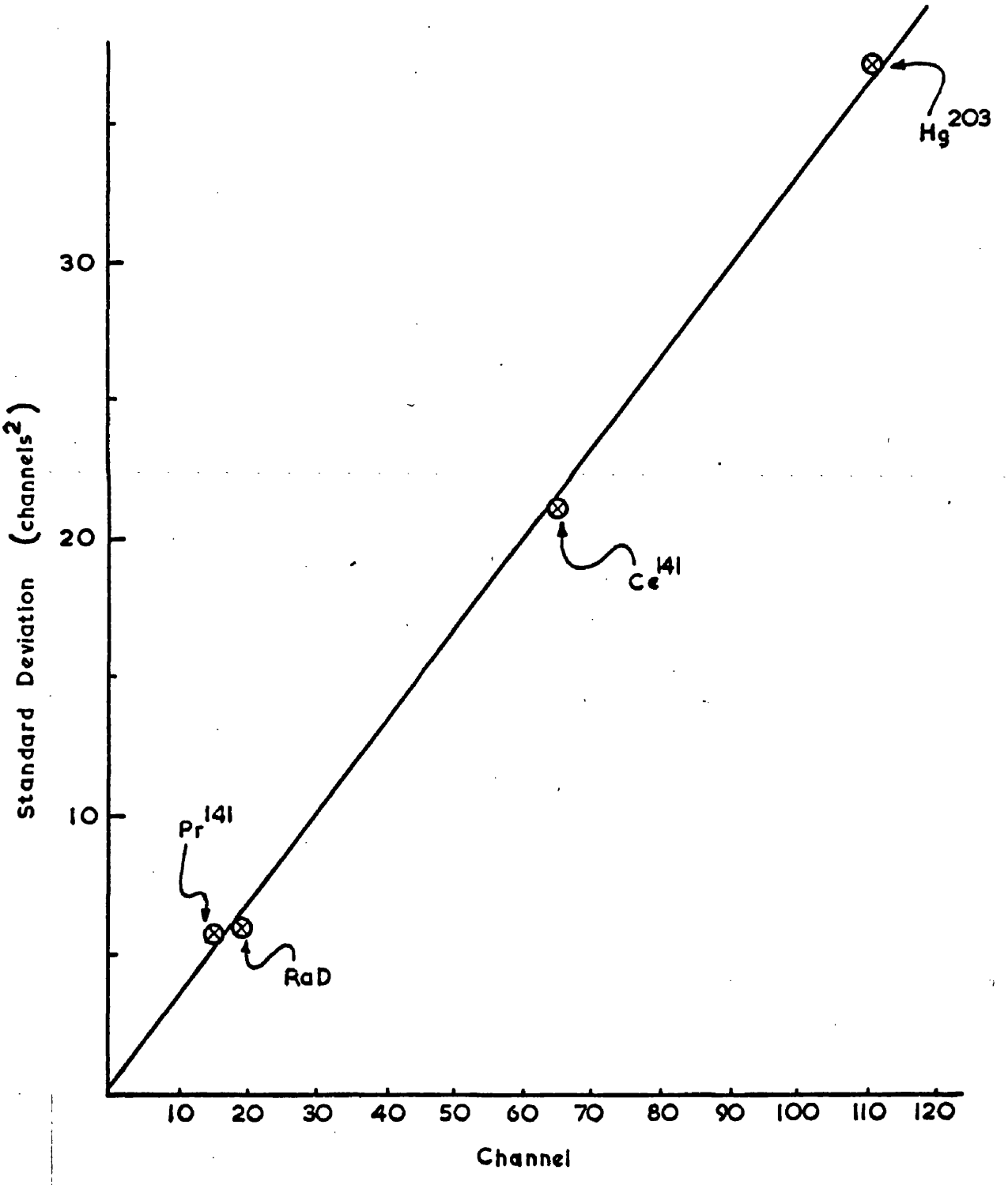

FIG. 3.8

Showing the variation of energy resolution with energy.

~~is 1/g and if there are R photoelectrons incident on the dynode the fractional variance on the number~~ leaving it will be $1/gR$. Similarly the fractional variances at the second, third etc. dynodes will be $1/g^2R$, $1/g^3R$ etc. Hence the total fractional variance is given by

$$v^2 = \frac{1}{R} + \frac{1}{gR} + \frac{1}{g^2R} + \text{----}$$

and since only the leading terms matter this can be written as:

$$v^2 = \frac{f}{R(g-1)} \qquad (3.7)$$

The fractional variance at different energies can be determined experimentally by measuring η where:

$$\eta = \frac{\text{full width at half height in keV}}{\text{energy in keV}} \qquad (3.8)$$

Now since, in general:

$$\text{FWR} = 2.36\,\sigma \qquad (3.9)$$

it follows that

$$\eta^2 = \frac{2.36^2 f}{R(g-1)} \qquad (3.10)$$

Hence if the stage gain g is known and if η is measured at a given energy R can be determined and hence F.

Fig. 3.8 is a graph of measured σ^2(in channels^2) plotted against the energy (in channels). Since this graph is roughly linear it means that η^2 varies as $1/E$ which

is as it should be. The stage gain g was determined for three stages as 4.1, 2.5 and 3.6, i.e. 3.4 on average. Since g cannot be determined for the first and most important dynode there is a considerable uncertainty in this factor. Altogether therefore the method is not very satisfactory.

The value finally determined for P was 2 ± 15% but this was not considered very reliable. The resolution can be degraded by various effects (Kelly et al. 1956, Derby et al. 1960, Monahan et al. 1960) and so the figure of 2 is acceptable only as a lower limit. In the next section it will be explained how a more accurate value of P = 25 ± 5% was obtained in quite a different way.

The results of this section are summarised in table 3.1.

Table 3.1

Scintillator	τ (sec) (*quoted by manufacturer)	Efficiency(%) of anthracene ± 2%	Photoelectrons per keV ± 5%
NaI(Tl)	$(2.34 \pm 0.12) \times 10^{-7}$	175	2.5
Anthracene	$(3.7 \pm 0.2) \times 10^{-8}$	100	1.4
Plastic NE 102	* 4×10^{-9} 7×10^{-9}	35	0.5
Liquid NE 211	* 3×10^{-9} 7×10^{-9}	33	0.47

(3.3) Main Measurements.

The quantities to be assessed were t_c and σ^2. Since the position of the centroid of any resolution curve depends, among other things, on the energies selected in the side channels a centroid shift method for determining t_c was adopted. The change in t_c produced by a change in energy was measured for a given scintillator by observing the centroid shift of the resolution curve. Thus the measurements of t_c were relative since the zero value of this quantity corresponds to the high energy limit and is inaccessible. When Bashandy (1960) was analysing his measurements he did so in terms of Δt in order to allow for this fact. This is not necessary however, and the interpretation is much more straightforward and the curves much clearer when t_c itself is used.

For each series of measurements a plastic scintillator was used in channel 1 and the energy selected in this channel was kept fixed. Thus the time delay for this channel was constant. The bias of the single channel analyser was first of all calibrated in terms of energy. This was done by gating energy pulses with the output of the analyser and feeding them to a kicksorter. Using a "window" of 0.5 volts (this means selecting a range of voltage of 0.5 volts) the kicksorter was calibrated in terms of the analyser bias. Different standard sources were then selected to produce

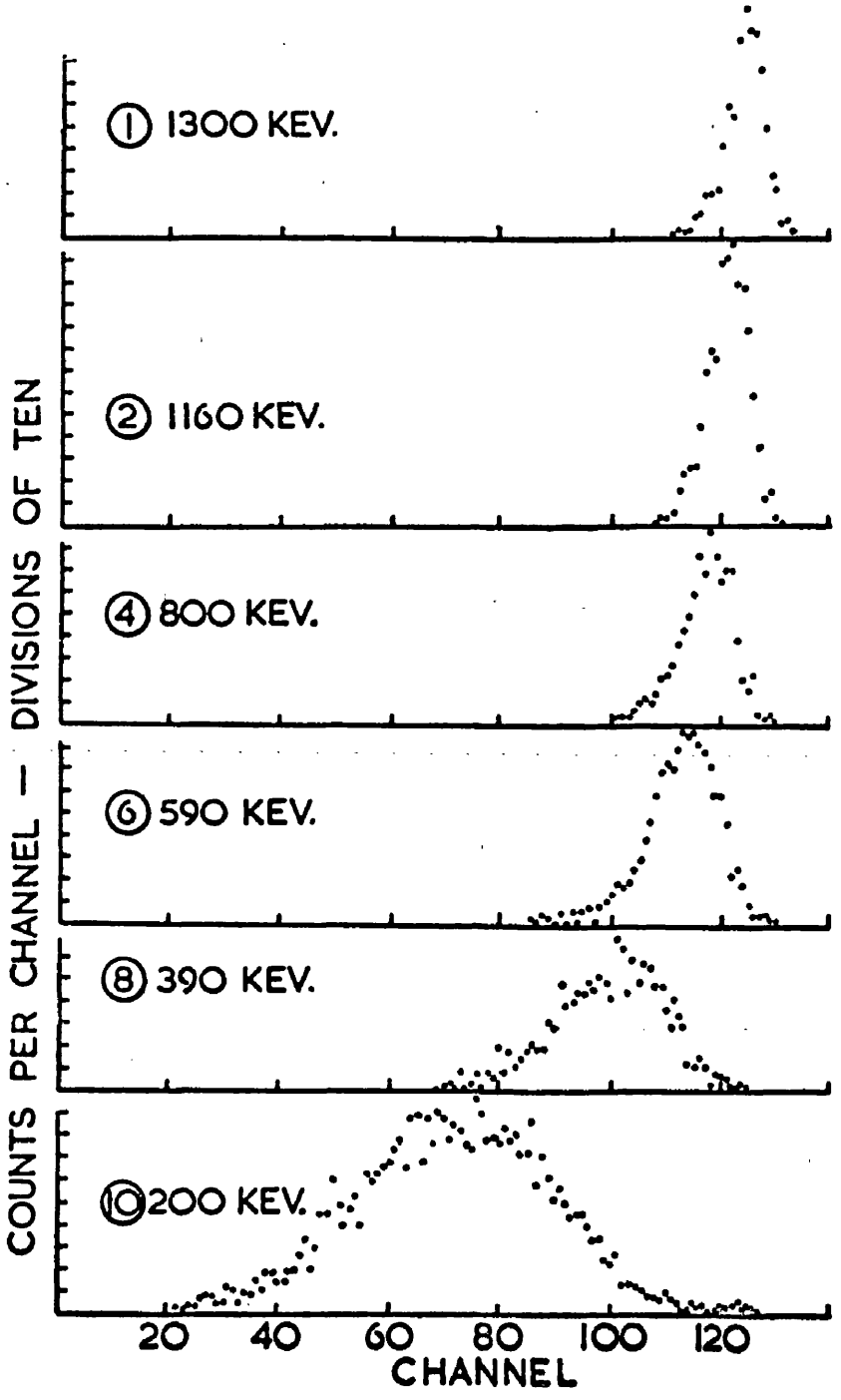

Illustrating how the change of instrumental time delay, t_c, with energy was measured for a NaI(Tl) scintillator in Channel 2. The peaks were recorded for the mean energies indicated. The odd numbered peaks (only No. 1 shown) were all recorded with electrons of 1300 keV and were used as reference peaks and for stability checks. In the case of NaI(Tl) and anthracene, the variation of resolving time with energy was also obtained from such shifted peaks.

FIG. 3.9

spectra on the kicksorter. From these an accurate calibration of single channel analyser bias in terms of energy could be quickly obtained.

The bias of the analyser in channel 2 was then varied systematically and coincidence resolution curves were recorded on the kicksorter for each bias and window setting. The results of such a series of measurements on NaI(Tl) are shown in fig. 3.9. The observed peaks give directly the variation of t_c with energy. Furthermore the broadening of these peaks at low energies is due almost entirely to statistical fluctuations in the emission of light from the NaI(Tl) and the contribution of this variance to the total width obviously outweighs the contributions from channel 1 and from other sources. Therefore these peaks are also adequate for obtaining the variation of σ^2 with energy for NaI(Tl).

With the organic phosphors the procedure was a little more complicated. In order to obtain large enough variations in t_c it was necessary to cover a wider range of energy than in fig. 3.9. This was best done by the use of Co^{60} γ-rays for high energies and Na^{22} γ-rays at low energies, thus avoiding overloading and paralysis troubles at low energies. For anthracene, plastic and liquid therefore, the curves giving t_c were obtained from a superposition of points obtained with different sources.

In the case of anthracene the variation of σ^2 could also be obtained from these shifted peaks, just as in the case of NaI(Tl). But with the plastic and liquid scintillators this method was not considered precise enough to give the small variations of σ^2 with energy, as found in these cases. The variation of t_c was found as above but that of σ^2 was obtained somewhat differently, as follows.

Both single channel analysers were calibrated in terms of energy and both were varied simultaneously so that the same energy range was selected in each channel. When this was done the centroid of the resolution curve did not move by more than $\pm 10^{-10}$ sec., thus indicating that the time delay in channel 1 was the same as that in channel 2. The changes in σ^2 were twice the changes which would have been produced had the energy been varied in only one channel, and a more accurate evaluation of the variation of σ^2 with energy could thus be obtained.

In most cases the measurements were repeated several times to improve the accuracy, especially at high energies where changes in t_c were small. Stability was checked all the time and energy and time calibrations were repeated frequently. In a series of measurements like those illustrated in fig. 3.9 the odd peaks (only No.1 shown) were all recorded at 1,300 keV and were used for stability

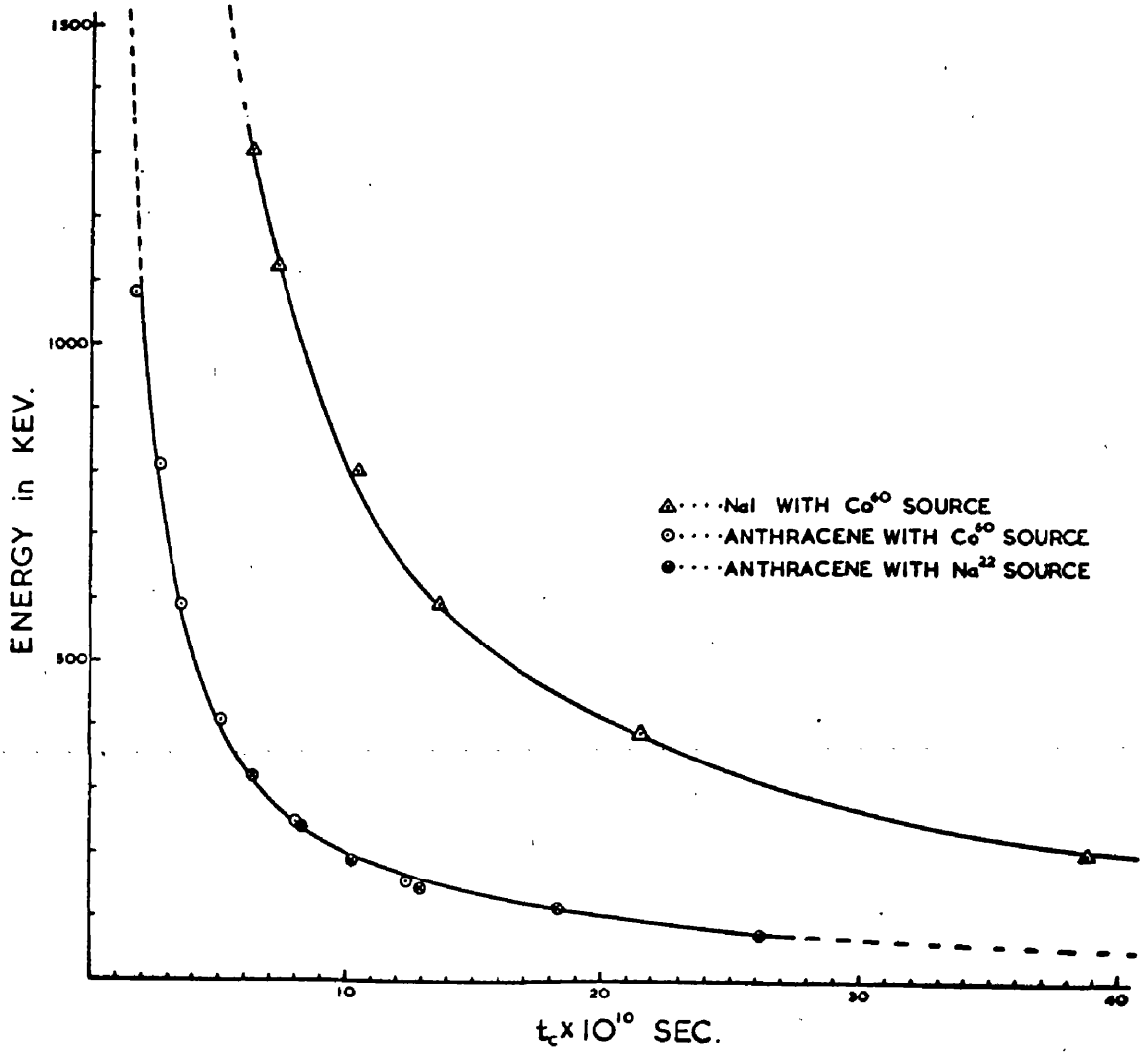

Change of instrumental time delay, t_c, with energy for NaI(Tl) and anthracene scintillators. The solid curves are the theoretical curves obtained from eq. (1) with $Q = 15$ and P (number of photoelectrons keV) = 2.5 and 1.4 for NaI(Tl) and anthracene respectively. The true zero of the t_c scale for the two curves (corresponding to the high energy limit) cannot be known experimentally. (The two experimental anthracene points at lowest energy were corrected to allow for slight non-linearity in the output of the scintillator.)

FIG. 3.10

checks. This was generally of the order of a few x 10^{-11} sec. over long periods.

It should be mentioned here that the problem of stability in the apparatus was a very serious one and held up these measurements for exactly one year. It was only after many tests and after the incorporation of numerous improvements that sufficiently good performance was obtained for the precision measurements of time delays etc. to be carried out.

(3.4) Results and Discussion.

(a) Time delays with NaI(Tl) and anthracene

The changes in time delay t_c for different energies in NaI(Tl) and anthracene scintillators are shown in fig. 3.10. For each material the experimental points were measured relative to one another. The solid curve drawn through the NaI(Tl) points was calculated from eq.(2.22) on the assumption that (Q + 1)/2 was the charge emitted at the photocathode by the liberation of 3.2 keV in the scintillator. Thus although Q itself was not known the ratio Q/R was essentially known and the points could be correctly plotted. The value of 3.2 keV for (Q + 1)/2 was chosen simply to make the curve fit the points, and the zero of the time scale was obtained from these considerations.

It was then found that the above figure for (Q + 1)/2, taken in conjunction with the measured relative efficiency

and decay time of anthracene gave the theoretical curve drawn through the anthracene points in fig. 3.10. The excellent fit in this case emphatically confirms the validity of the method and the correctness of the data.

When it was first attempted to make the data for the NE 102 plastic scintillator fit this scheme good agreement could not be obtained. Not only did the relative efficiency and decay time of NE 102 fail to give values of t_c consistent with the results for NaI(Tl) and anthracene, but the shape of the curve drawn through the plastic points was wrong. These points could not be fitted by an equation of the type (2.22) for any values of τ or Q. This matter will be reconsidered a little later.

(b) Determination of P and Q.

It has already been said that for a completely satisfactory description of time delays and resolution it is necessary to know Q and R as numbers of photoelectrons. In the last section it was seen that attempts to determine P, and hence R, by consideration of the energy resolution were neither accurate nor convincing enough to meet this demand. In the course of the work another method was found which does allow an accurate determination of Q. This method is neat and much more convincing than any of the earlier methods for the determination of either Q or P.

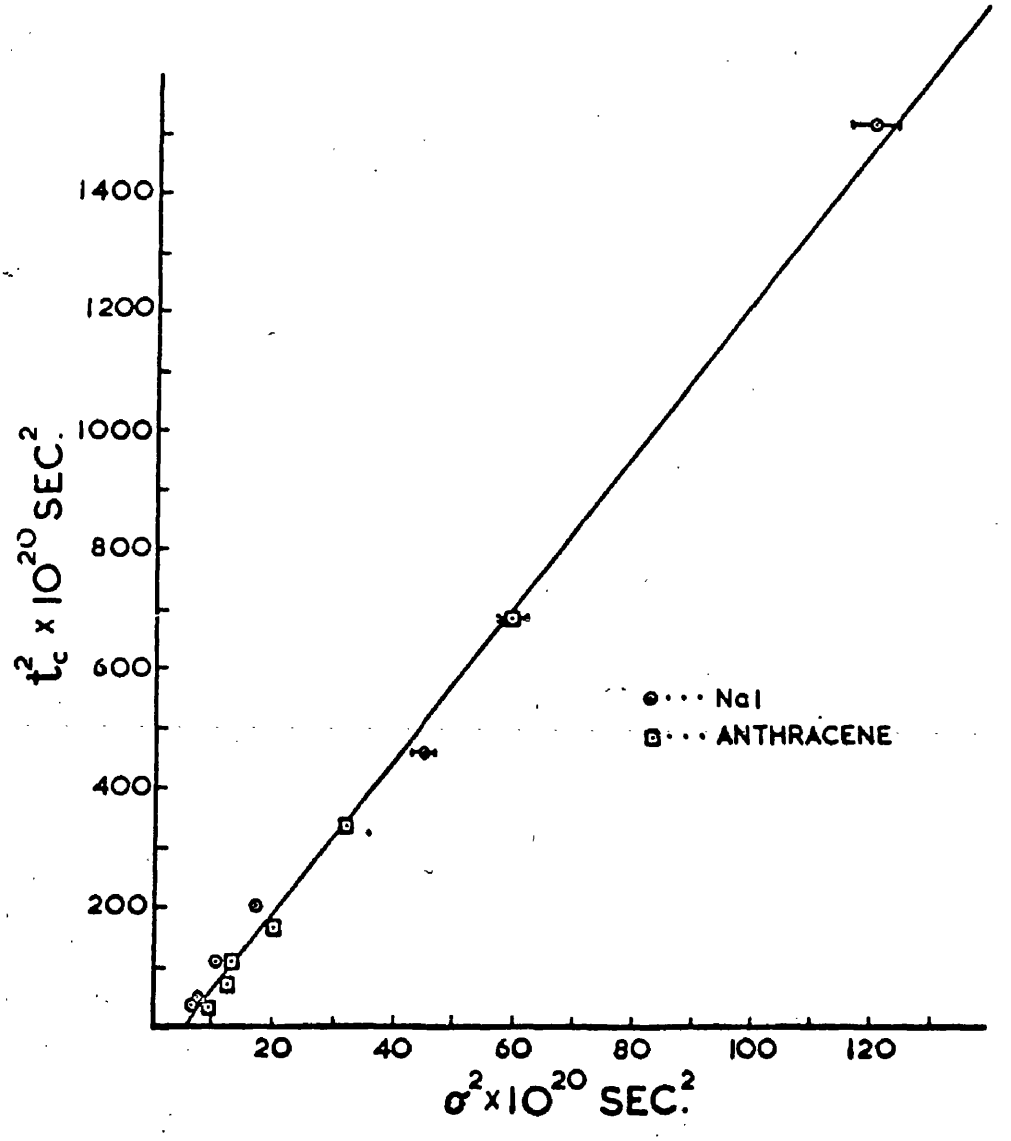

t_c^2 plotted against the variance for NaI(Tl) and anthracene for large values of t_c. By the use of eq. (4) and the gradient of the mean line drawn through the points, a value of 15 was obtained for Q, showing overall consistency of interpretation for large t_c. The line does not go through the origin because of the contribution to the variance from channel 1 scintillator and the multipliers.

FIG. 3.11

In the original Post-Schiff treatment an equation was given (eq. (2.14)) linking σ^2 and t_Q. To first order this equation is independent of R, viz:

$$\sigma^2 = \frac{1}{Q} t_Q^2 \qquad (3.11)$$

In the more accurate Gatti treatment the analogue of this equation is obtained from equations (2.22) and (2.23) and is

$$\sigma^2 = \frac{4}{3} \frac{Q}{(Q+1)^2} t_c^2 \qquad (3.12)$$

Since σ^2 and t_c^2 can be obtained directly from the curves of fig. 3.9 a plot of these can be made and should give a straight line with gradient determined by Q. This is shown in fig.3.11. Here points are plotted for both NaI(Tl) and anthracene. It will be noted that a line drawn through the points for NaI(Tl) makes an intercept on the σ^2 axis. This is the contribution to σ^2 from the multipliers and from the plastic scintillator in channel 1. It will be noticed also that the intercept for the anthracene points is slightly larger than for the NaI(Tl) points. The reason for this is that the anthracene points were obtained with a Na^{22} source, the NaI(Tl) points with a Co^{60} source. Hence the contribution from channel 1 was greater in the case of anthracene.

From the mean line drawn through the points a value of 15 is obtained for Q. This figure, taken in conjunction

with the value of 3.2 keV for $(Q + 1)/2$ quoted earlier gives a result for NaI(Tl) of:

$$P = 2.5 \pm 5\% \text{ photoelectrons/keV}$$

(c) Time delays with plastic and liquid.

It has been stated that the measured changes in t_c for plastic and liquid scintillators could not be accounted for by eq. (2.22). The reason for this is that in the case of these fast scintillators there is a considerable effect due to the parameter λ, eq.(2.26). This effect is most serious when λ/τ is appreciable and when $t_c \lesssim \lambda$. As explained in chapter 2, $C = Q$ only in the ideal case when $\lambda/\tau = 0$. In all other cases $C<Q$. This is because the limited speed of response of the multiplier (as measured by λ) to a delta function input (single photoelectron) introduces an additional delay whose energy dependence is different from that given in eq. (2.22). Put another way: when the limiter valve is cut off by C equivalent photoelectrons some of the information from the scintillator is still in transit in the multiplier. Hence Q, the number of actual photoelectrons is greater than C by the amount which is, effectively, still in transit.

It is to be expected therefore that the curves of Colombo et al. (1957), based on a full consideration of the implications of λ, will more adequately describe the performance of the plastic and liquid scintillators.

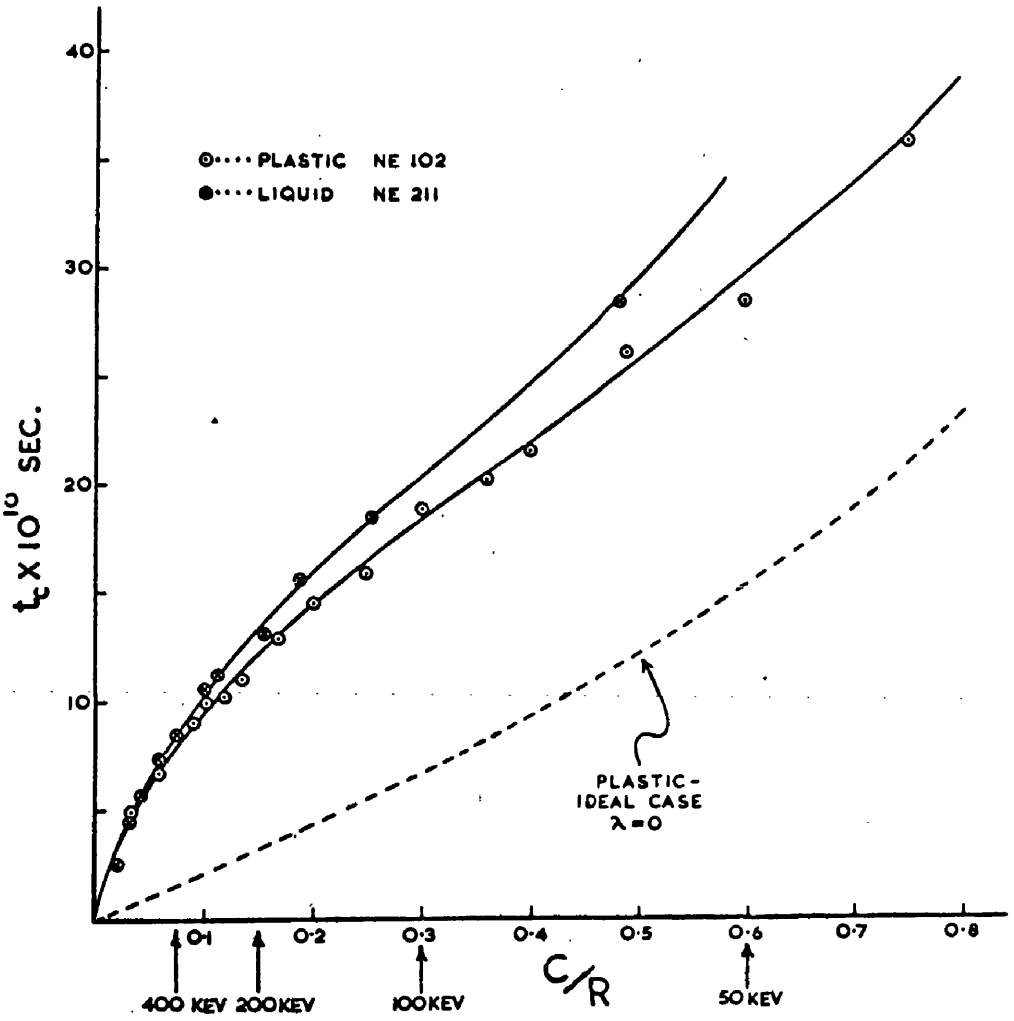

Fig. 8. Change of instrumental time delay with energy for plastic and liquid scintillators. This figure should be compared directly with fig. 7 of ref.[4]). C is the number of photoelectrons equivalent to the cut off charge. $C/R \propto 1/E$ where E is the energy liberated in the scintillator.

FIG. 3.12

Fig. 3.12 shows the data for these scintillators plotted after the fashion of fig. 2.10b which was taken from Colombo et al. (1957). If these two figures are compared it will be apparent that the Gatti description is a good one.

Following Colombo et al., calculations have been made in an effort to determine λ. In their paper it is shown that

$$C(t_1) = \int_0^{t_i} \underline{i}\,(t)dt \qquad (3.13)$$

where C is the charge collected in time t_1 and $\underline{i}(t)$ is the current output pulse of the photomultiplier:

$$\underline{i}(t) = \int_0^t I(t')\, f(t-t')dt' \qquad (3.14)$$

In (3.14) I(t) is the illumination function of the photocathode which, for simplicity, can be assumed in the calculations to be

$$I(t) = \frac{R}{\tau} \qquad (3.15)$$

Also, in (3.14) f(t) is the single electron response of the multiplier, assumed to be:

$$f(t) = c\left(e^{-\frac{1}{2}ct} - e^{-ct}\right) \qquad (3.16)$$

where $c = \sqrt{5}/\lambda$ in order to satisfy eq. (2.26).

In the paper referred to it is also shown that:

$$t_c = \frac{\int_0^{t_i} t\ \underline{i}\ (t)\ dt}{\int_0^{t_i} \underline{i}\ (t)\ dt} = \frac{\int_0^{t_i} t\ \underline{i}\ (t)\ dt}{C(t_i)} \qquad (3.17)$$

Assuming (3.15) and (3.16) calculations of t_c were made for various values of λ and it was found that the plastic curve of fig. 3.12 could be obtained roughly with $\lambda \approx 10^{-9}$ sec. The shape was not quite correct but this was probably due to the inadequacy of eq.(3.16). It was concluded therefore that the 6342-A tubes used for the measurements gave a single electron output whose second moment was ~1 nsec. That is to say the intrinsic rise time of the photomultiplier is ~2 nsec.

It may be asked whether or not λ has any effect on the NaI(Tl) and anthracene data. It can be seen in fig. 3.12 that for E ≤ 100 keV the actual curve for t_c has very much the same shape as the broken curve calculated from eq.(2.22). Thus the effect of λ at these energies is essentially an alteration in the zero of the time scale, by ~1.3 nsec. in this case. Calculations in which λ was assumed to be 1 nsec. showed that for NaI(Tl) and anthracene the shapes of the curves would not be affected in the energy ranges considered but that the zero of the time scale would be shifted by ~ 9 x 10^{-10} sec. in the case of the former and

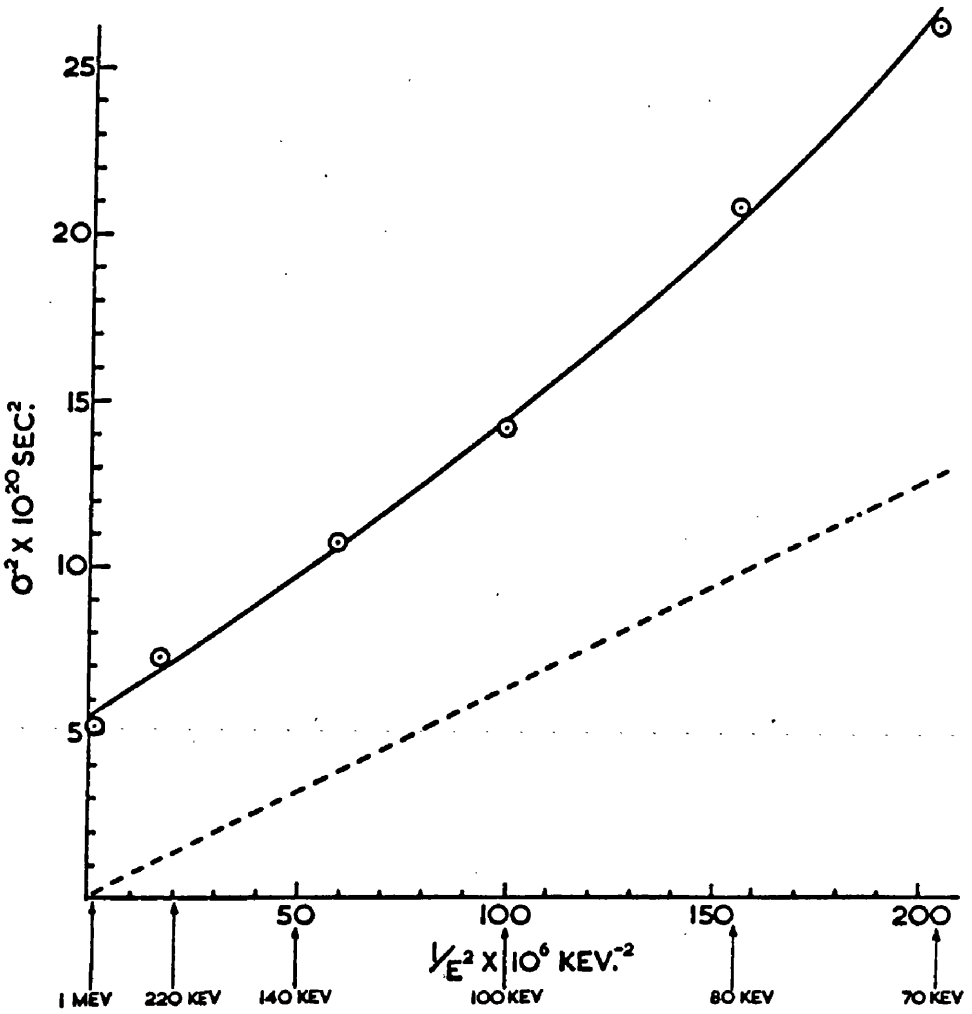

. A plot of the variance as a function of energy for a system of two counters with plastic scintillators. The energy "window" was changed by equal amounts in the two channels. The dotted curve shows the contribution to be expected from both scintillators on the basis of eq. (2). At high energies dominant contributions to the variance are attributable to the photomultiplier transit time variances (cf. text).

FIG. 3.13

$\sim 1.0 \times 10^{-9}$ sec. in the case of the latter. Only at very high energies would eq. (2.22) be seriously misleading for these scintillators. Thus, consideration of λ does not alter the earlier analysis of these data.

(d) Resolution with plastic.

It was explained in the last section how measurements of σ^2 for plastic were made by changing the energy in both channels simultaneously by equal amounts. The results were corrected for finite "window" width, i.e. allowance was made for the variation of t_c in the energy range selected by the use of fig. 3.12. Were eq. (2.23) for the variance strictly valid the contribution of the two plastic scintillators to the total variance would be correctly given by the broken curve of fig. 3.13 (assuming the data of Table 3.1 and $Q = 15$). The inclusion of a second order term in eq. (2.23) and the effects of gain fluctuations in the photomultiplier would raise the broken curve slightly at lower energies and make it concave upwards like the experimental curve. But there would still be a substantial gap $\gtrsim 5 \times 10^{-20}$ sec.^{2} between the two curves. The effect of the electronics, as exhibited by curve A in fig. 3.2b is of only minor importance and so this contribution of $\gtrsim 5 \times 10^{-20}$ sec.^{2} to the total variance must be largely the result of time spread in the photomultipliers, i.e.

interdynode fluctuations ε_{dd}^2 and photoelectron transit time fluctuations ε_{ph}^2.

As explained in chapter 2 these effects have been considered in detail by Colombo et al. (1957) and Gatti and Svelto (1959). In the latter paper it is assumed that λ arises from the cumulative effects of interdynode fluctuations and is given by

$$\lambda^2 = (n - 1)\,\varepsilon_{dd}^2 \qquad (3.18)$$

where n is the number of dynodes. This should not be confused with the variance on the centroid of the single electron response or with the variance on λ itself. From eq.(3.18) it follows that for the 6342-A and $\lambda \approx 10^{-9}$ sec., $\varepsilon_{dd} \approx 3 \times 10^{-10}$ sec. The effect that this has on σ^2 can be understood in terms of equations (2.29) and (2.30). The function Q(R) is always greater than Q so that σ_s^2 is increased by the effect of λ and σ_n^2 is decreased. Q(R) was obtained graphically from fig. 2.10a and it was found that the experimental curve of fig. 3.13 could be accounted for in the range 500 keV - 70 keV if it were assumed that:

$$\varepsilon_{ph} \approx 7 \times 10^{-10} \text{ sec.}$$

This is very reasonable since the maximum time delay between photoelectrons leaving the centre of the photocathode and others leaving the circumference of a circle 2.85 cm. in diameter is quoted by the manufacturers of the 6342-A as

1.3 nsec. For a circle 2.5 cm. in diameter, as used in the measurements, the maximum relative delay will be 1.0 - 1.2 nsec. and the r.m.s. delay should be about $1/\sqrt{2}$ times this, i.e. $\sim 8 \times 10^{-10}$ sec. It must be remembered that in the experiment the tubes were run at higher voltages than recommended so that ε_{ph} should be lower than the figure just quoted. Also it is apparent from eq. (2.24) that there is a contribution to ε_{ph} from the dynodes. However, this is only ~6% and so ε_{ph}^2 can be almost entirely attributed to the transit time fluctuations between photocathode and first dynode.

Above about 500 keV only one measurement was made, not sufficient to give the exact variation of σ^2 with $1/E^2$. From equations (2.29) and (2.30) it is expected that σ^2 should tend to zero at very high energies (several MeV). This would mean that the solid line in fig. 3.13 would not intersect the σ^2 axis at the point shown but at a lower point determined mainly by the electronics.

An important conclusion to be drawn from all this is that in the apparatus used for these measurements the contribution of the scintillators (in the case of plastic) to the FWR is outweighed by the contribution from the multipliers. Fig. 3.13 reveals that at 1 MeV the contribution of the scintillators accounts for less than 10% of the total variance. Here then it is desirable to

minimise σ^2. The procedure is, however, not as simple as eq. (2.20) suggests. The effect of λ must be taken into account. This matter has not yet been pursued any further but as a result of some correspondence with R.E.Bell it is intended to make further measurements which, it is hoped, will show how σ^2 may be minimised.

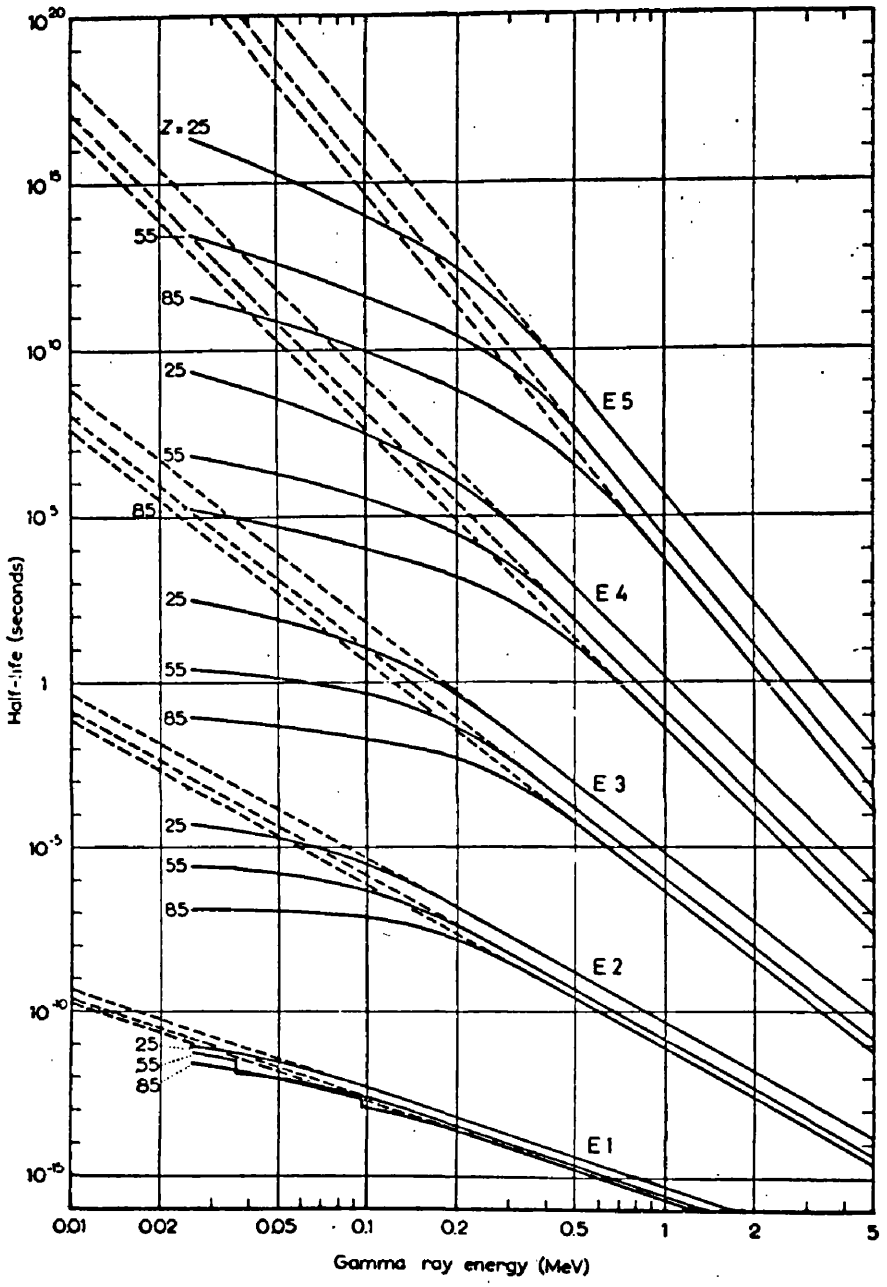

Fig. 4.1 Half-lives for gamma ray emission (Weisskopf estimate) with (drawn lines) and without (dashed lines) correction for conversion. Electric multipoles.

CHAPTER 4

LIFETIME OF THE 2.083 MEV LEVEL IN Ce^{140}.

(4.1) Introduction

After several unsuccessful attempts had been made to observe perturbed angular correlation effects in the decay of Hf^{181} and Hg^{199} (for which see chapter 7) it was decided to attempt some measurements of isomeric lifetimes. Two of these had already been investigated (see also chapter 7) but without any success, and as there has been quite an intensive study of the lifetimes of excited states in recent years there is not a great deal of scope for measurements in this field. By the use of 14 MeV neutron reactions a number of interesting sources can be made and in chapters 5 and 6 the usefulness of this technique will be shown. This method of activation is one which seems never to have been used for the purpose of isomeric studies.

Another line of enquiry is the investigation of very low energy levels. Such levels are interesting not only from the general standpoint of nuclear isomerism but also from the point of view of the Mossbauer effect. They present quite a difficult problem in measurement techniques because although the radiative lifetime may be quite long, internal conversion is usually the dominant decay mode and the observed lifetime can therefore be quite short (see figs. 4.1 and 4.2). Two further factors that make such

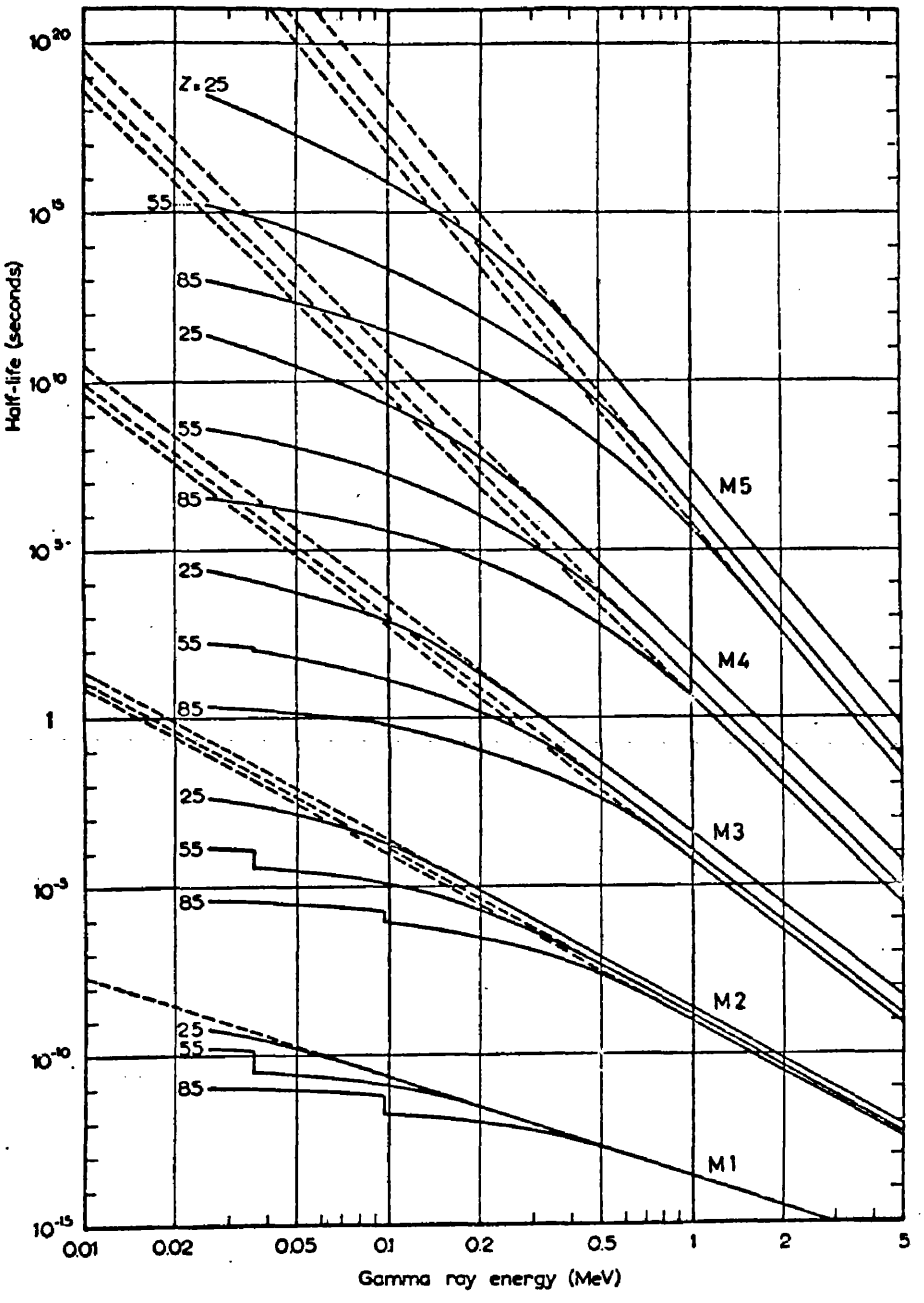

Fig. 4.2 Half-lives for gamma ray emission (Weisskopf estimate) with (drawn lines) and without (dashed lines) correction for conversion. Magnetic multipoles.

measurements difficult are the increased resolving time of fast coincidence systems at low energies and the widening gulf between photopeak energies and Compton edge energies. This last fact means that low-Z plastic scintillators, which have the best resolving times, become rapidly ineffective for Y-ray detection and time resolution as the energy is lowered.

As a result of these various factors a decrease in energy for any kind of transition faster than E3 is accompanied at ~100 keV by a more rapid increase in the time resolution than in the observed lifetime. Consequently low energy measurements are difficult. This has lead to a number of variations in measuring techniques. Since conversion coefficients increase as the energy is lowered it is better to detect the conversion electrons rather than the Y-rays. By this means Bell et al. (1960) have been able to determine mean lives of 3×10^{-10} sec. or so for levels as low as 43 keV from the slope of the delayed resolution curve. Beekhuis and de Waard (1958) developed a special technique of accelerating the low energy conversion electrons before detecting them and by this means were able to measure the lifetime of the 8 keV M1 transition in Tm^{169}. By the same means Beekhuis (reported in Boskma and de Waard 1959) was unable to determine the lifetime of the 30 keV level in La^{140}. He obtained only an upper limit of 3×10^{-9} sec. for this transition.

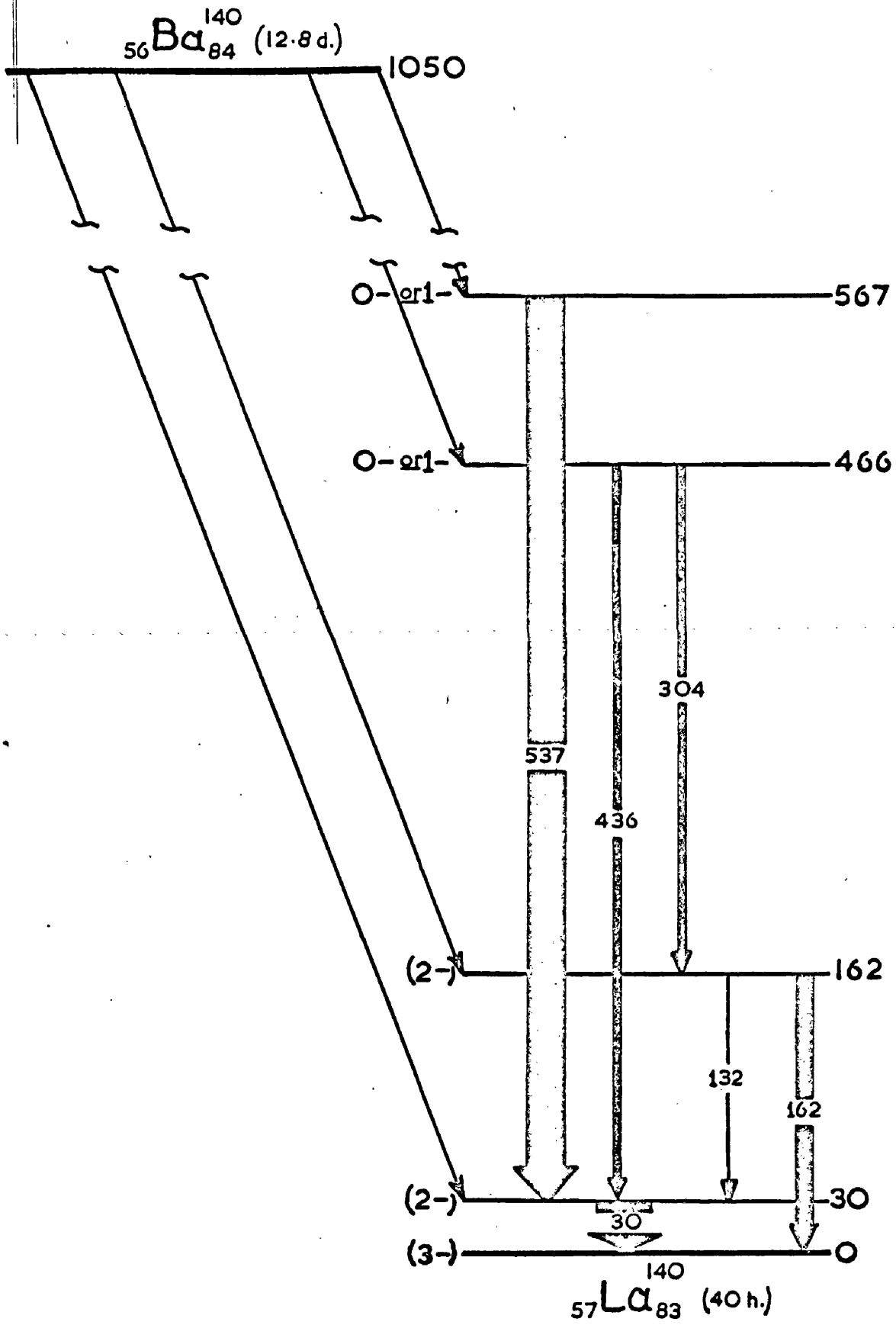

FIG. 4.3

Decay scheme of Ba^{140}

It seemed, therefore, that it might just be possible to determine this lifetime with the apparatus described in chapter 3. It was thought possible to obtain a FWH of $\sim 2 \times 10^{-9}$ sec. with one counter detecting 30 keV conversion electrons, in which case a lifetime of ~1 nsec. or more could be determined from the slope of the delayed resolution curve. On the basis of these considerations an attempt was made to measure the lifetime of the 30 keV level in La^{140} using a 13 day source of Ba^{140}, fig. 4.3

For the detection of conversion electrons the source has to be very thin and either placed directly on the scintillator or diffused within it. One drawback of the project was thought to be the radiation from the decay of the daughter La^{140}. This decay scheme (fig. 4.5) involves several high energy γ-rays which would prove a nuisance in the examination of the 30 keV level in La^{140}. Selection of the low energy radiation in the presence of so many high energy events would be difficult and overloading and paralysis effects would impair the time resolution.

For these reasons a specially thin scintillator (3.5×10^{-3} inches) was prepared for counter 2 and was mounted on a recently obtained 56AVP photomultiplier. Channel 1 detector consisted of a 6342-A multiplier with a disc of Ne 102, $\frac{1}{4}$ inch thick. The thin scintillator was prepared by placing a pellet of NE 102 between two plates of glass and loading with 12-14 lead blocks in an oven.

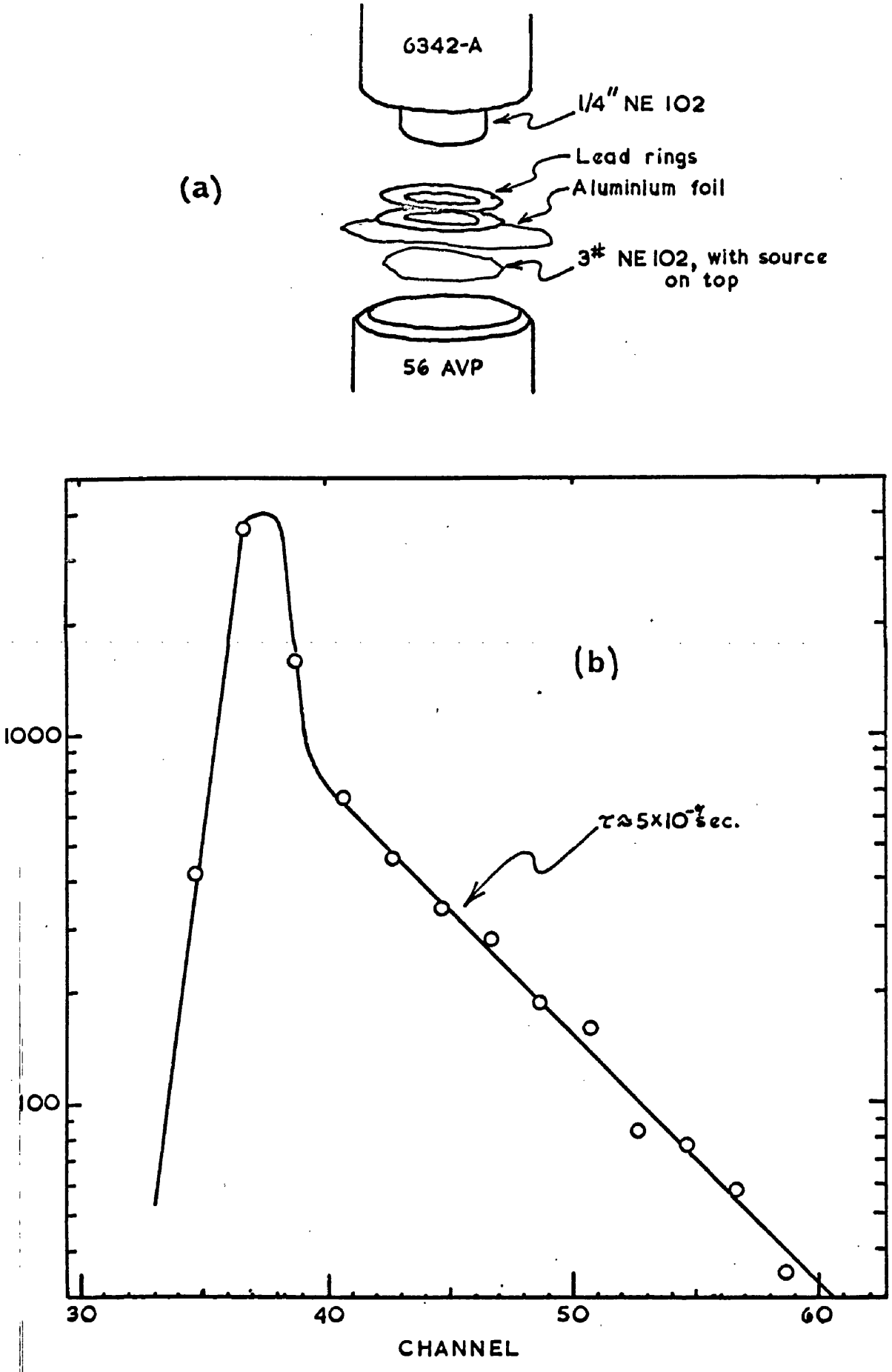

FIG. 4.4

Source arrangement and first delayed coincidence curve from Ba^{140} source.

The source was placed on the thin scintillator and the arrangement completed as shown in fig. 4.4a.

The time analyser was adjusted so that delayed conversion electrons detected in the thin scintillator would give rise to a delayed tail on the resolution curve, this tail coming on the lower or left hand side of the main peak. That is to say, events delayed in counter 2 would shift the peak to the left. When a pulse height spectrum was recorded the opposite was found. Fig. 4.4b was the first spectrum obtained. It suggested that the delayed events were being detected in counter 1 and that the mean life for these events was $\sim 5.3 \times 10^{-9}$ sec.

The only events which could be detected by counter 1 were the β-particles and the γ-rays. By varying the energy selection in channel 1 it was determined that the very highest energy pulses in counter 1 produced delayed events. It was concluded therefore that these events must be produced in the decay of La^{140}, i.e. the delayed level was in Ce^{140}. By further investigation with the Ba^{140} source it was established that the 2.083 MeV level in Ce^{140} (fig.4.5) was the delayed one. In order to eliminate the possibility of error or contamination a La^{140} source was obtained and was used to produce the results which will now be given.

The lifetime of the 30 keV state in La^{140} was never determined but will be the subject of further investigation

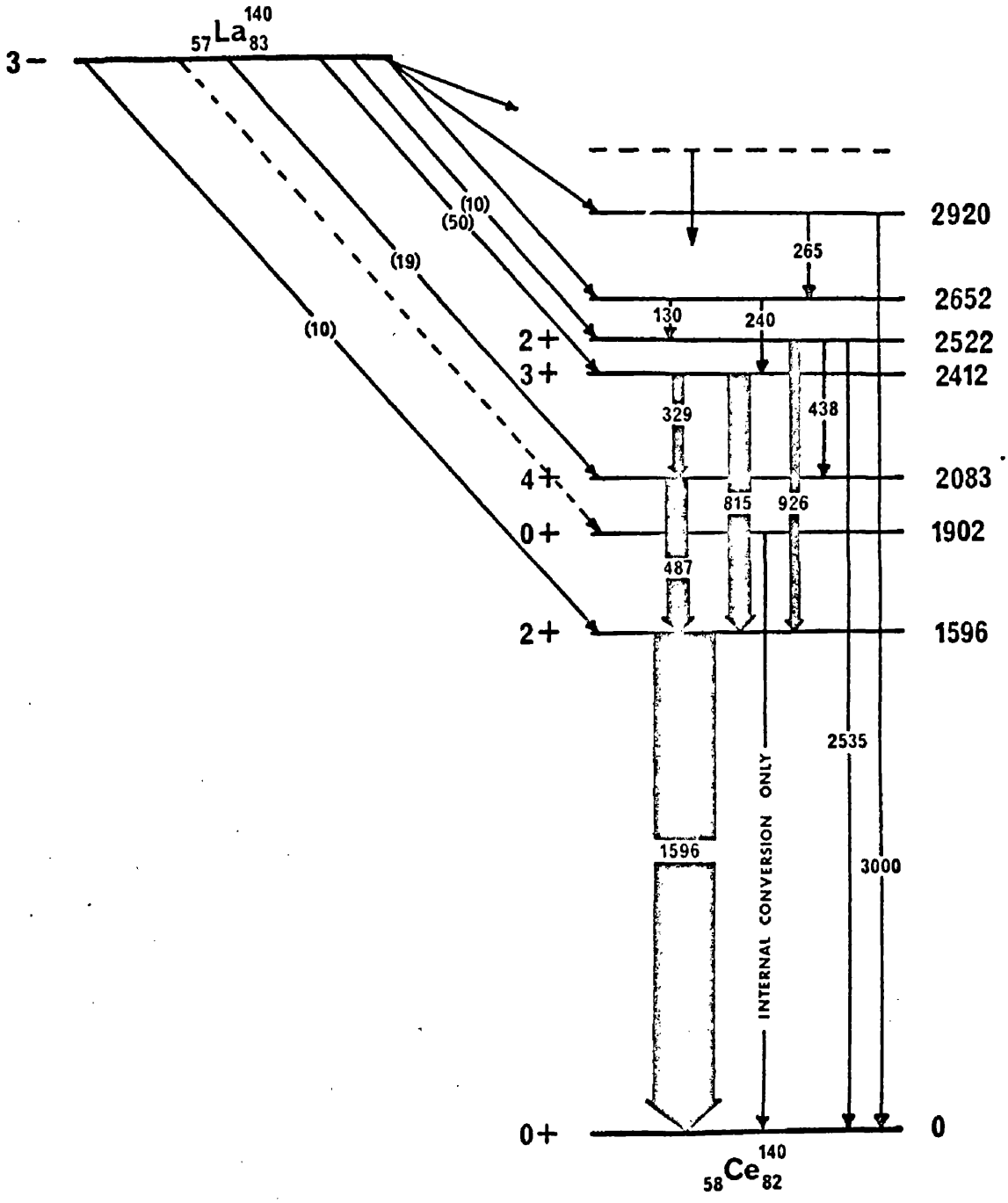

FIG. 4.5

Decay scheme of 40h La^{140}

with an improved technique for low energy work.

(4.2) Technique and Measurements.

The apparatus used in this experiment was essentially the same as that described in the last chapter. However, in order to demonstrate conclusively which level was the delayed one a special technique was used and for the clarification of this technique a block diagram of the system is given in fig. 4.6a.

Fig. 4.6b shows the sort of pulse height distribution which might be obtained from a time-to-pulse height converter when the source of the radiations contains both prompt and delayed levels (cf. fig. 4.4b). It is a mixture of a prompt peak and a delayed curve. Fig. 4.6a shows that the pulses from the time sorter (time-to-height converter) pass from amplifier 4 through a discriminator to the slow triple coincidence unit to provide a gating signal. At the same time these pulses are fed to a second discriminator (upper disc). When the latter fires, a veto pulse is applied to the gate cancelling the event. Thus if the lower discriminator is set at a level corresponding to A in fig. 4.6b and the upper discriminator at a level corresponding to B the lengthening gate passes pulses only when a prompt coincidence occurs. Similarly, if the discriminator levels correspond to C and D the gate will open only for delayed events.

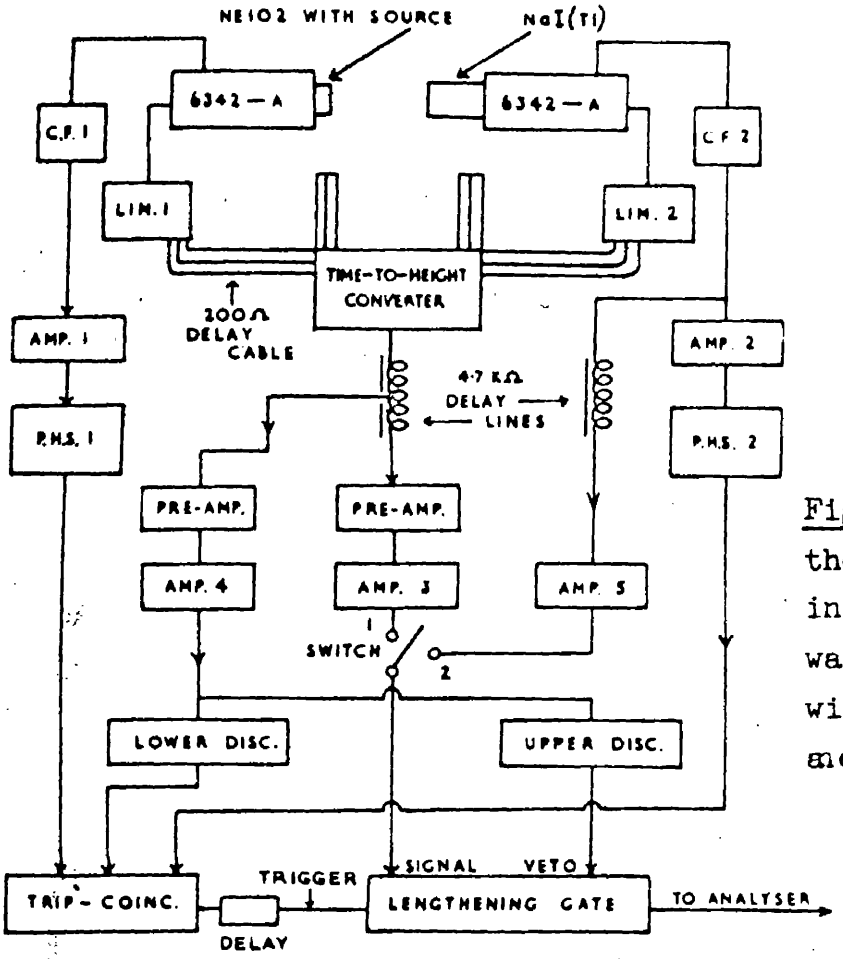

(A)

Fig.4.6(A) Block diagram of the apparatus. With the switch in position 1 a time spectrum was passed to the gate while with the switch in position 2 an energy spectrum was obtained.

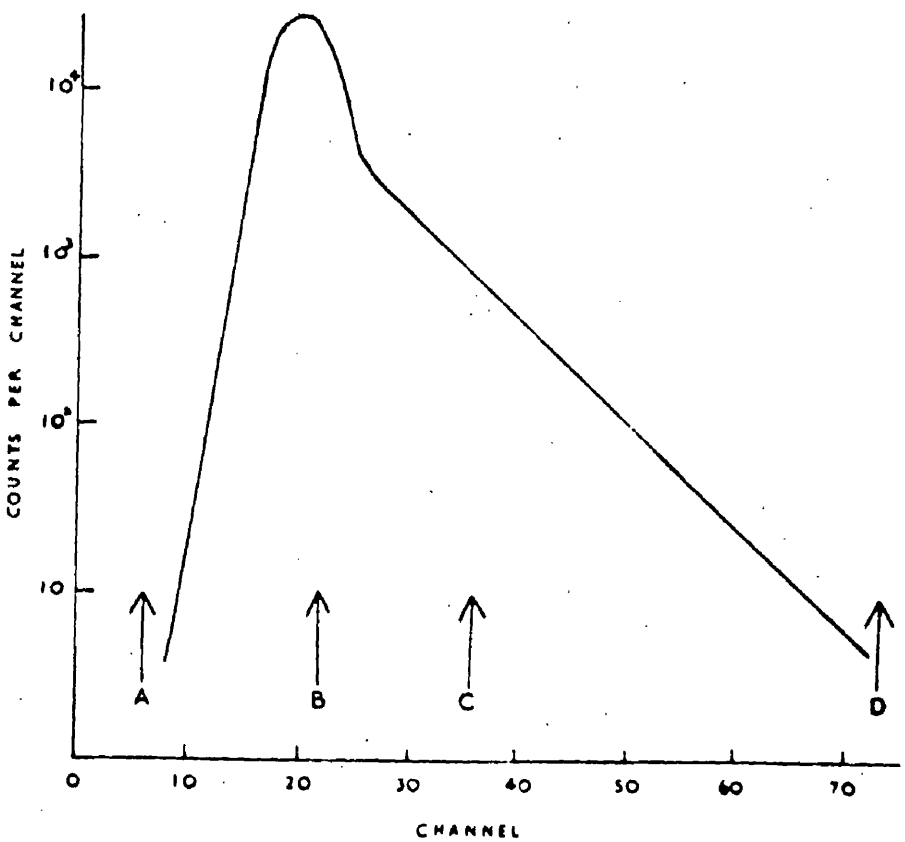

(B)

Fig.4.6(B) A typical time spectrum for a mixture of prompt and delayed events. Arrows A and B indicate the respective levels of the lower and upper discriminators used to open the gate for prompt events. Arrows C and D indicate the corresponding levels for delayed events. Details in text.

With the switch (fig. 4.6a) in position 1 the discriminators were adjusted while the delayed coincidence spectrum was observed on the screen of a multichannel analyser. The adjustment could be made so that the gate opened for prompt, delayed or all events as desired. The switch was then turned to position 2 so that energy pulses from channel 2 passed to the gate. In this way the radiations associated with prompt and delayed events could be analysed. Techniques of this kind have been used before. For instance a more rudimentary form of the present arrangement was used to elucidate a similar situation in the decay of Pb^{204m}(Krohn and Raboy 1954).

A minute quantity of active La_2O_3 was rubbed on to a disc of NE102 plastic scintillator 1.25cm x 1.9 cm. diam., and covered with aluminium foil. This scintillator, mounted on a 6342-A photomultiplier, constituted the β-detector (channel 1). The second detector(channel 2) for γ-rays was a 1" x 1" diam. NaI(Tl) scintillator also mounted on a 6342-A.

In order to use the technique just described it was necessary to take coincidences between β-particles stopping in the plastic scintillator and γ-rays stopping in the NaI(Tl). It was further necessary to select as wide an energy range as possible in the NaI(Tl), i.e. to select all energies above a certain minimum, this minimum being

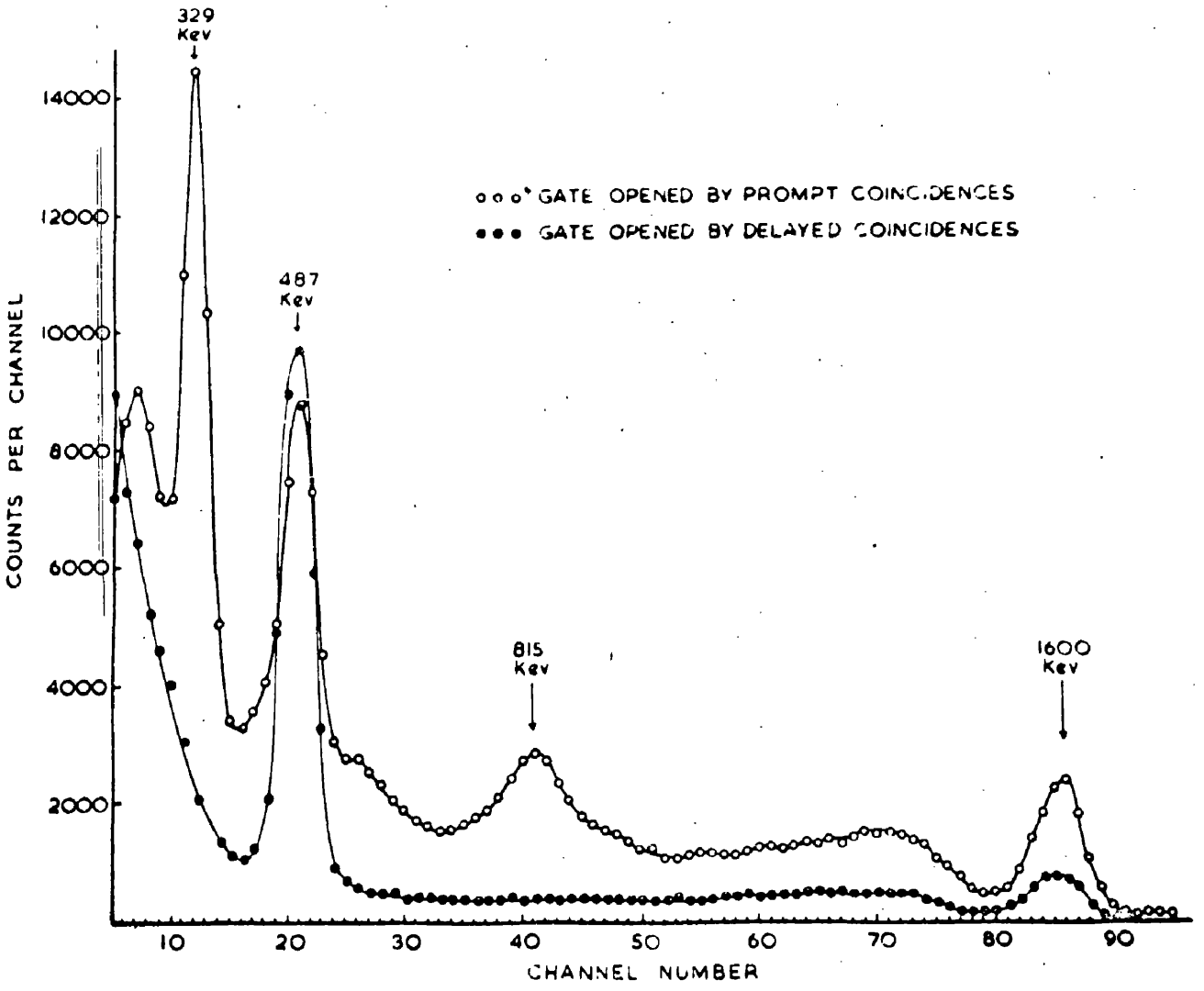

Fig. 4.7 γ-ray energy spectra from NaI(Tl) obtained by using first prompt, and then delayed β-γ coincidences to open the lengthening gate of fig. 4.6A, the switch being in position 2. These curves show that the 329 and 815 keV γ-rays are only in prompt coincidence with the β's while the 487 keV and 1.596 MeV γ-rays are also in delayed coincidence with them.

determined by the pulse height selector in that channel. The use of such a wide range of energies results in poor overall time resolution, not merely because σ^2 gets large at low energies but also because of the time delays t_c which augment σ^2 when t_c varies markedly over the energy "window".

In the present case the resolution of the γ-channel and its inherent time delays were small enough for delayed events to be separated unequivocally from prompt events even when the pulse height selector in this channel was set to select all energies above about 180 keV. Under these conditions, of course, the lower discriminator level (C in fig. 4.6b) had to be set quite high so as to exclude all low energy events delayed in the instrument. From fig. 3.10 it can be concluded that the delay associated with a 180 keV event in NaI(Tl) is $\sim 5 \times 10^{-9}$ sec. greater than that associated with a 1 MeV event, i.e. the difference in delay is about the same as the lifetime being measured. This consideration and the increased resolving time at 180 keV meant that, speaking in terms of time, level C had to be $\sim 10^{-8}$ sec. away from the high energy prompt peak, and this in turn led to a rather reduced counting rate.

With plastic as the β-detector in channel 1 a wide range of energies could be selected with little deterioration of resolving time. In this way, with the

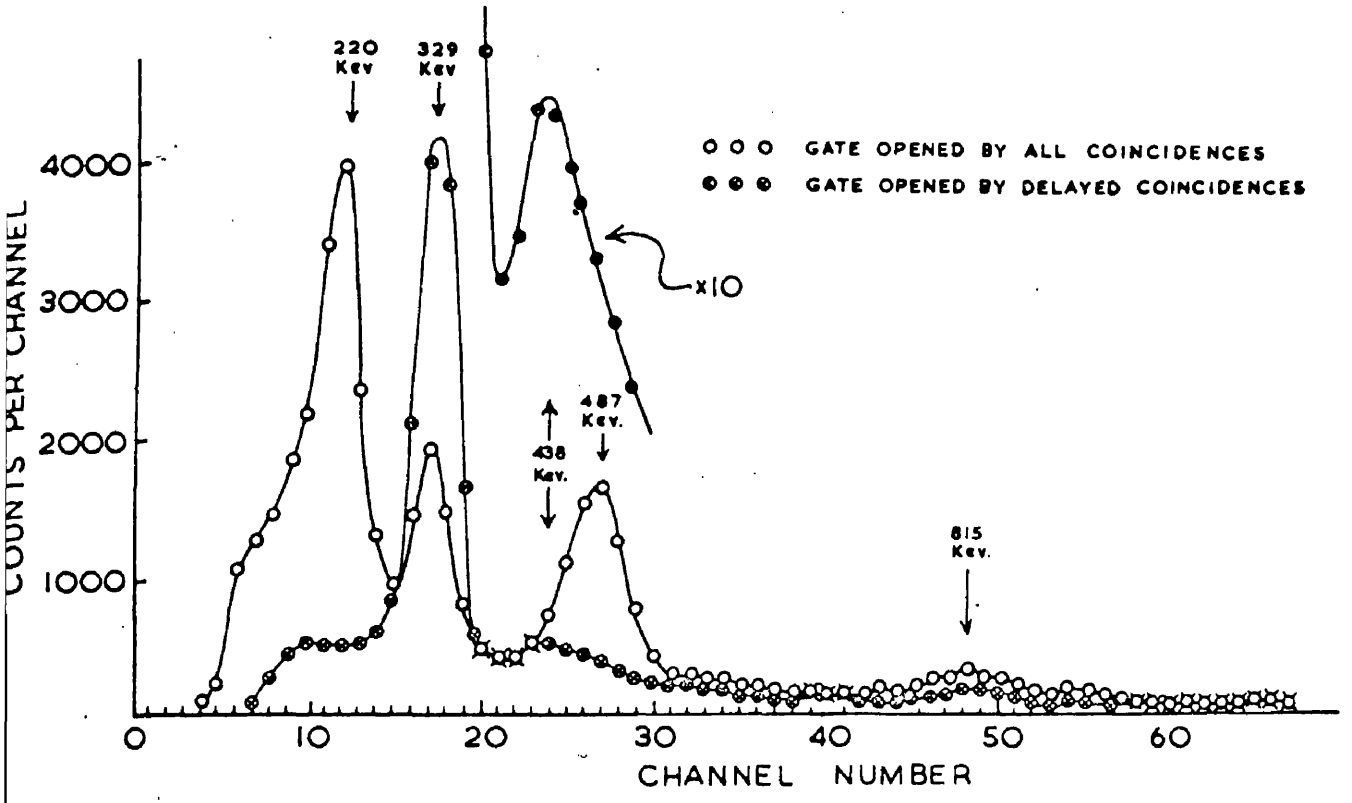

Fig. 4.8 γ-ray energy spectra from NaI(Tl) obtained by using first all, and then delayed γ-γ coincidences to open the lengthening gate of fig. 4.6A. One channel selected only the 1.596 MeV γ-ray while the other channel detected radiations in coincidence with this. The curves show that the 329 and, less clearly, the 438 keV γ-rays are in advance of the 1.596 MeV radiation. The peak at 220 keV was caused by back scattered photons from the 1.596 MeV γ-ray stopping in plastic.

two detectors pressed together and a fairly high counting rate in the β-channel both a good coincidence counting rate and a good real/random ratio were achieved.

With the arrangements just described the Y-ray spectra associated with both prompt and delayed events were recorded. These are shown in fig. 4.7. From these curves it can be inferred that the 487 keV and the 1.596 MeV Y-rays are delayed with respect to β-rays while the 329 and 815 keV Y-rays are not. This evidence by itself indicates the 2.083 MeV level as the delayed one.

For confirmation of these results the plastic disc in channel 1 was replaced by a larger encapsulated plastic scintillator and an external source was employed. Channel 1 was then used to detect the 1.596 MeV Y-ray while the NaI(Tl) scintillator in channel 2 detected Y-rays in coincidence with this radiation. Under these circumstances delayed coincidences in channel 2 were, strictly speaking, prior events; i.e. they were caused by Y-rays preceding the 1.596 MeV level by more than the resolving time of the apparatus.

Spectra were obtained for events both in general and in delayed coincidence with the 1.596 MeV radiation. These results are shown in fig. 4.8 from which it is apparent that the 329 and 438 keV Y-rays are advanced relative to the 1.596 MeV Y-ray while the 487 and 815 keV radiations are in prompt coincidence with it. This confirms that the 2.083

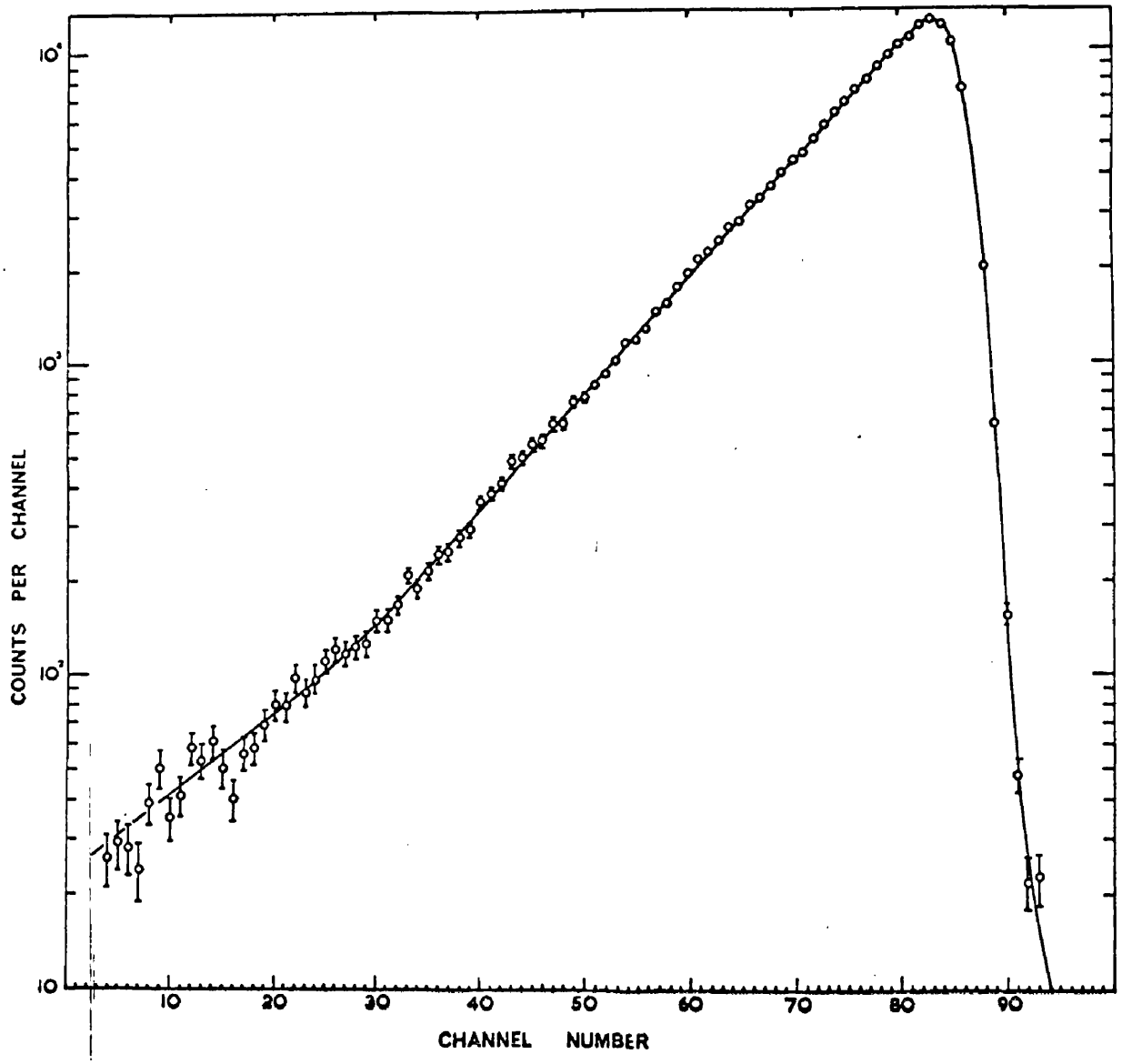

FIG. 4.9

Delayed coincidence curve obtained from β-γ coincidences with NaI(Tl) as the γ-ray detector and with the pulse-height selector in the γ-channel set on the central part of the 487 keV photopeak (1 channel = 4.25×10^{-10} sec). The extra counts below about channel 30 were caused by instrumental effects. From this curve the value $\tau = (4.96 \pm 0.13) \times 10^{-9}$ sec was found. From the average of three such curves each calibrated independently a value of $(4.97 \pm 0.09) \times 10^{-9}$ sec was obtained for the mean life, the greater part of the uncertainty being that of the cable velocity

MeV level is the delayed one. The "delayed" curve of fig. 4.8 is the only one which shows the 438 keV photopeak clearly. In the "all" curve of fig. 4.8 and the "prompt" curve of fig. 4.7 this peak is rendered invisible by the much larger 487 keV peak. The absence of the 438 keV contribution is nevertheless noticeable in the "delayed" curve of fig. 4.7. The 220 keV peak appearing in the "all coincidences" curve of fig. 4.8 was caused by Compton backscattered photons from the 1.596 MeV γ-ray stopping in the plastic scintillator.

The lifetime curve (fig. 4.9) was obtained from β-γ coincidences with the pulse height selector in the γ-channel set on the central part, of the 487 keV photopeak (see fig. 4.10). For this reason the admixture of prompt events is small.

(4.3) Result and Discussion.

A mean life of $(4.97 \pm 0.09) \times 10^{-9}$ sec. was obtained from the average of three separate measurements each giving a delayed coincidence curve like that of fig. 4.9. Since the internal conversion coefficient for this transition is ~0.01 (Bashilov et al. 1958, Bolotin et al. 1955) $\tau_\gamma \approx 5$ nsec by equation (1.9). The reduced lifetime is therefore

$$\tau_{red} = \tau_\gamma A^{4/3} E^5$$

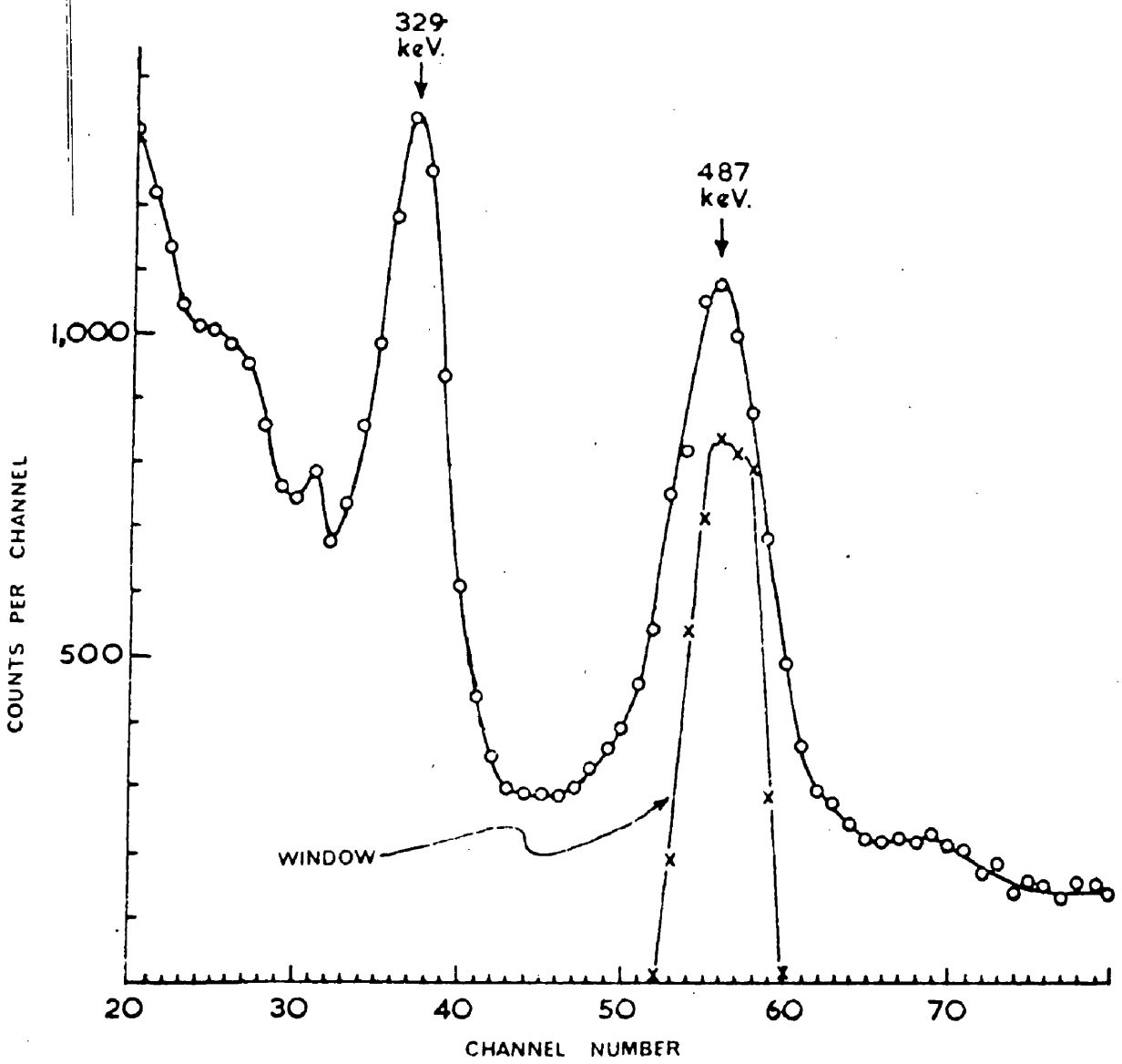

Fig. 4.10 Showing the "window", or range of energy selected in the γ-channel when fig. 5 was being recorded.

where E is in MeV. This gives almost exactly 10^{-7} sec. for the reduced lifetime, compared with the single particle estimate of 5.6×10^{-9} sec. for an E2 transition obtained from eq. (1.10). Thus, assuming an E2 transition the measured lifetime is 18 times longer than the single particle estimate. This contrasts strongly with the lifetime of the 1.596 MeV level which has been determined by nuclear resonance scattering to be $(1.10 \pm 0.15) \times 10^{-13}$ sec., 17 times shorter than the single particle estimate (Ofer and Schwarzschild 1959).

It would seem therefore that these two transitions in Ce^{140} are quite different in their reduced lifetimes. The difference was so marked that it was wondered if the 487 keV transition was M2. For an M2 transition of this energy eq. (1.11) gives 7.8×10^{-8} sec. for the single particle lifetime. This is just 15.5 times longer than the observed lifetime. The observed lifetime is therefore closer to the M2 prediction than to the E2 prediction. But according to fig. 1.4 the tendency (on the little data available) is for M2 lifetimes to be longer than the single particle estimate, not shorter. On the other hand the tendency is for E2 lifetimes to be shorter than the single particle estimate, not longer.

These doubts concerning the character of the 487 keV radiation were settled by an examination of the published data. Both the spins and the parities of the principal Ce^{140} levels were investigated by Bishop and Percy Y Yorba (1954).

For the first three excited states (excluding the 0+ state) they inferred two possible schemes: 2+, 4+, 3- or 2-, 4-, 3+. On the assumption (hydrodynamical model) that the first state must be a 2+ one they concluded that the first scheme was correct. If their experiment is assumed to have been unreliable the next two possibilities are 2+, 4+, 3+ and 2-, 4-, 3- which still imply an E2 transition from the 2.083 MeV level. The measurements would have to be in error by as much as 12% before the scheme 2+, 4-, 3- would be reasonable, making possible an M2 transition from the 2.083 MeV level.

Bolotin et al. (1955), Coleman (1955) and Kelly and Wiedenbeck (1956) also studied this scheme and on the basis of conversion coefficients and ratios, and directional correlation measurements they all found agreement with the assignment 2+, 4+, 3-. It did not seem reasonable in the face of so much evidence to regard the 487 keV transition as anything but E2.(note: none of these investigators were aware of the 0+ level at 1.9 MeV, concerning which see chapter 7)

The result of the measurement on Ce^{140} was thus concluded to be an unusually long E2 lifetime, and an explanation was therefore sought. The result was compared with known data on E2 lifetimes in even-even nuclei within the range $82 \leq N \leq 126$. This was done after the manner of fig. 1.10 (Sunyar 1955), as shown in fig. 4.11. Some

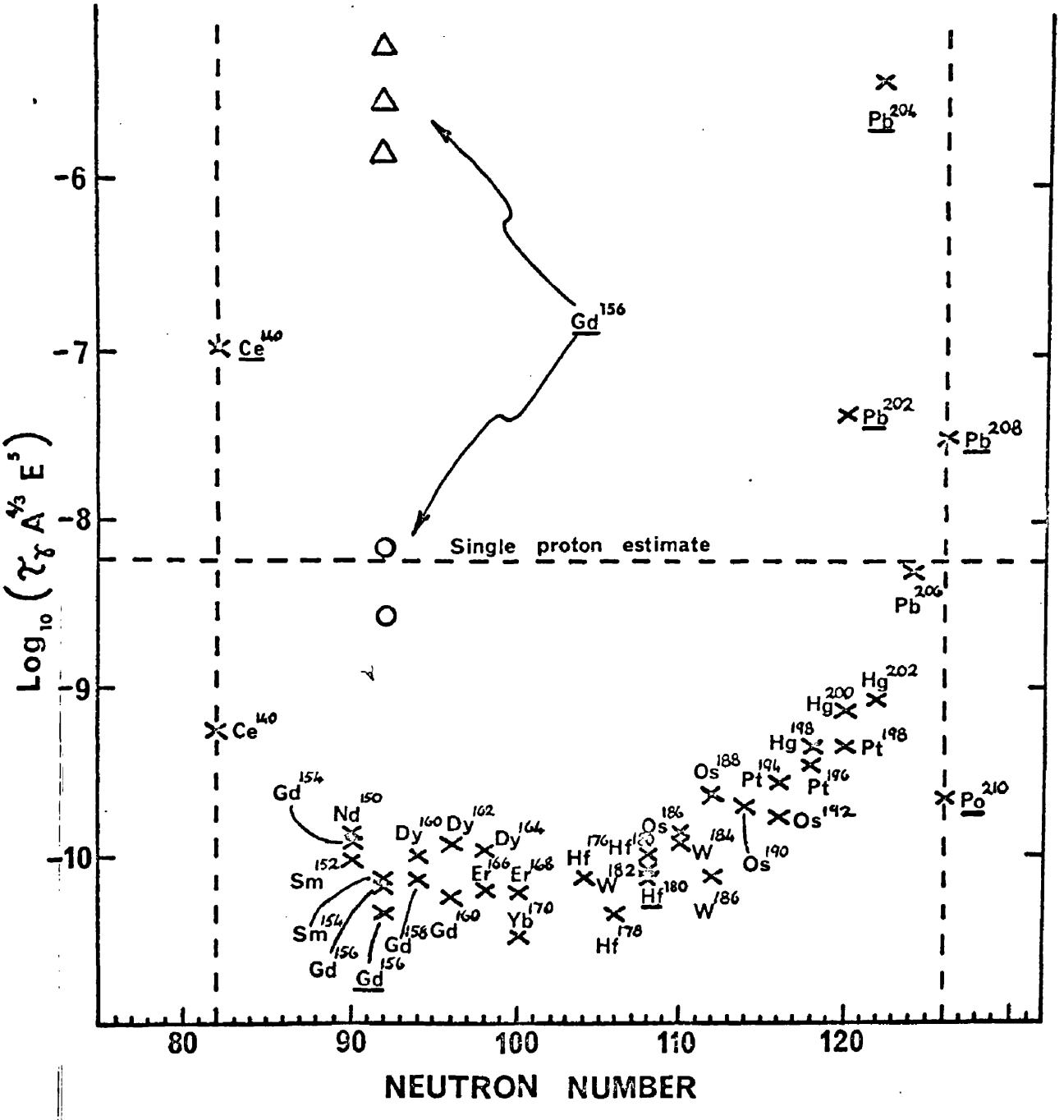

FIG. 4.11

Up-to-date plot of comparative E2 lifetime in the region $82 \leqq N \leqq 126$. The horizontal hatched line is the single proton estimate and underlined symbols refer to excited states higher than the first. The open circles ($\Delta K = 2$) and triangles ($\Delta K = 4$) are approximate and refer to the five branches in the decay of the 1.5 MeV level [19–21]) in Gd^{156}. In obtaining the points, measured values of conversion coefficients and ratios were used where possible and where not possible the tables by Rose [14]) were used. The figure should be compared with those in refs. [15, 16]).

discussion of these results is called for.

It can be seen that most recent data are in agreement with the general tendency for E2 lifetimes in this part of the periodic table, i.e. enhanced transition probabilities resulting from collective effects. Most of the data refer to first excited states, i.e. low lying rotational states, although the 2+ states in Ce^{140} and Pb^{206} are vibrational in nature. As explained in chapter 1 all these transitions should have enhanced probabilities. In Gd^{156} and Hf^{180} (Sunyar 1955, Birk et al. 1959, Sunyar 1958, Bell and Jørgenson 1959, Ofer 1959, Goldring and Vager 1961) the lifetimes for both the 2+ and the 4+ states of the K=0 band are known. As discussed in chapter 1 these should be in the ratio 10/7 (i.e. 1.43). The ratios for the measured values are approximately

Gd^{156} $\quad \frac{5.56}{4.0} = 1.39$ approx.

Hf^{180} $\quad \frac{10}{7.25} = 1.38$ "

Dy^{160} (Burde and Rakavy 1961) $= 1.65 \pm 0.33$

The last named figure is from a recent publication not available when fig. 4.11 was prepared. The agreement is quite good and suggests that this prediction of the unified model is precisely correct.

Fig. 4.11 shows several points which do not conform to the general rule. In the case of Gd^{156} the reason is

to be found in the discussion of chapter 1. There it was pointed out that where a transition between rotational states involves a change in the intrinsic state of the nucleus selection rules are liable to hinder the process. In fig. 4.11 the triangles and circles refer to the various branches in the decay of the 1.507 MeV level in Gd^{156} (Gregers-Hansen et al. 1959, Ofer 1959). The lifetime of this state has been measured, (Bell and Jørgensen 1959) and the branching ratios are known. On the basis of the interpretation of Gregers-Hansen et al. (1959) three of the branches have $\Delta K = 2$. Those are shown as circles in fig. 4.11 where it can be seen that they fall close to the single particle estimate. The other three are K-forbidden, with $\Delta K = 4$. They are represented by the triangles in fig. 4.11 and are slower than the single particle estimate by about 10^3. Thus, while purely collective effects always speed up an E2 transition, the combination of collective and intrinsic or single particle states can result in considerable slowing down of the decay process.

The other even-even levels with hindered E2 transitions can be seen in fig. 4.11 to be all higher than the first excited state and to occur in nuclei close to the magic numbers. These nuclei are not deformed and can more correctly be described by the hydrodynamical model. Pb^{208} is rather exceptional in having both N and Z magic. Pb^{204}, Pb^{202} and Ce^{140} all have similar spectra and the

hindered transitions are all from the second 4+ state to the first 2+ state. In the Pb isotopes there is also a higher 4+ state which probably corresponds to the two phonon excitation. The lower 4+ state is therefore a particle excitation of the 2+ state. The same applies to the 4+ state in Ce^{140}. Its first excited state is close (0.94) to the prediction of the hydrodynamical model (Coleman 1958). Hence the 4+ $\longrightarrow$ 2+ decay in each of these nuclei is rather similar to the K-forbidden decay in Gd^{156}, and the fact that these transitions are slower than the single particle estimate is in qualitative agreement with what happens in deformed nuclei when there is mixing of states.

In view of these various remarks it appears that the result for Ce^{140} is consistent with other data on collective effects. There is no precise theoretical prediction with which the result can be compared, as in the case of rotational excitations, but the overall systematics for E2 lifetimes in this region of the periodic table render the result much less surprising than it appeared at first.

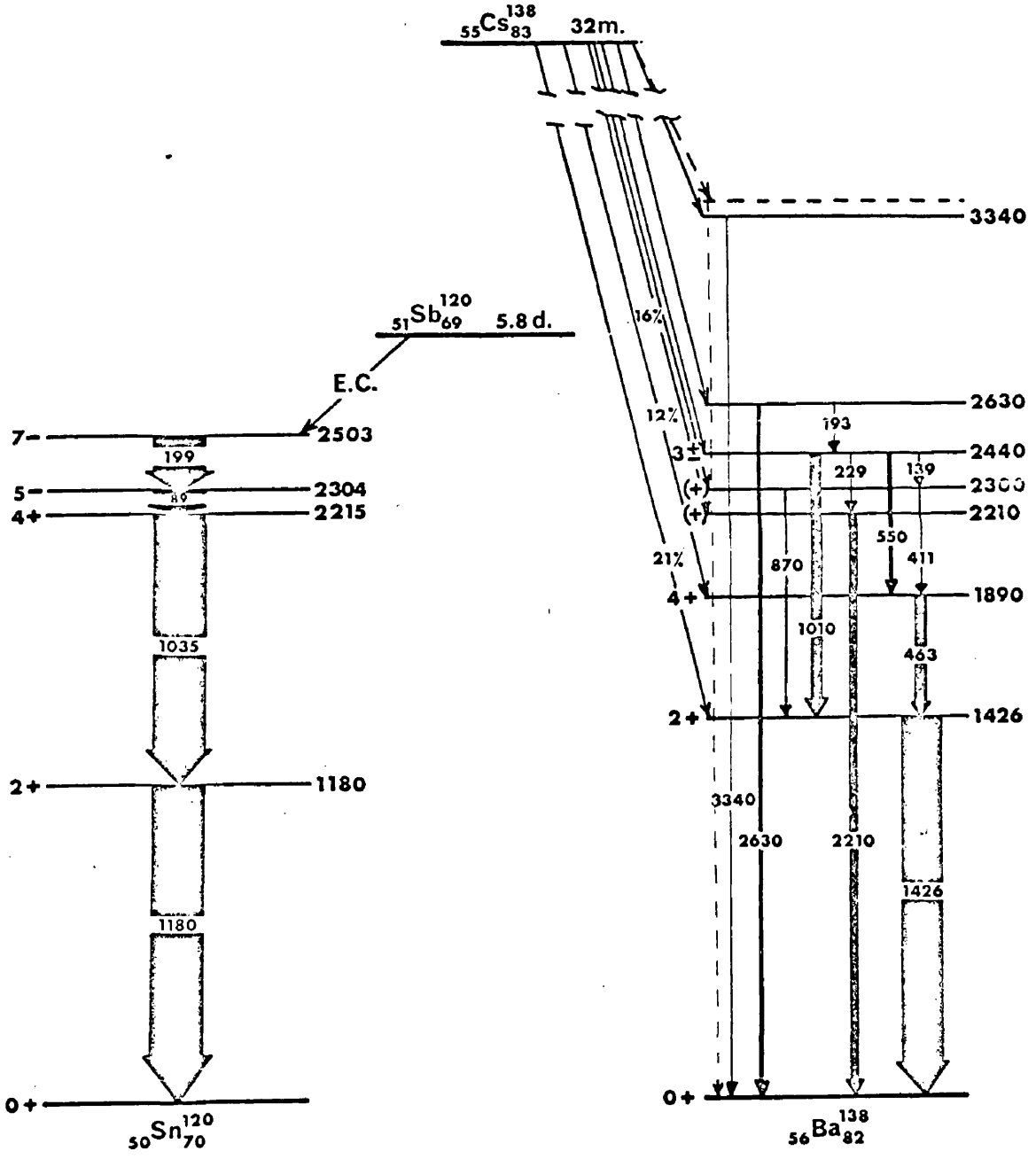

(a) (b)

FIG. 5.1

Decay schemes of Sb^{120} and Cs^{138}

CHAPTER 5.

ISOMERIC LIFETIMES IN Sn^{120} AND Ba^{138}.

(5.1) Introduction.

Following the discovery of the unusually long E2 lifetime in Ce^{140} other spherical nuclei showing both vibrational and particle excitations were sought. The possibility of similarly retarded E2 transitions in such nuclei was envisaged and it was considered a worthwhile matter for investigation. Great stress has been laid in the literature on the enhancement of most E2 transition probabilities and consequently a series of transitions of this multipolarity and character which did not exhibit the usual enhancement would provide an interesting addition to the data on isomeric states.

The first obvious nucleus for study was Ba^{138} (Thulin 1954, Bunker et al. 1956). This is produced by the decay of Cs^{138} and has a level structure, fig. 5.1b, very similar to that of La^{140}, cf. fig. 4.5. Ba^{138} also has N = 82 and the close resemblance between its levels and those of La^{140} immediately suggests that the 1.89 MeV level is a 4+ state and that the 463 keV transition from this level to the 1.43 MeV 2+ level is E2 and is retarded.

Cs^{138} (32m.) could be produced by the (n,p) reaction on Ba^{138} with 14 MeV neutrons from the H.T. set. The use of 14 MeV neutrons for source preparation had been tried quite a

long time before this and found very successful. It is discussed more fully in chapter 6.

Another nucleus to which some attention was given is Ba^{136}. The level scheme of this nucleus is rather different from that of Ba^{138} (Girgis and Van Lieshout 1959) and the parent Cs^{136} has a half-life which is rather long (13 days) for preparation by the above method. Production of this isotope would be both expensive and difficult. For these reasons it has not so far been explored.

No other nuclei in the region of $N = 82$ were found suitable for study. Attention was therefore directed to the regions of $Z = 50$ and $N = 50$. The only nucleus which was found to have a promising decay scheme and which could be obtained easily was $Sn^{120}(Z = 50)$. This is produced by the decay of Sb^{120}(5.8d) and has particle excitations superimposed on the two phonon excitation at 2.22 MeV (fig. 5.1a). The transition $6+ \longrightarrow 4+$ might therefore have quite a long lifetime. The parent nucleus could be produced by the (n, 2n) reaction on Sb^{121}.

(5.2) Lifetime of the 1.89 MeV Level in Ba^{138}.

Natural barium consists of 72% Ba^{138}, so if it is irradiated by 14 MeV neutrons 2.6 minute Ba^{137m} should be produced by the (n,2n) reaction, and 32 minute Cs^{138} by the (n,p) reaction (Thulin 1954, Bunker et al. 1956). (n,2n) reactions have quite high cross sections in general while the

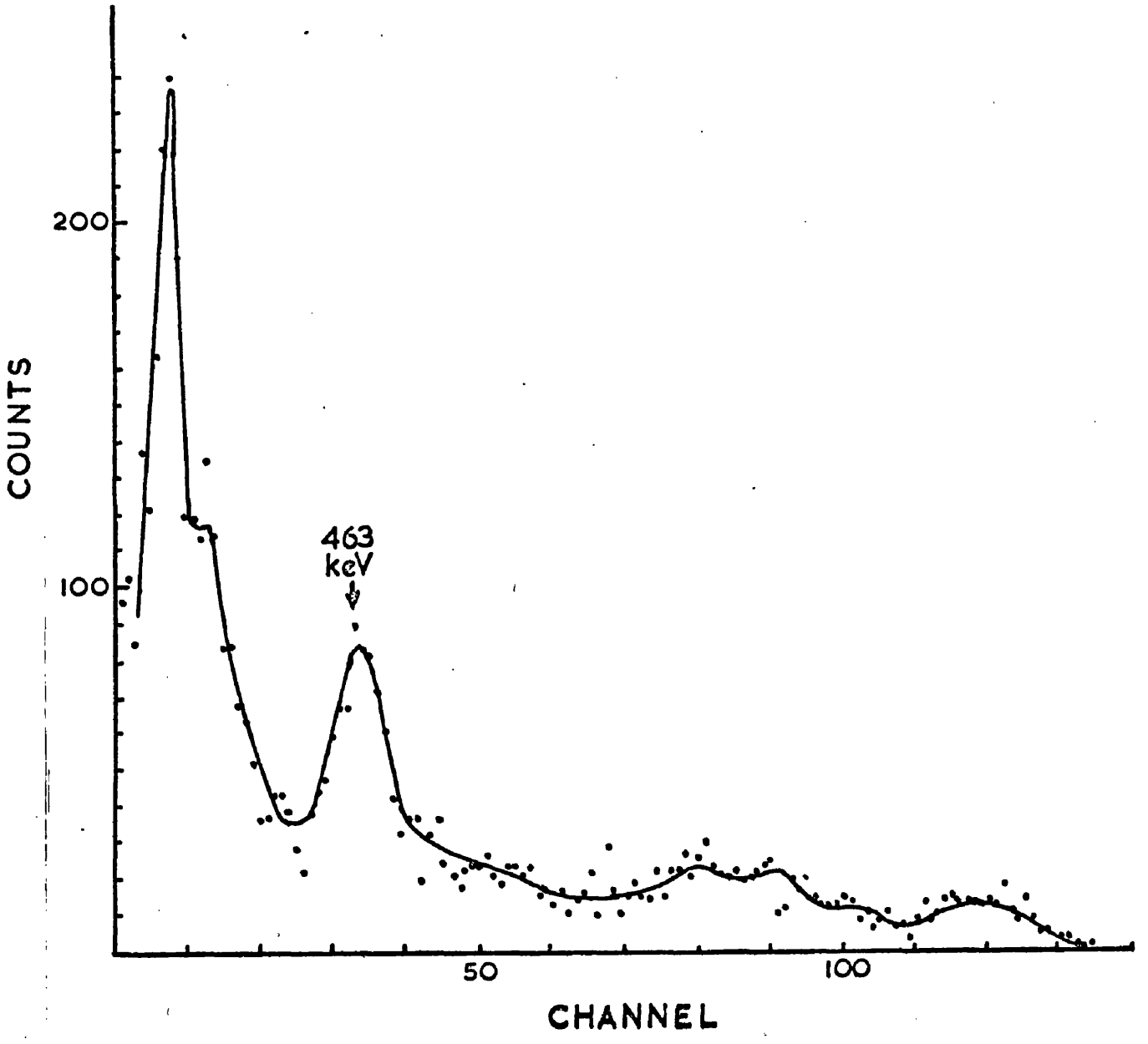

FIG. 5.2

Energy spectrum of Ba^{138} (gated by fast β-γ coincidence pulses)

(n,p) reactions are normally much less productive. Furthermore many early estimates of (n,p) cross sections have more recently been shown to be too high. For instance Paul and Clarke (1953) quoted the (n,p) cross section for Ba^{138} as 6.3 mb., while Coleman et al. (1959) obtained a figure of only 2.2 mb. for the same reaction. The production of Cs^{138} cannot therefore be expected to be very great.

Ordinary $BaSO_4$ was irradiated in the H.T. set and the resulting irradiations examined for the Cs^{138} activity. This could not be found. Instead, after the rapid decay of the 662 keV Ba^{137m} radiation, a prominent Y-ray of 385 keV, having a half-life of 2.8 hr. was observed. Other Y-rays were also observed but the 385 keV one stood out particularly and prevented any small 462 keV peak being seen. This 385 KeV Y-ray was not identified. Ba CO_3 was irradiated with the same result.

To get rid of the unwanted radiations 200 mg. of separated Ba^{138}, enriched to 97% and in the form of 287 mg. of $BaCO_3$, was bought from Oak Ridge National Laboratory. When this material was irradiated the only activities produced to a measureable degree were those of Ba^{137m} and Cs^{138}. That of Ba^{137m} was dominant but by the use of fast β-Y coincidences to open the gate (see fig. 4.6A) the energy spectrum in fig. 5.2 was obtained. This spectrum is not very impressive but it does show the 463 keV photopeak

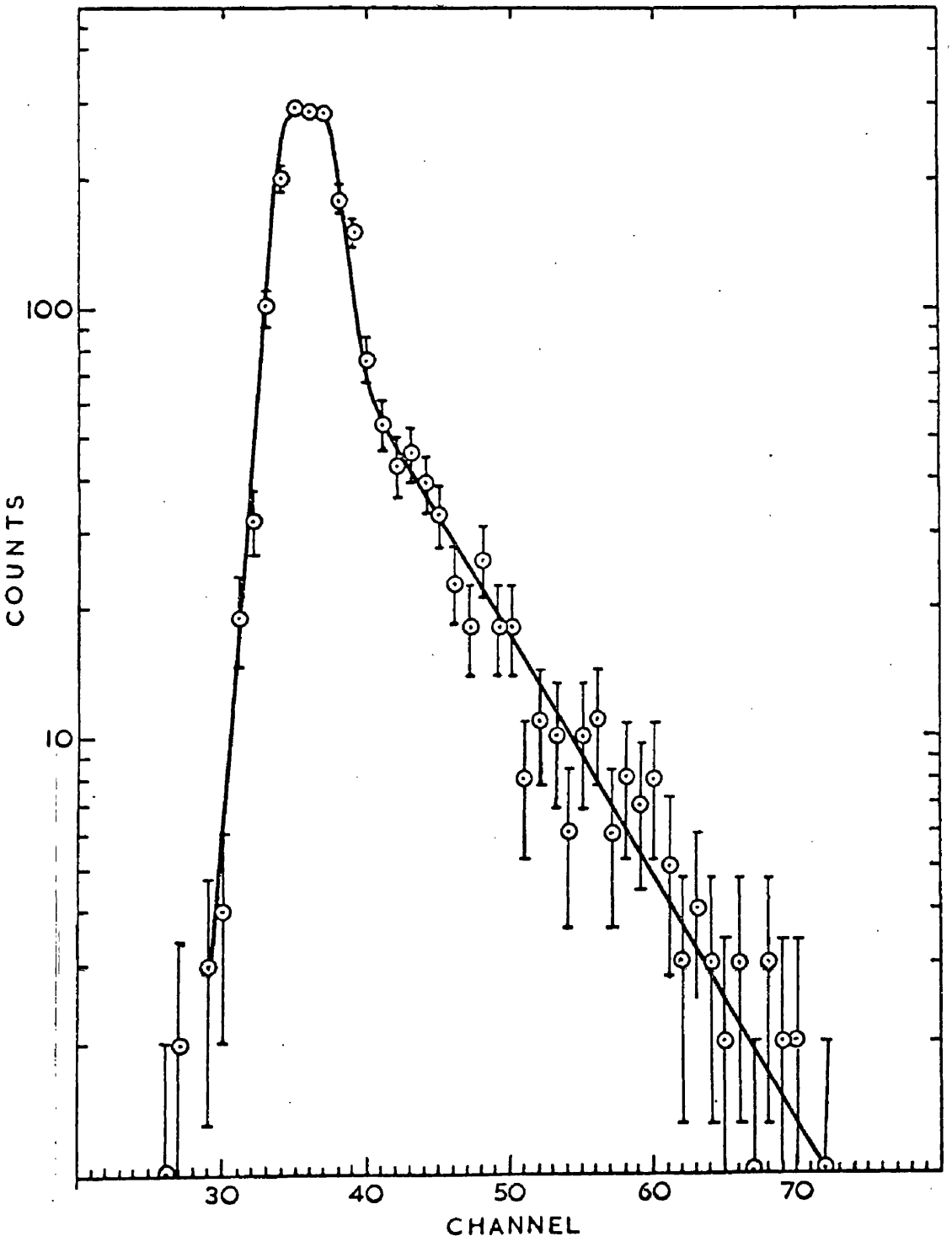

FIG. 5.3

β-γ delayed coincidence curve for the 1.89 MeV level of Ba138, yielding $\tau = (2.9 \pm 0.2) \times 10^{-9}$ sec.

and it was considered to be a reliable enough identification of the Ba^{138} activity.

The apparatus was then arranged for time measurement. A ¼" thick NE102 plastic scintillator, covered by thin aluminium foil and mounted on a 6342-A photomultiplier constituted the β-detector, while the Y-detector was a 1" x 1" diam. NaI(Tl) scintillator, also on a 6342-A. The energy selection window in the Y-channel was set roughly on the 463 keV photopeak and the delayed coincidence spectrum recorded for about three hours. The result is shown in fig. 5.3.

From this curve the mean life is derived as:

$$\tau = (2.9 \pm 0.2) \times 10^{-9} \text{ sec.}$$

Consequently the transition is just slightly slower than the single proton estimate. It is not as slow as its analogue in Ce^{140}, but neither is it enhanced as in so many other cases. Hence it may reasonably be concluded that the original thought concerning this transition was justified, and the result may therefore be lumped with those for Ce^{140} and the Pb isotopes as illustrating a slower kind of E2 transition which occurs when there is a mixing of states.

(5.3) Lifetime of the 2.31 MeV Level in Sn^{120}.

The level scheme of Sn^{120} has already been given, fig. 5.1a. This is the revised scheme. As originally proposed the second highest level was at 2.42 MeV and the

two low energy γ-rays were emitted in the opposite order from that shown in fig. 5.1a. It is only this experiment which allows the radiations to be put definitely in the order shown in fig. 5.1a.

The two high energy γ-rays are probably both E2 radiations from the decay of vibrational states, although the lifetime of the first state at 1.18 MeV is only slightly shorter than the single particle estimate. It was determined by Coulomb excitation to be 7×10^{-13} sec. (Stelson and McGowan 1957). The two low energy radiations are therefore very likely to come from the decay of mixed state similar to those in Ce^{140} and Ba^{138}.

The decay of Sb^{120}(5.8d) was investigated by McGinnis (1958). He showed by delayed coincidence methods that the 2.51 MeV level had a half-life of 11 μsec., and on the basis of the internal conversion coefficients he concluded that the 89 and 199 keV γ-rays were E1 and E2 respectively. McGinnis did not determine directly the order of these two γ-rays but inferred that the 89 keV photon was emitted first by the following argument.

The E1 transitions in Ag^{103} and Ag^{109} from the 410 keV 5/2 - level to the 7/2 + level have a half-life of $\sim 9 \times 10^{-9}$ sec. which is 10^6 times longer than the single proton estimate. If the 89 keV E1 γ-ray is emitted in the decay of the 11 μsec. level in Sn^{120} its lifetime is 4×10^7 times greater than the single particle estimate, while if this level decays by the

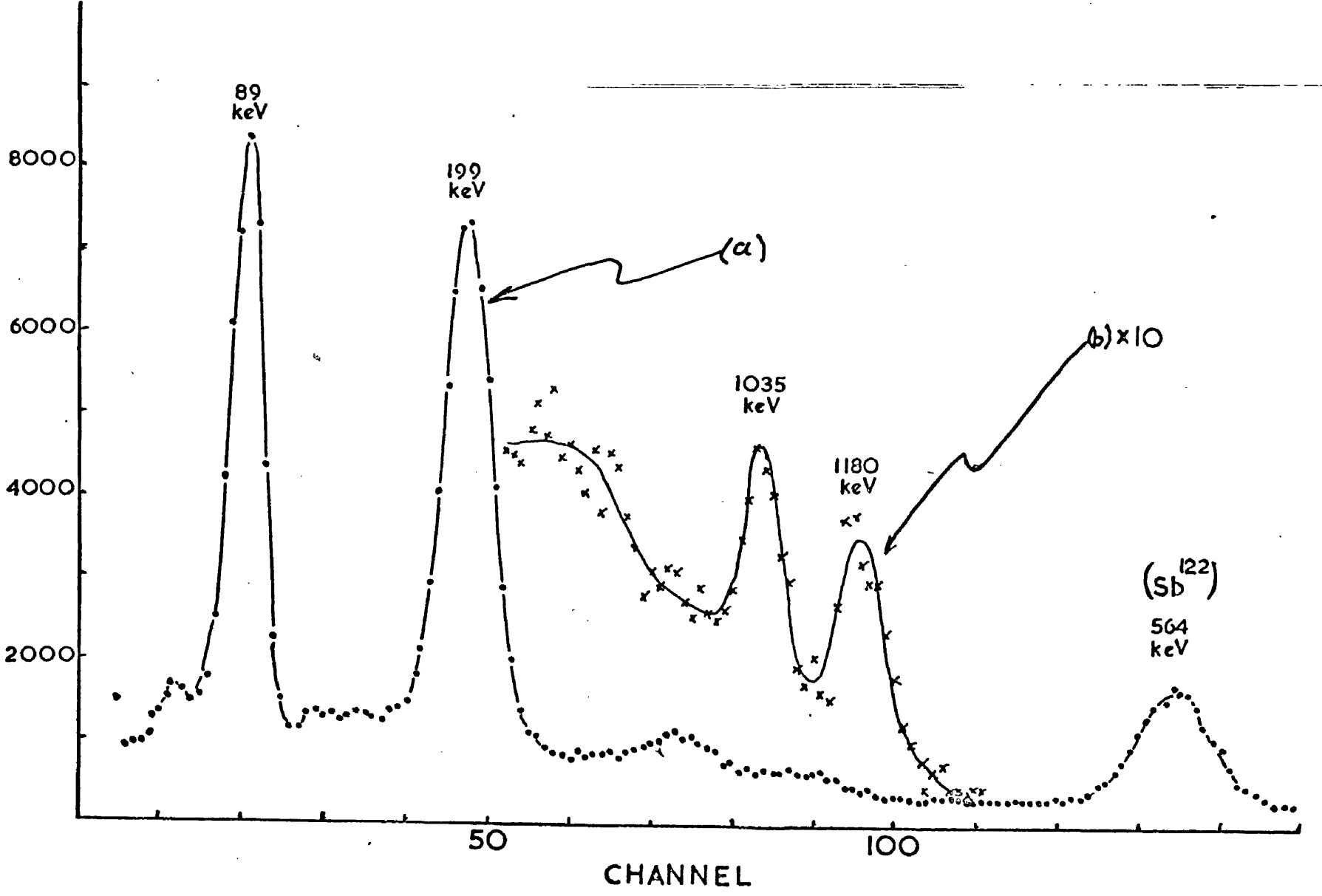

FIG. 5.4

Energy spectra for both high and low energy Y-rays from irradiated antimony.

emission of the 199 keV γ-ray the transition would be 300 times slower than the single particle estimate for an E2 transition. Since E2 transitions are generally faster than predicted by this model it is reasonable to associate the the 11 μsec. half life with the 89 keV E1 γ-ray.

As is about to be shown, the order of the γ-rays is not in fact that concluded by McGinnis, and in view of the findings reported in this thesis it is not unreasonable to accept the E2 transition as 300 times slower than the Weisskopf estimate. The slow E2 transition in Pb^{204} is 600 times slower (fig. 4.11) than this estimate.

Ordinary antimony powder was irradiated by 14 MeV neutrons in the H.T. set for several hours each day over a period of about a week. These irradiations were done at the same time as those on chromium (next chapter), the antimony and chromium being placed simultaneously in a special container. The cross section for the (n,2n)reaction on Sb^{121} (57% of natural Sb) leading to the 5.8 day activity is 1,100 mb. (Prestwood and Bayhurst 1961), and in accordance with this high value a good activity was obtained. Sb^{122} (2.8d) was also produced but presented no problem. The low energy γ-ray spectrum obtained from antimony is shown in fig. 5.4a, the high energy spectrum in fig. 5.4b.

The lifetime which was wanted was that of the 199 keV transition which, according to McGinnis (1958) is E2 and

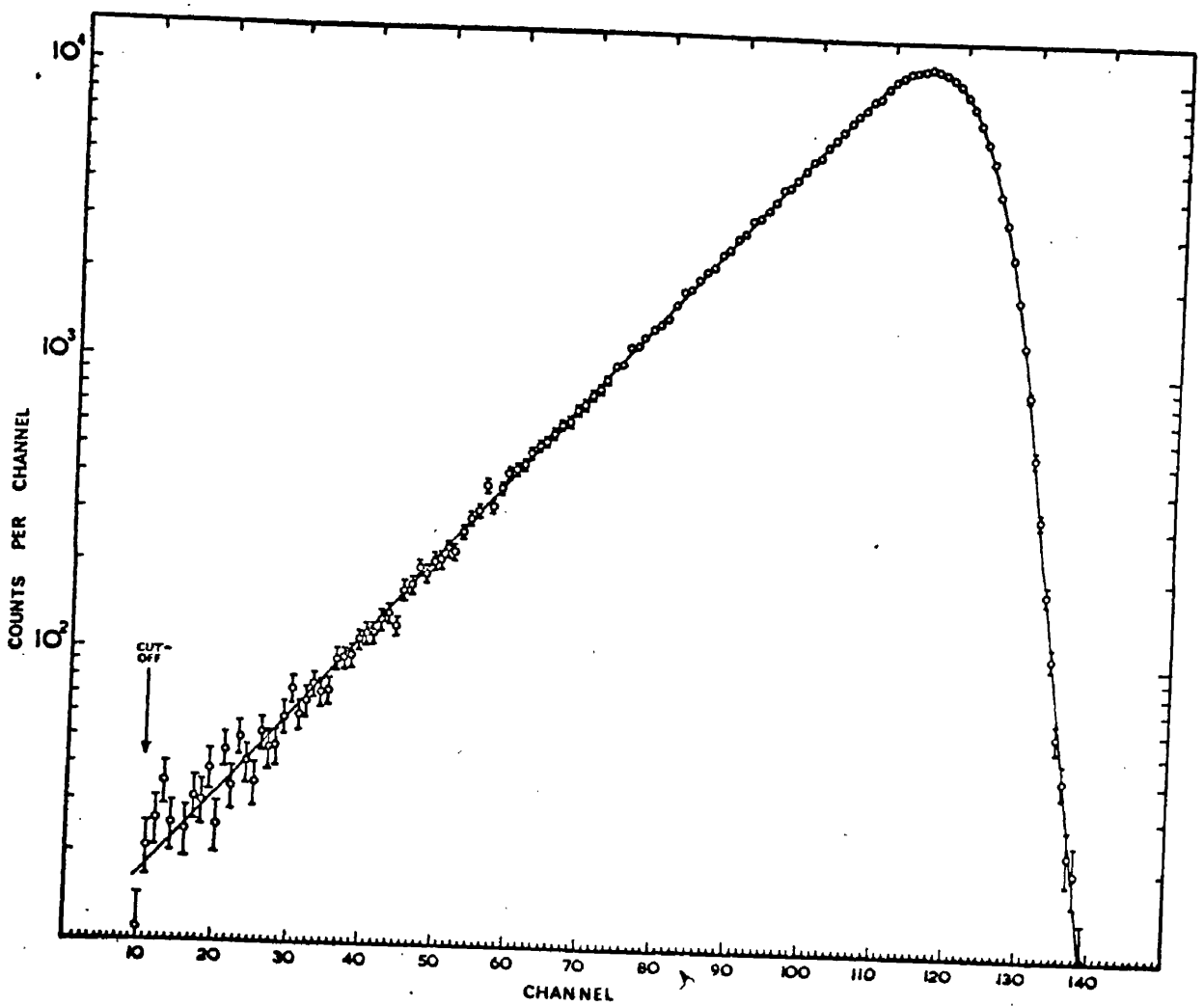

FIG. 5.5

Delayed coincidence curve for the two low energy radiations from Sb^{120}. From the slope of this curve $\tau = (8.45 \pm 0.18) \times 10^{-9}$ sec.

follows the 89 keV transition. On the basis of the results for Ce^{140} and Ba^{138} this lifetime was expected to be quite long, perhaps $\sim 10^{-8}$ sec. It was therefore considered worthwhile attempting the measurement with two NaI(Tl) scintillators, one for the 89 keV photon and the other for the 199 keV photon. With such scintillators and low energy radiations the time resolution would be poor, but for a long enough lifetime the measurement would be possible.

This was found to be the case. Fig. 5.5 shows a delayed coincidence spectrum obtained by taking coincidences between the two low energy γ-rays. The energy "windows" were set on the photopeaks for those radiations. It will be noticed that this curve is better than that (fig. 4.9) obtained for Ce^{140}, in the sense that it is linear over a greater range. The reason for this is that steps were taken to overcome the "instrumental effects" referred to in fig. 4.9. The time constants of the limiter circuits were altered and the counting rates were kept low to ensure that the standing currents through the limiter valves were maintained as nearly constant as possible. In this way paralysis effects were kept to a safe level.

But fig. 5.5 is revealing in two ways. It shows directly in conjunction with the settings used in the apparatus at the time - that the 199 keV γ-ray precedes the 89 keV radiation and that it is the latter which is responsible for the lifetime apparent in fig. 5.5. From the data this lifetime is determined as:

$$\tau = (8.45 \pm 0.18) \times 10^{-9} \text{ sec.}$$

This means that it is the 199 keV radiation which decays with a mean life of 1.45×10^{-5} sec. ($T_{\frac{1}{2}} = 1.1 \times 10^{-5}$ sec.). With these findings the scheme of McGinnis needs re-examination.

It seems very likely that the two high energy Y-rays are E2. The angular correlation results of McGinnis support this view, as also does his value for the conversion coefficient of the 1.04 MeV radiation. In addition, as has been pointed out already, this conclusion is consistent with the expectations of the hydrodynamical model. The first two excited states are therefore undoubtedly 2+ and 4+. The conversion coefficients quoted by McGinnis for the other two radiations and the theoretical predictions are given in table 5.1.

Table 5.1

EY (MeV)	$\alpha \times 10^3$ (exp.)	Theoretical $\alpha(\times 10^3)$				Assignment
		E1	E2	M1	M2	
0.089	0.29 ± 0.05	0.24	2.30	0.80	8.9	E1
0.199	0.13 ± 0.025	0.025	0.12	0.093	0.52	E2

These data leave no alternative to his conclusions that the 89 keV Y-ray is E1 and the 199 keV one E2. This conclusion is supported by his angular correlation data. Hence there is an E2 transition of 199 keV having a radiation lifetime

of 1.64×10^{-5} sec. and an E1 transition of 89 keV with a radiation lifetime of 1.09×10^{-8} sec. By fig. 4.1 these are respectively 2.7×10^{4} and 300 times longer than the single proton estimate. Here then is another case of a retarded E2 transition, once again where there is mixing of collective and individual particle excitations. In accordance with these conclusions the third and fourth excited states have to be 5- and 7- respectively.

CHAPTER 6.

LIFETIME OF THE 152 keV LEVEL IN V^{49}.

(6.1) Introduction.

In giving consideration to the measurement of isomeric lifetimes special attention was paid to the short lived isotopes which could be produced by one or other of the reactions (n,2n),(n,p), (n,α). The nuclei which can be produced in piles by the common (n,γ) reaction have been studied very thoroughly and in consequence there are very few likely isomeric levels which have not been examined by delayed coincidence methods. But many of the nuclei which are produced by the (n,2n) and other reactions have not been studied in detail and it seemed that there was quite a range of such nuclei which could profitably be investigated. One of the reasons why some of these isotopes have escaped detailed attention is that they are often short lived, a few minutes to a few hours. For this reason they must be prepared and investigated in the same place.

From the viewpoint of the present work the short half-lives of these (n, 2n) products is an advantage because in many cases sufficient activity can be obtained only when the irradiation lasts for several half-lives. The optimum lifetime is therefore 2-3 hours.

Of the three reactions mentioned at the beginning

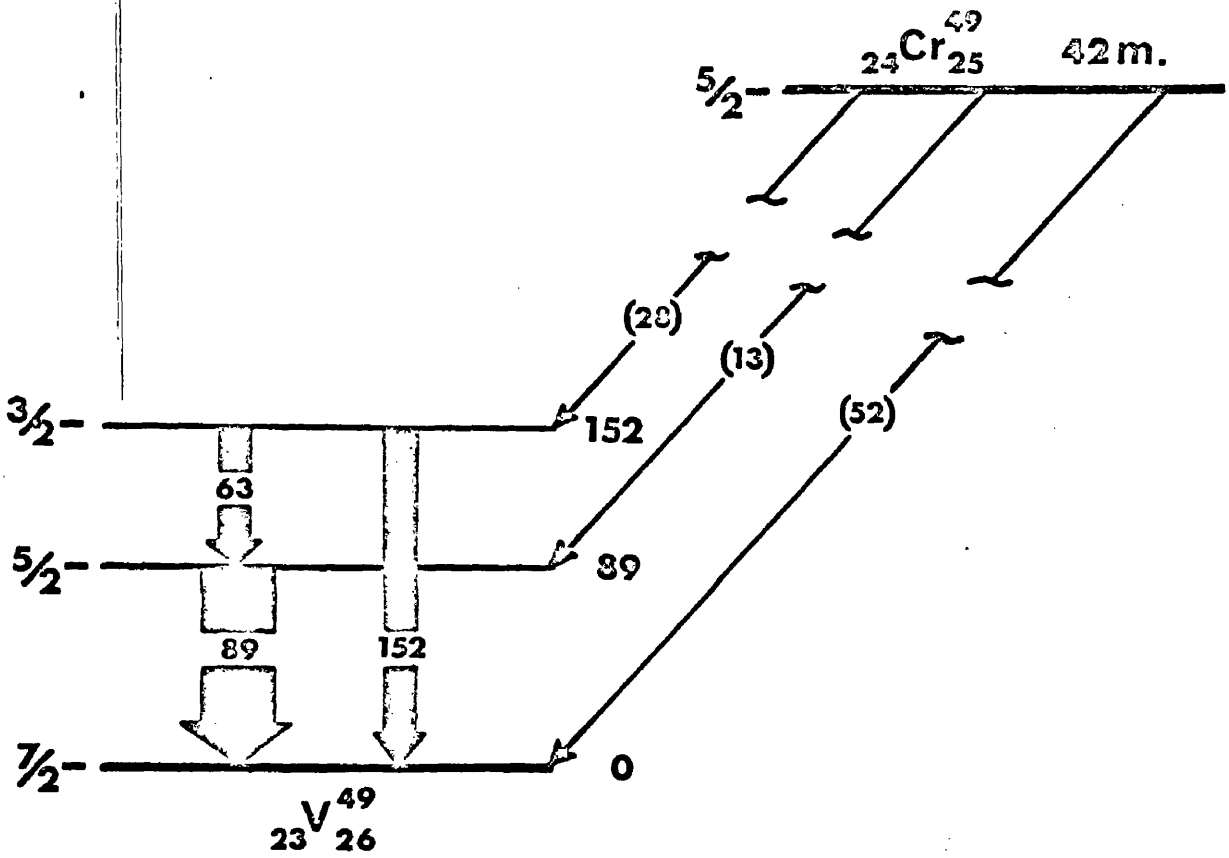

FIG. 6.1

Decay scheme of Cr^{49}.

the (n,2n) one is the most productive having a cross section $\gtrsim$1b in many heavy nuclei. The (n,p) and (n,α) reactions have much lower cross sections especially in heavy nuclei, where Coulomb effects are strong. Proton reactions were also considered and a number of them included in the programme but so far this process has not been utilised. It requires the use of the large H.T. set while all the work to date has been done on the small H.T. set. The latter when functioning at its best produces up to 7×10^9 14 MeV neutrons per second, isotropically distributed over a solid angle of 4π. A special target was prepared for this work. It allowed the material for irradiation to be placed very close to the tritium target but without its being in the vacuum. The material could therefore be removed very quickly and replaced by a fresh sample without the vacuum being broken.

The 152 keV level of V^{49} (fig. 6.1) is expected to have quite a long lifetime. Nussbaum et al.(1954) looked for this with a minimum resolving time of 2×10^{-7} sec. but obtained no positive results. In spite of this it looked as though this was a case of a level whose lifetime could be measured very easily with a delayed coincidence apparatus. The only difficulty was the production of the source.

Cr^{50} has an abundance of only 4.3% and the cross section for the reaction Cr^{50}(n,2n) Cr^{49} is only 26 mb.(Rayburn 1961). Hence the production of 42 minute Cr^{49} was likely to be

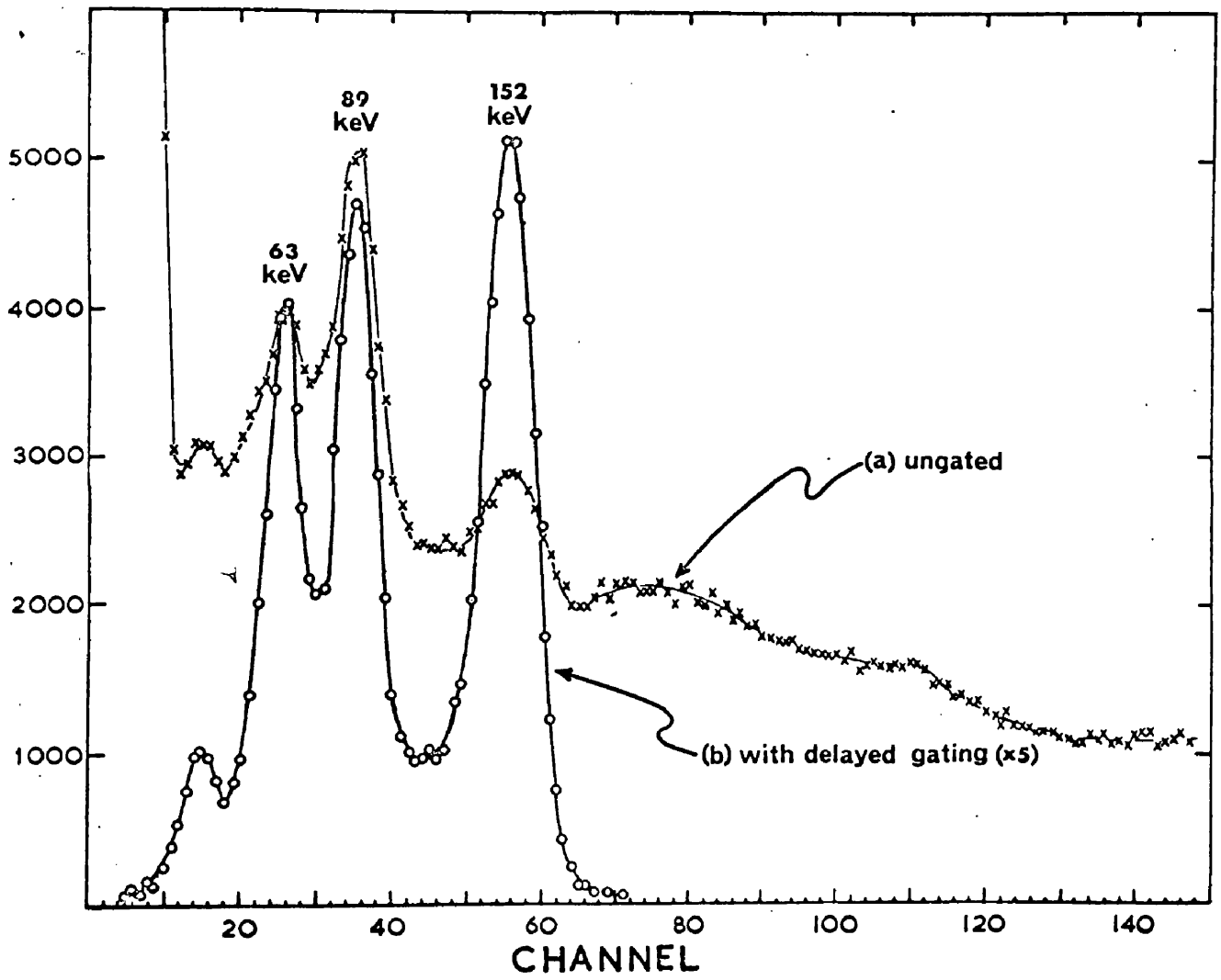

FIG. 6.2

Energy spectra from Cr^{49}, a) without gating and b) with "delayed gating". These curves show that the 63,89 and 152 keV γ-rays are delayed with respect to β-particles, and that the 152 keV level of V^{49} is responsible for the measured decay period.

difficult, especially as so many other reactions take place when chromium is bombarded with neutrons. Notwithstanding, the isotope has been prepared and the measurement made. Fig. 6.2(curve a) shows the low energy spectrum obtained from ordinary chromium irradiated for a short time in the H.T. set.

(6.2) Measurements and Results.

The experiment was tried first of all with plastic scintillators because it was expected that the lifetime would be quite short, perhaps a few nsec. This was unsuccessful and the quest was almost abandoned when it was noticed that the number of non-prompt, random coincidences was rather inordinate. Thereupon two NaI(Tl) scintillators were put in place of the plastic ones and a delayed coincidence spectrum was quickly obtained, the lifetime being quite long and requiring very long clipping lines for its determination.

In order to demonstrate that the observed period was that of the 152 keV level in V^{49} the delayed gating technique described in chapter 4 was used. One counter was set to select the photopeak of the $\frac{1}{2}$ MeV annihilation radiation from the Cr^{49} positrons while the energy pulses from the other counter were gated by the delayed coincidence pulses as described in section 4.2. The result was the curve b of fig. 6.2 which clearly verifies that the 152 keV level is responsible for the delayed coincidences.

It will be noticed that the 89 keV photopeak is larger

than that of the 63 keV radiation. Considerations of the detection efficiency and conversion coefficients do not lead to this conclusion. If the data of Nussbaum et al. are correct the two photopeaks should have approximately the same area because nearly every 89 keV γ-ray should be accompanied by one of 63 keV. This suggested that the 89 keV level also had quite a long half life and that some of the delayed photons from this level were associated with positrons feeding the level directly. To check this possibility the amount of 200Ω delay cable used to separate the delayed from the prompt coincidences was varied to see if the ratio of 89 keV/63keV areas would change. There was no significant variation. This implies firstly that the 89 keV level is short lived and secondly that the conversion coefficients quoted by Nussbaum et al. are incorrect. These authors realised this possibility and stated that the figures might be in error by a factor of two. It seems now that this is so and that a_K for the 63 keV transition is considerably greater than the value reported in the above paper. This would be consistent with the rather long lifetime of the 152 keV level on the one hand and with the short lifetime of the 89 keV on the other.

For the lifetime of the 152 keV level the "window" in channel 2 was set on the 152 keV photopeak and the delayed coincidence spectrum recorded. The measurement was hindered by the presence of so many other undesirable high energy radiations. Although the Cr^{49} activity was weak the total

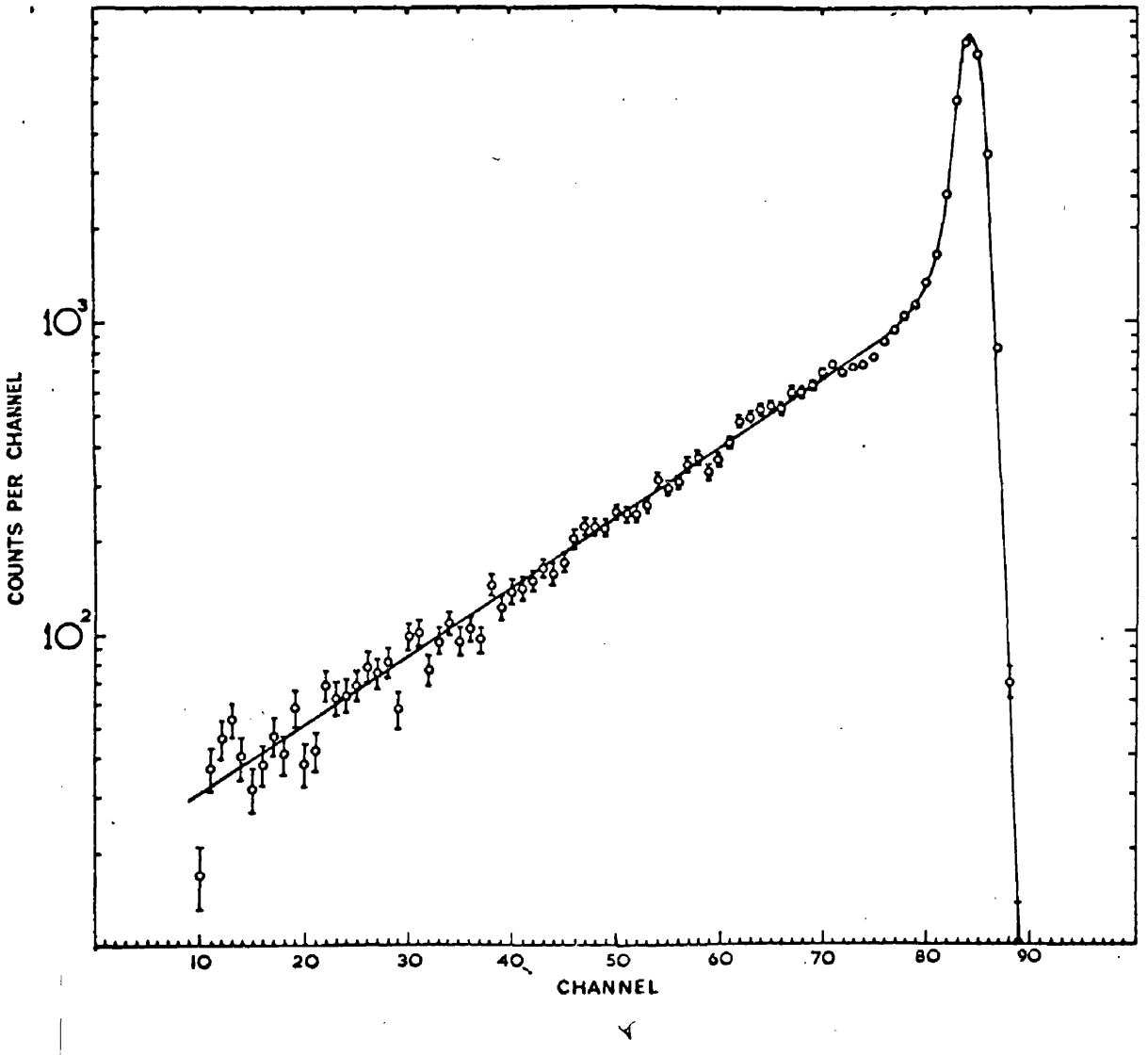

FIG. 6.3

Delayed coincidence curve for the 152 keV γ-ray following the decay of Cr^{49}. From the slope $\tau = (3.05 \pm 0.08) \times 10^{-8}$ sec.

counting rate was quite high. Added to the long clipping times this meant that paralysis troubles were encountered at quite low counting rates. As a result the chromium activations had to be kept short and had to be made frequently. Also a delay of half an hour had to be allowed between activation and use to permit the decay of short lived components.

The curve of fig. 6.3 was recorded with 6 irradiations made over a whole day. A time calibration was made halfway through. From this curve the mean life has been calculated as:

$$\tau = (3.05 \pm 0.08) \times 10^{-8} \text{ sec.}$$

From this result the radiation lifetimes for the M1 and E2 transitions can be calculated. Assuming Nussbaum's result for the E2 transition, $\alpha_K = 0.16$, and a value $\alpha_K \approx 0.25$ for the M1 transition, the radiation lifetimes are derived as 7.7×10^{-8} and 7.2×10^{-8} respectively. For the E2 transition this is ~ 3 times shorter than the single proton estimate while for the M1 transition the result is ~ 700 times longer than the single particle estimate. These results are in general agreement with comparative data.

CHAPTER 7.

PERTURBED ANGULAR CORRELATIONS IN Ta^{181} AND OTHER WORK.

(7.1) Introduction.

In chapter 1 some consideration was given to collective effects in nuclei and it was shown that quite a few of the properties of deformed nuclei can be fairly precisely predicted by the simple treatment given there. In particular it was pointed out that the quadrupole moments of the different levels of a rotational band should be related by eq. (1.46). In this connection, therefore, the theory provides a specific theoretical prediction, applicable chiefly to excited states. The other theoretical predictions concerning spins, parities, energies and transition rates have all been well substantiated and it is therefore hardly credible that the prediction concerning quadrupole moments should not also be correct. But, while this is so, an experimental verification of eq. (1.46) would still be very gratifying and it is in any case desirable that this equation should be tested for at least one particular case.

The problem raised in the preceding paragraph is a difficult one, namely the measurement of the quadrupole moment of an excited nuclear state. The determination of ground state quadrupole moments is difficult enough ,and

generally speaking, for an excited or unstable nucleus the standard techniques are not applicable and in only a few cases is a measurement possible.

Melissinos and Davis (1959) have studied the optical lines of 65 hour radioactive Hg^{197} and 25 hour isomeric Hg^{197} and in this way have determined the quadrupole interaction energies. On the basis of certain assumptions they were able to derive values for the quadrupole moments of these unstable nuclei. It is to be noted that, as in all determinations of quadrupole moments, these measurements required assumptions to be made. The reason is that controlled artificial field gradients sufficient to produce measurable effects cannot be manufactured in the laboratory. Consequently any measurements, whether by resonance, optical spectra or angular correlations, will yield only the interaction frequency ν_Q of eq. (1.32). Assumptions have therefore to be made about $\partial E/\partial z$ before Q can be evaluated.

In section 1.3b it was explained how measurements of perturbed angular correlations, especially delayed angular correlations, could lead to a value for the quadrupole interaction frequency. Such measurements are equivalent to those made on stable nuclei by other means. They are, however, liable to special complications. When the γ-rays follow a β-particle there is a change in Z with consequent effects due to shake-off electrons. Also there may be a

considerable recoil of the nucleus, and when electron capture takes place there will be effects due to the residual electron hole and to Auger transitions. These effects must be considered and, if possible, evaluated in the interpretation of results for, as has been pointed out by several authors (e.g. Pettersson et al. 1961), the interplay between these effects and the static quadrupole interaction may considerably affect the angular correlation.

The most reliable way of investigating the static quadrupole interaction would be by a delayed angular correlation measurement as described and illustrated in section 1.36. Such a measurement might allow a clear distinction to be made between static quadrupole and other effects and it would in any case be the most accurate method for determining the precessional frequency. The method has already been used (Lehman and Miller 1958) with the results shown in fig. 1.9b. In this investigation static quadrupole and K-capture effects (not illustrated in fig. 1.9) were clearly distinguished in the time dependent measurements of anisotropy. The resultant value for ν_Q was rather different from that obtained by integral correlation measurements (Steffen 1956, using eq. (1.29)) and indicates the superiority of the delayed method. Where the precessional period is short compared with the isomeric lifetime the delayed method becomes more desirable and in the limit of a "hard core" integral correlation only the delayed method offers any chance of yielding the

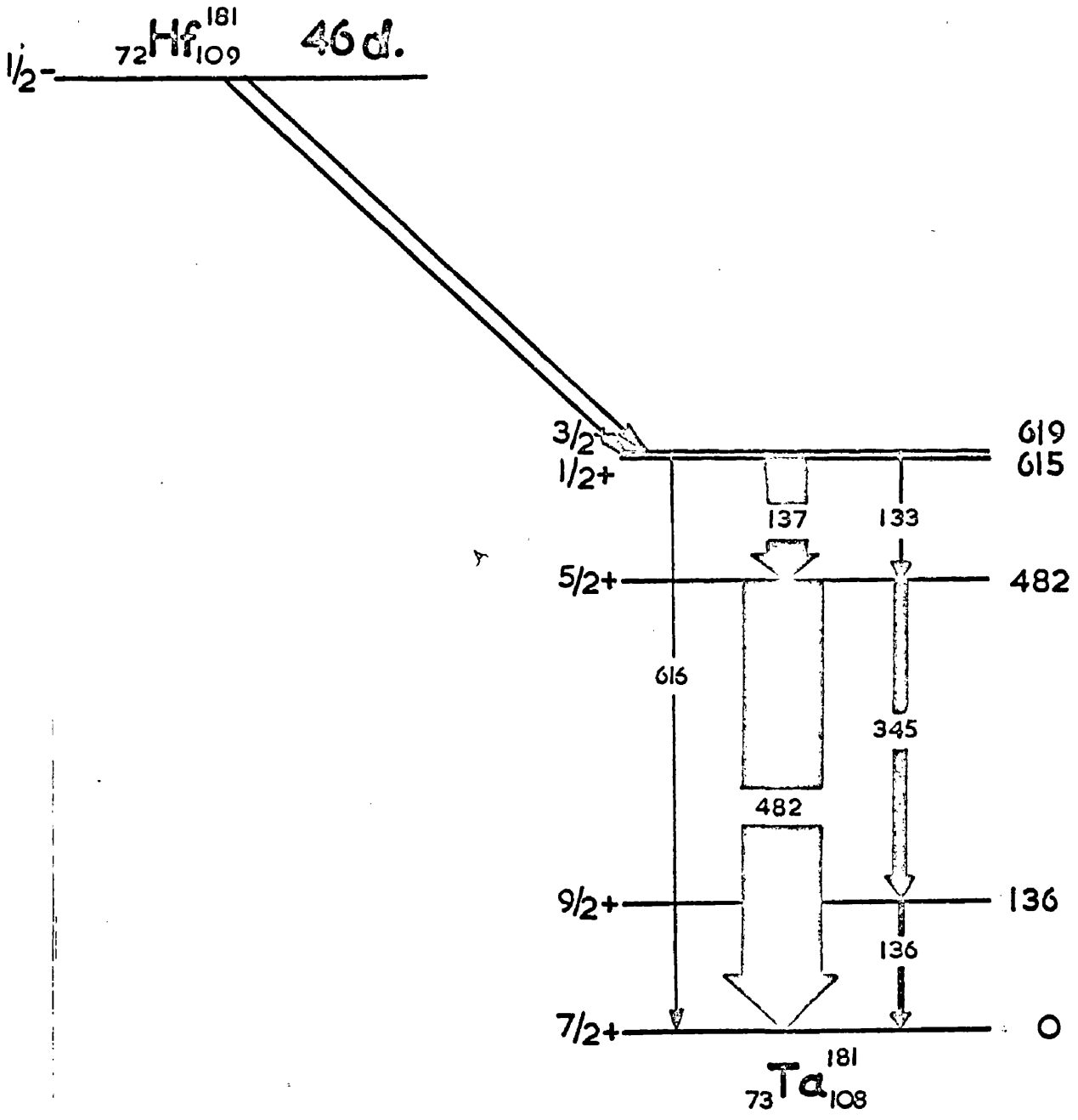

FIG. 7.1

Decay scheme of Hf^{181}

interaction strength.

The case of Cd^{111} is similar to the cases of Ta^{181} and Hg^{199} in that the spins of the intermediate state is 5/2 in each case. Hence the attenuation function is given by eq. (1.30). The same effect has been studied in Pb^{204} (Wertheim and Pound 1956) where the relevant spin is 4 and the attenuation function is more complicated. As in the case of Cd^{111} the lifetime (0.27 μsec.) and precessional period (~0.1 μsec.) are long and measurements of the delayed correlation were possible.

The measurements which have been attempted on Ta^{181} and Hg^{199} and which will now be reviewed briefly are an extension of the work on Cd^{111} and Pb^{204} into the sub-nanosecond region. The technique is more difficult but the experiments are perhaps more worthwhile (at least in the case of Ta^{181}) since it might be possible to relate the results to the collective model.

(7.2) Experiments with Ta^{181} and Hg^{199}.

The decay scheme of Hf^{181} is given in fig. 7.1. The 5/2 level at 482 keV is the first state of the K=5/2 band (Mottelson and Nilsson 1959). The ground state has K=7/2. These two states are therefore not in the same rotational band; they are intrinsically different, which is the reason for the long lifetime of the 482 keV level. Despite the

intrinsic difference between these states it is unlikely that Q_o will differ very much between them. Hence Eq.(1.46) should be quite a reliable guide to the difference in the relative magnitudes of their quadrupole moments. According to (1.46)

$$\frac{Q(7/2)}{Q(5/2)} \approx 1.3$$

Thus if the quadrupole interaction frequency were determined for the ground state by, say, resonance methods, and for the excited state by correlation methods they would be expected to be in this ratio.

Unfortunately things are not quite so straightforward. In the angular correlation measurements a tantalum nucleus is precessing in a hafnium lattice. For a strict comparison to be made between the two levels both experiments would have to be carried out under identical conditions. This might be possible if a strong source of Hf^{181} were allowed to decay for many half-lives(40d.) and if the resulting material were then used in resonance measurements. Notwithstanding these difficulties, as a first step towards the goal mentioned in the previous paragraph and as an example of the technique on investigation of the delayed angular correlation in polycrystalline HfO_2 was undertaken.

In the decay of Hf^{181} a fairly low energy β-particle is emitted and subsequently the 482 keV level of Ta^{181} is

fed principally through the 19 μsec. level at 619 keV. As a result it is expected that recoil and ionisation effects will not interfere with the precession of the 482 keV level and only the static quadrupole interaction will influence the correlation. The problem has been studied by Debrunner et al. (1956) using the method of integral correlations. In the case of HfO_2 they found only the "hard core" correlation and hence concluded that $\nu_Q >$ 350 Mc/sec. Now for I = 5/2 the fundamental frequency of precession is given (Heer and Novey 1959) by:

$$\omega = \frac{3}{2I(2I-1)} \frac{eQ}{\hbar} \frac{\partial E_z}{\partial z}$$

$$= \frac{3(2\pi)}{2I(2I-1)} \nu_Q$$

$$= \frac{12}{20} \nu_Q$$

Since the separation of the main peaks in the curve of fig. 1.9a for I=5/2 is $2\pi/\omega$ this separation must be less than about 2×10^{-8} sec. The matter was pursued by Lewis and Azuma (1957), prior to the author's work, who concluded that their FWR of 4 nsec. was insufficient (i.e. too large) to reveal the modulations in the delayed coincidence curve. On this account it seemed that the fundamental period of precession was much less than 2×10^{-8} sec. and that only an apparatus of very high resolution would permit its measurement.

As a sequel to the work of Lewis and Azuma various attempts have been made by the author to obtain a delayed coincidence lifetime curve showing modulations roughly like those of fig. 1.8. These efforts have met with no success.

The failure of the experiments on HfO_2 was perhaps due in part to inexperience since this was the first investigation undertaken by the author. The time resolution was poor, the apparatus was not very stable nor perfectly linear and the preparation of sources was not planned in the most efficacious way. As mentioned at the end of section 3.3 much time was spent in improving the apparatus, and it was really only after the work on instrumental effects that the correlation experiment could be tackled in a knowledgeable way. By this time more consideration had been given to the work of other people and a different course of action was adopted.

Debrunner et al. (1956) in their work on the Hf^{181} decay scheme used sources of $(NH_4)_3HfF_7$ and $Rb_2Hf\ Cl_6$ in which the quadrupole interaction is much weaker than in HfO_2. In the case of $(NH_4)_3Hf\ F_7$ ν_Q = 59 Mc/sec. so that the modulation to be looked for in the delayed angular correlation would be much slower than in the case of HfO_2. The only problem with this source was its preparation. In this connection the author received advice and assistance from many people, including Debrunner himself, but did not

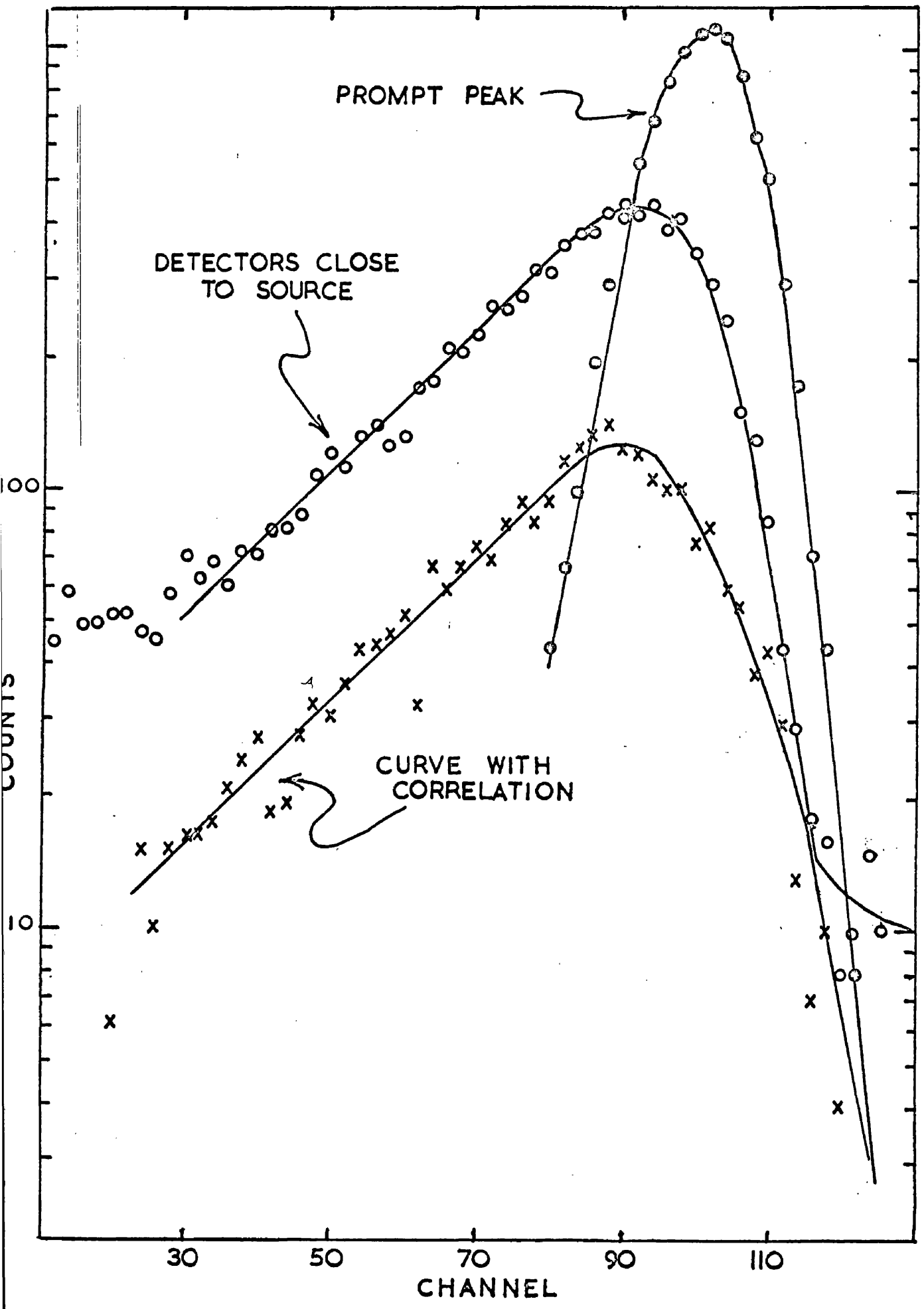

FIG. 7.2

Delayed coincidence curves obtained with Hf^{181}.

succeed in demonstrating the effect.

The preparation of $(NH_4)_3$ Hf F_7 or of the very similar $(NH_4)_3$ Zr F_7 has been described by several people(Debrunner et al. 1956, Haendler et al. 1952, Hampson and Pauling 1938, Von Hevesy and Jantzen 1923, Baker 1879). It was attempted both with ordinary and with radioactive HfO_2 both by the author and by two chemists. The U.K.A.E.A. Radiochemical Centre, Amersham declined to make it and Debrunner at Zurich and Haddock at Cambridge were consulted. The results were never conclusive. Finally the Wah Chang Corporation, Albany Oregon kindly offered their help. They supplied different samples of HfO_2 and $(NH_4)_3$ Hf F_7. They also enclosed 18 mg. of the latter in a special quartz phial which was sent to them. This was irradiated at Harwell and the active double fluoride extracted and put immediately under liquid paraffin, to prevent exposure to the atmosphere. Various sources of this material were studied both with NaI(Tl) and with specially shaped conical plastic scintillators and many delayed resolution curves were recorded. Fig. 7.2 shows two delayed coincidence curves, one recorded with the detectors close to the source, the other with the detectors further back so that angular correlation effects would become apparent. There is no indication of non linearity in the curve, and even although the statistics are poor the result was considered

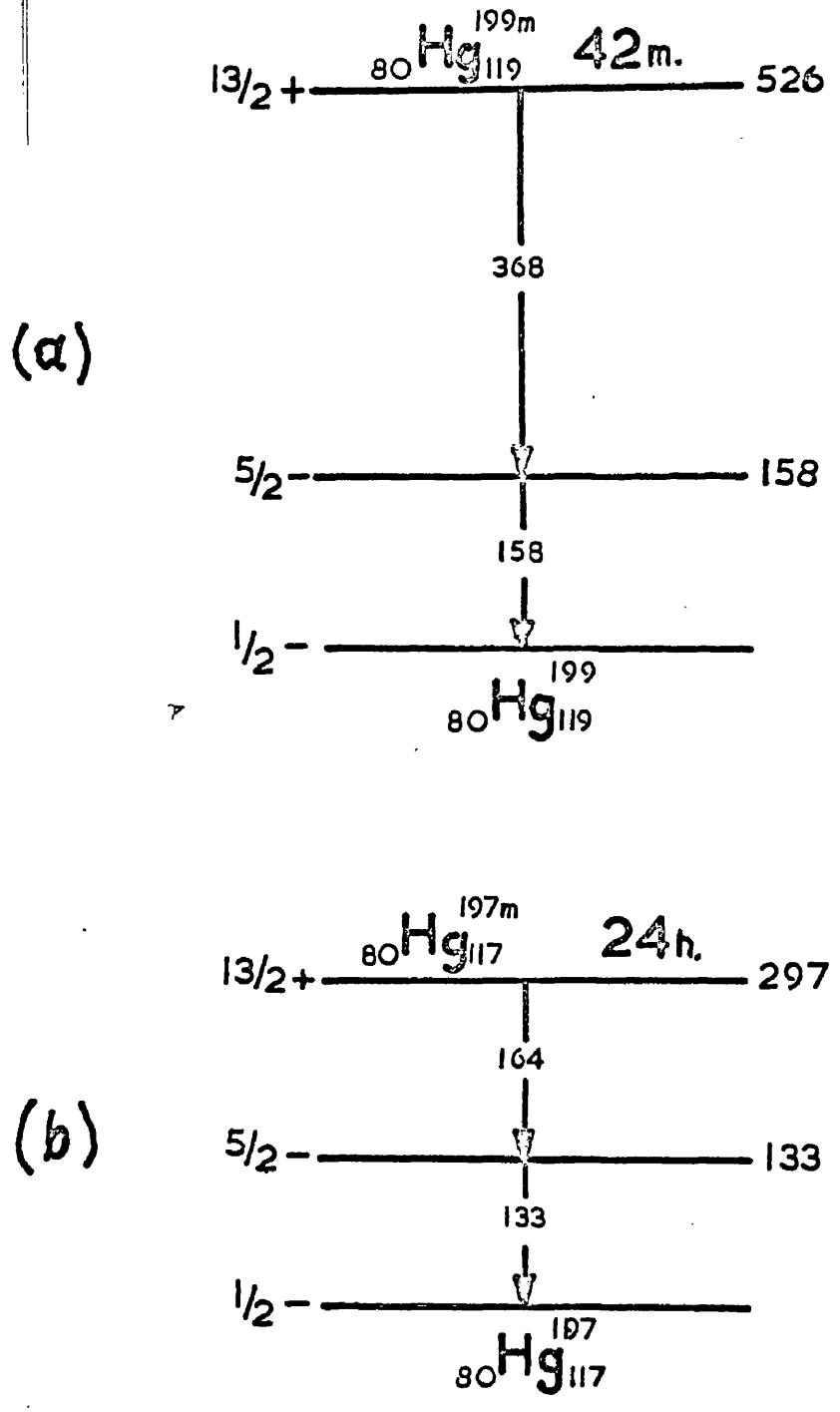

FIG. 7.3

The excited states of Hg^{199} and Hg^{197}.

significant. The large anisotropy of nearly 40% in Ta^{181} should make the perturbation quite apparent. It was concluded that radiation damage to the double fluoride had altered the internal fields near radioactive nuclei.

In the course of the work attention was turned to other nuclei which might prove more suitable for this kind of experiment. In some respects Hg^{199} and Hg^{197} (fig. 7.3) seemed preferable to Ta^{181}. In both cases the state of interest has I=5/2. Both levels can be obtained in mercury itself if metastable Hg^{199m} and Hg^{197m} are used as sources. This would permit excited state and ground state quadrupole moments to be compared under identical conditions. The half-lives of the levels are acceptable, 2.4 and 7.0 nsec. respectively and the energies are just tolerable.

Both levels have been studied before, by Coburn and Frankel (1955) and Pound and Wertheim (1956). Coburn and Frankel measured the K-γ correlation for Hg^{197} in various chemical forms. In the case of $Hg(NO_3)$ they concluded that the attenuation arose from ionisation effects. This would not apply to a γ-γ correlation. Pound and Wertheim studied the case of Hg^{199} using liquid, frozen metal and $HgCl_2$. They deduced interactions of 590 Mc/sec. and 1,100 Mc/sec. in the frozen metal and $HgCl_2$ respectively. Thus the modulations to be expected would have periods of about 10 and 5 nsec. respectively and this should come within the scope of the apparatus.

The chief disadvantage of such a short lived source as Hg^{199m} is that it has to be prepared on the premises by the reaction $Hg^{200}(n,2n)\ Hg^{199m}$. The cross section for this reaction is quite high (~1b.), the abundance of Hg^{200} is quite good (23%) but in spite of this it has not been possible to obtain a high enough specific activity for these rather difficult measurements. Special conical plastic scintillators were obtained in an effort to improve the detection efficiency but to no avail. It seems that such an experiment is not practicable on Hg^{199}. Hg^{197} has not been investigated but is under consideration. The best course seems to be thermal neutron irradiation of enriched Hg^{196} with rapid delivery from Harwell. The radiations are lower in energy and the experiment is being left until some improvements in technique have been accomplished.

(7.3) Other Work.

(a) On the 0^+ level in Ce^{140}.

As shown in fig. 4.5 there is a 0+ level at 1.9 MeV in Ce^{140} (Cork et al. 1951, Dzelepov et al. 1958, Dzelepov et al. 1958a, Langer and Smith 1960). This level decays by internal conversion only and can be expected to have a lifetime of a nanosecond or so. The number of transitions through this channel is very low, 0.013%, (Dzelepov et al. 1958, Bashilov et al. 1958), and so coincidences between

β-particles and conversion electrons would be rare.

During the work on Ce^{140} a search was made for high energy e-e coincidences but only a prompt peak could be obtained. Whether this prompt peak included the desired coincidences or not was uncertain. With such a low yield of conversion electrons the summing effects of the other radiations becomes quite important and the experiment was finally abandoned as being too impracticable. It could be done with a magnetic spectrometer but even then it would be quite difficult.

(b) On Rb^{84}.

When 14 MeV neutron activation was first adopted as a means of source production one of the levels investigated was the 240 keV level of Rb^{84}. 23 minute Rb^{84m} decays by a 220 keV Y-ray followed by one of 240 keV. The metastable isomer was easily prepared using $Rb_2 CO_3$ and coincidences were obtained. These were prompt and formed a resolution curve just like that obtained with annihilation radiation. There was no difference in the widths of the curves and so it seemed that the lifetime of the first excited state of Rb^{84} is very short $< 10^{-10}$ sec.

(c) On Sb^{122}.

The decay of Sb^{122m} is similar to that of Rb^{84m} except that the Y-rays have lower energy. The metastable state is reported to have a half-life of 3.5m. (der Meteosian and

Goldhaber 1951). It was found however to decay with a half life of 6m., which was rather puzzling. Thin plastic scintillators were used on two counters in an effort to obtain coincidences between conversion electrons from the two cascade transitions. Coincidences were certainly obtained but the resolution curve was prompt, suggesting a very short half-life.

Since this work was done der Mateosian and Sehgal (1962) have investigated this decay scheme again and found that the first excited state has actually a long half-life of 1.8 μsec. On the basis of conversion coefficients this slow γ-ray is concluded to be E1 while the first γ-ray with 3.5 m(?) half life is E2. Thus the transitions are retarded by $\sim 10^6$ and $\sim 10^8$ respectively.

In a private communication der Mateosian has referred to some work by Meyer-Berkhout which indicates another level in Sb^{122}, with perhaps a very low energy transition of a few keV. In view of this it is intended to pursue the matter further.

(d) Future plans.

As a result of private communications with R.E.Bell it has been decided , as mentioned at the end of section 3.4, to add a little to the work on instrumental effects, principally to demonstrate the effectiveness of minimising σ^2 and to compare different multipliers. This will be done immediately

since the information will be of considerable practical value to other experimenters.

After that it is intended to carry on the work on lifetime measurements and also the work on delayed angular correlations. In particular an improved technique for centroid shift measurements may be tried out and quite a few sources will be prepared by 14 MeV neutron bombardment and investigated.

A particular development which may permit the measurement of lifetimes of low energy states is a cooled crystal spectrometer, now almost ready for use. This is a cryostat in which it is intended to cool crystals of pure NaI and CsI to 80^{o}K or less. At these temperatures the pure scintillators are very efficient and much improved in speed. The light from them will be extracted through a 7" quartz light pipe to a 56UVP photomultiplier. If the system works as planned quite a number of measurements should be possible.

REFERENCES.

A.ABRAGAM and R.V. POUND(1953) Phys.Rev. 92 943

ALAGA, ALDER, BOHR and MOTTELSON (1955) K.Dan.Vid. Selsk. mat. -fys. Medd. 29 No. 9.

K. ALDER (1952) Helv. Phys. Acta 25 235.

AMALDIE, D'AGOSTINO, FERMI, PONTECORVO and SEGRE (1935) Ricerea sci. 61 581.

R.E. AZUMA and G.M. LEWIS (1957) Phil. Mag. 2 1325.

H. BAKER (1879) J.Chem. Soc. 35 760.

E. BASHANDY (1960) Nucl. Instr. and Meth. 6 289.

BASHILOV, DZELEPOV, NOVOSIL'TSEVA and CHERVINSKAYA (1958) Izv. Akad. Nauk S.S.S.R., Sev. fiz. 22 No.2.

Z. BAY (1951) Phys. Rev. 83 242.

H. BEEKHUIS and H. de WAARD (1958) Physica 24 767.

BELL, GRAHAM and PETCH (1952) Can. J. Phys. 30 35.

R.E. BELL and M.H. JØRGENSEN (1959) Nuc.Phys. 12 413.

" " (1960)Can. J. Phys. 38 652.

BELL, BJØRNHOLM and SEVERIENS (1960) K. Dan. Vid. Selsk. mat.-fys. Medd. 32 No.12.

L.C. BIEDENHARN and M.E. ROSE (1953) Rev.mod.Phys. 25 729.

BIRK, GOLDRING and WOLFSON (1959) Phys.Rev. 116 730.

G.R. BISHOP and J.P. PEREZ Y JORBA (1954) Phys.Rev. 98 89.

A. BOHR (1952) K. Dan. Vid. Selsk. mat.-fys. Medd. 26 No.14

A. BOHR and B.R. MOTTELSON (1953) K.Dan. Vid. Selsk. mat.-fys. Medd. 27 No.16.

BOLOTIN, PRUETT, ROGGENKAMP and WILKINSON (1955)
Phys. Rev. 99 62 and 670.

M. BONITZ and E.J. BERLOVITCH (1960) Nucl.Instr. and Meth.
9 13.

P. BOSKMA and H. de WAARD (1959) Nuc.Phys. 14 145.

F.D. BROOKS (1956) Progress in Nuclear Physics 5 252.

BUNKER, DUFFIELD, MIZE AND STARNER (1956)
Phys. Rev. 103 1417.

C.F. COLEMAN (1955) Phil. Mag. 46 1132.

" " (1958) Nuc. Phys. 7 488.

COLEMAN, HAWKER, O'CONNOR and PERKIN (1959)
Proc. Phys. Soc. 23 215.

COLOMBO, GATTI and PIGNANELLI (1957) Nuovo Cimento 52 1739.

E.U. CONDON and G.H. SHORTLEY (1935) Theory of Atomic Spectra
(Cambridge University Press).

C. COTTINI, E. GATTI and G. GIANELLI (1956) Nuovo Cimento
4 156.

C. COTTINI and E.GATTI (1956) Nuovo Cimento 4 1550.

CORK, LE BLANC, STODDARD, MARTIN, BRANYAN and CHILDS
(1951) Phys. Rev. 83 856.

S.M. DANCOFF and P. MORRISON (1939) Phys. Rev. 55 122.

DEBRUNNER, HEER, KUNDIG and RÜETSCHI (1956) Helv.
Phys. Acta. 29 463.

S. DEVONS and L.J.B. GOLDFARB (1957) Encyclopedia of
Physics, Vol. 42. (Springer-Verlag, Berlin).

H.de WAARD (1958) Nucl.Instr. and Meth. 2 73.

E. der MATEOSIAN and M. GOLDHABER (1951) Phys. Rev. 82 115.

E. der MATEOSIAN and M.L.SEHGAL (1962) Phys. Rev. 125 1615.

DZELEPOV, KHOLNOV and PRIKHODTSEVA (1958) Dokl. Akad. S.S.S.R. 121 995.

DZELEPOV, KHOLNOV and PRIKHODTSEVA (1958a) Nuc. Phys. 9 665.

F.S. EBY and W.K. JENTSCHKE (1954) Phys.Rev. 96 911.

A.R. EDMONDS (1957) Angular Momentum. Princeton U.P. 1957.

FALKOFF and UHLENBECK (1950) Phys.Rev. 79 323.

U. FANO (1953) Phys.Rev. 90 577.

M. FIERZ (1949) Helv. Phys. Acta. 22 489.

H. FRAUNFELDER (1955) in SIEGBAHN 1955.

J.B. GARG (1960) Nucl. Instr. and Meth. 6 72.

E. GATTI and V.SVELTO (1959) Nucl. Instr. and Meth. 4 189.

A. GEIGER and E. MARSDEN (1913) Phil.Mag. 25 604.

R.K. GIRGIS and R. VAN LIESHOUT (1959) Nuc. Phys. 12 204.

M. GOLDHABER and A.W. SUNYAR (1951) Phys.Rev. 83 906.

M. GOLDHABER and R.D. HILL (1952) Rev. mod. Phys. 24 179.

M. GOLDHABER and A.W. SUNYAR (1955) in SIEGBAHN 1955.

G. GOLDRING and Z. VAGER (1961) Nuc.Phys. 26 250.

R.E. GREEN and R.E. BELL (1958) Nucl.Instr. and Meth. 3 127.

GREGERS-HANSEN, NIELSEN and SHELINE (1959) Nuc.Phys. 12 389.

HAENDLER, WHEELER and ROBINSON (1952) J. Am.Chem.Soc. 4 235.

O. HAHN (1921) Chem.Ber. 54 1131.

D.R. HAMILTON (1940) Phys.Rev. 58 122.

HAMPSON and PAVLING (1938) J.Am.Chem.Soc. 60 2702.

HAXEL,JENSEN and SUESS(1960) Z.Physik 128 301.

H.H.HEBB and G.E. UHLENBECK (1938) Physica 5 605.

E.HEER and T.B. NOVEY (1959) Solid State Physics Vol.9, 200.

W. HEISENBERG(1925) Z.Physik 33 879.

W. HEITLER (1936a) Proc.Camb. Phil.Soc. 32 112.

" " (1936b) The Quantum Theory of Radiation (Oxford University Press).

HUUS, BJERREGAARD and ELBECK (1956) K.Dan.Vid. Selsk. Mat.-fys. Medd. 30 No.17.

KANE, PIXLEY, SCHWARTZ and SCHWARTZSCHILD(1960) Phys.Rev. 120 162.

KELLEY, BELL DAVIS and LAZAR (1956) Nucleonics 14 No. 4, 53.

W.H.KELLY and M.L. WIEDENBECK (1956) Phys.Rev. 102 1130.

V.E. KROHN and S. RABOY (1954) Phys.Rev. 95 1354.

KURCHATOV, KURCHATOV, MYSSOWSKI and ROUSSINOV (1935) C.R.Acad.Sci. 200 1201.

L.M. LANGER and D.R. SMITH (1960) Phys.Rev. 119 1308.

P. LEHMAN and J.MILLER (1956) J. Phys. Radium 17 526.

C.L. McGINNIS (1958) Phys.Rev. 109 888.

J. MARSHALL (1952) Nucleonics 10 No.3, 38 .

M.G. MAYER (1951) Phys.Rev. 78 16 and 22.

A.C. MELISSINOS and S.P. DAVIS (1959) Phys.Rev. 115 130.

G.H. MINTON(1956) J.Res. Nat. Bur. Stand. 57 119.

MONAHAN, RABOY and TRAIL (1960) Bull. Am. Phys. Soc. 5 104.

B.R. MOTTELSON and S.G. NILSSON (1959) K.Dan.Vid. Selsk.

K. MURAKAWA and T. KAMEI (1957) Phys.Rev. 105 671.

S.G. NILSSON (1955) K.Dan.Vid.Selsk. Mat.-fys. Medd. 29 No.16.

L.W. NORDHEIM (1951) Revs.Mod.Phys. 23 322.

NUSSBAUM, WAPSTRA, NIJGH, ORNSTEIN and VERSTER (1954) Physica 20 165.

S. OFFER (1959) Phys.Rev. 115 412.

S. OFFER and A. SCHWARZSCHILD (1959) Phys.Rev. 116 725.

E.B. PAUL and R.L. CLARKE (1953) Can.J.Phys. 31 267.

PETTERSSON, THUN and GERHOLM (1961) Nuc.Phys, 24 223.

H.B. PHILLIPS and R.K. SWANK (1953) Rev.Sci.Instr. 24 611.

R.F. POST and L.I. SCHIFF (1950) 80 1113.

R.F. POST (1952) Nucleonics 10 No.6, 56.

J. RAINWATER (1950) Phys.Rev. 79 432.

L.A. RAYBURN (1961) Phys.Rev. 122 168.

M.E. ROSE (1953) Phys.Rev. 91 610.

M.E. ROSE (1958) Internal Conversion Coefficients (North-Holland).

E. SEGRE and A.C. HELMHOLTZ (1949) Revs.Mod.Phys. 21 271.

K. SIEGBAHN - Editor (1955) Beta and Gamma Ray Spectroscopy (North-Holland).

P.C. SIMMS, N. BENCZER-KOLLER and C.S. WU(1961) Phys.Rev. 121 1169.

R.M. STEFFEN (1955) Advances in Physics 4 294.

R.M. STEFFEN (1956) Phys.Rev. 103 116.

P.H. STELSON and F.K. McGOWAN (1957) Bull.Am.Phys.Soc. Ser.II 2 267.

STROMINGER, HOLLANDER and SEABORG (1958) Revs.Mod.Phys. 30 585.

A.W. SUNYAR (1955) Phys.Rev. 98 653.

" " (1958) Private communication quoted in Strominger et al. (1958).

SYMPOSIUM (1952) Nucleonics 10 No.3, 32.

L. SZILARD and T.A. CHALMERS (1935) Nature 135 98.

S. THULIN(1954) Arkiv for Fysik 9 137.

W. VAN SCIVER (1956) Nucleonics 14 No. 50.

VON HEVESY and JANTZEN (1923) Chem.News. 127 353.

R.S. WEAVER and R.E. BELL (1960) Nucl.Instr. and Meth. 9 49.

V. WEISSKOPF (1951) Phys.Rev. 83 1073.

WU, AMBLER, HAYWARD, HOPPES and HUDSON (1957) Phys.Rev. 105 1413 and 106 1361.

ZERBY, MAYER and MURRAY (1960) Bull.Am.Phys.Soc. 5 417.

STUDIES IN THE TECHNIQUE OF SHORT TIME MEASUREMENT AND ITS APPLICATION TO NUCLEAR ISOMERISM.

by

W.M. CURRIE

(June 1962)

Submitted to the University of Glasgow as a Thesis for the degree of Doctor of Philosophy.

SUMMARY.

The work reported in this thesis was concerned with the use of a fast coincidence measuring system, i.e. an apparatus using scintillation counters for the measurement of short tim intervals between nuclear radiations. The results deal partly with the technique itself and partly with its application to the study of nuclear isomerism.

It has been recognised for a long time now that there are certain inherent limitations to the measurements which ca be made with a fast coincidence system. In the first place there is a lower limit to the resolving time which can be obtained and in the second place almost all fast coincidence systems generate by virtue of their detection processes energ dependent, instrumental time delays. This means that the apparent time of an event is influenced by the energy of the radiation. These two aspects of instrumentation are of great practical importance where very short times are being measured.

Chapters 2 and 3 are concerned with these problems of instrumentation, chapter 2 with the development and theory of the subject and chapter 3 with the precise experimental study instrumental time delays and resolution. The results are v satisfactory. They demonstrate the actual performance of a system, provide illustrative curves and numbers, and indicate the manner in which any other system may be quickly assessed and its limitations ascertained. In addition the

measurements provide pleasing confirmation of the latest theoretical work which has been done on the subject and reveal the inadequacy of some of the earlier treatments.

The rest of the thesis is concerned mainly with the measurement of isomeric lifetimes, four new results being reported and discussed. The background to the subject is considered in chapter 1 where the various features of γ-ray emission from nuclei are reviewed in simple terms and the relationship between these electromagnetic phenomena and the shell and collective models of the nucleus is described. The value of the measurements lies principally in their bearing on these models, and while they provide only a small addition to the already substantial data on the subject they are not insignificant. Three of the measurements have yielded results which do not accord with the general tendency of enhanced rates for E2 transition probabilities, thus emphasising the need for more detailed knowledge of nuclear states, particularly where there is mixing of collective and single particle excitations.

The first lifetime measured was in semi-magic Ce^{140}. It is an E2 lifetime, 17 times longer than the single proton estimate. This was at first found rather surprising since another E2 lifetime in Ce^{140} had already been determined as 17 times shorter than this estimate. As explained in chapter 4, the result is not quite so surprising when more careful consideration is given to the results for other nucle

This investigation suggested that there might be some other retarded E2 transitions in nuclei similar to Ce^{140}, tha is to say in other semi-magic nuclei which seemed to exhibit mixed excitation modes. An immediate choice for further study was Ba^{138}, and Sn^{120}, with Z = 50 rather than N = 82, was also selected for experiment. This work is described i chapter 5. In both cases successful measurements were made the result for Ba^{138} being very similar to that for Ce^{140}, an the Sn^{120} result not only giving a lifetime but also correcting an earlier misinterpretation of the decay scheme.

In chapter 6 the measurement of a mixed E2 and M1 transition rate in V^{49} is reported. This work was carried out as part of a plan for the investigation of many isomeric levels using sources prepared on the H.T. set by 14 MeV neutr activation. The work on Ba^{138} and Sn^{120} was also carried out by this means but only after the efficacy of the procedu had been demonstrated in other cases.

The four measured mean lives are:-

2.083 MeV level in Ce^{140} .....$(4.97 \pm 0.09) \times 10^{-9}$ sec.

1.890 " " " Ba^{138} .....$(2.8 \pm 0.2) \times 10^{-9}$ sec.

2.304 " " " Sn^{120} .....$(8.45 \pm 0.18) \times 10^{-9}$ sec.

152 keV " " V^{49} .....$(3.05 \pm 0.08) \times 10^{-8}$ sec.

Finally, in chapter 7 (and part of the introduction) there is a discussion of an unsuccessful attempt to observe the electric quadrupole perturbation in the delayed angular correlation between the 133 and the 482 keV γ-rays of Ta^{181}

This was the initial project undertaken by the author. It took up the greater part of $3\frac{1}{2}$ years without yielding any positive results. The reason for this lies simply in the difficulty of the experiment, which was tackled in several ways and which will be the subject of still further study,